

# Catalytic Chemical Vapor Deposition of Carbon Nanotubes for Field Emission and Field Effect Transistor Applications



蔡春鴻 教授 Prof. C. H. Tsai

\*[chtsai@ess.nthu.edu.tw](mailto:chtsai@ess.nthu.edu.tw)

國立清華大學 工程與系統科學系

奈米碳管實驗室

<http://www.ess.nthu.edu.tw/~cnt/index.htm>

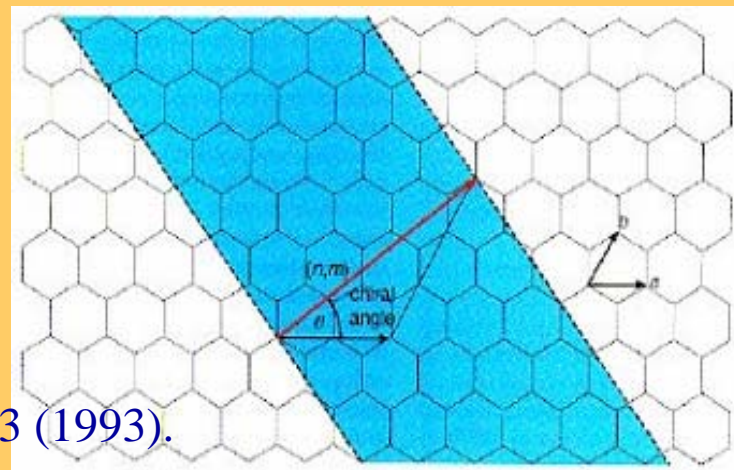
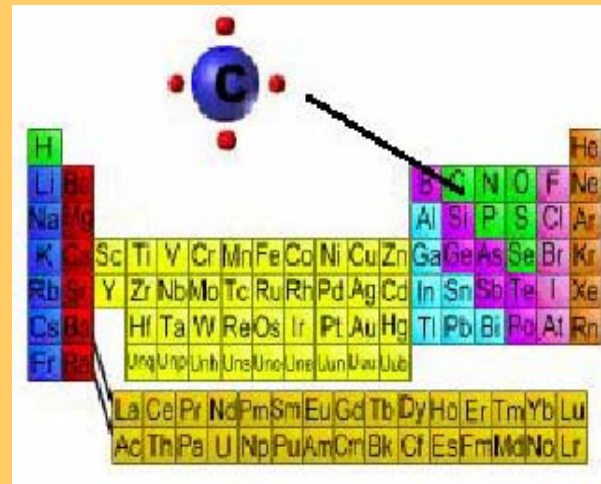
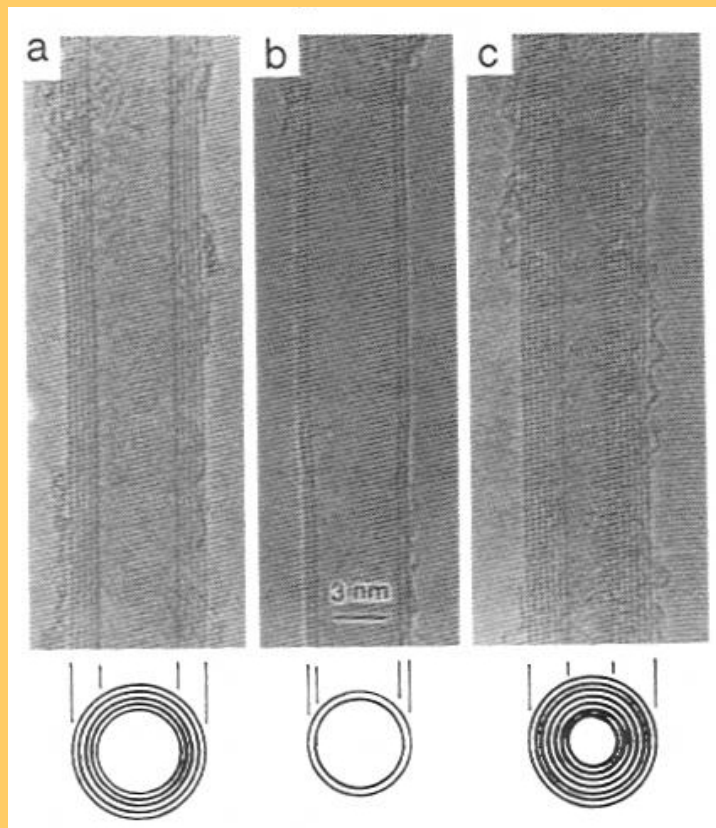
May 10, 2006 Dept. of Physics, NTHU

# First Discovery of Carbon Nanotubes by Prof. Sumio Iijima

Multi-wall carbon nanotubes (MWNTs) were first directly imaged by HRTEM by S. Iijima, NEC 1991



Sumio Iijima

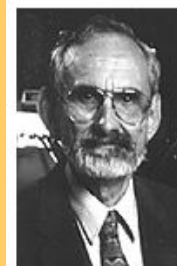


S. Iijima, *Nature* **354**, 56 (1991).

S. Iijima and T. Ichihashi, *Nature* **363**, 603 (1993).

# First Discovery of C<sub>60</sub> Fullerene

C<sub>60</sub> “fullerene” was first detected by Laser Vaporization Mass Spectrometry in Harry Kroto, Robert Curl Jr. and Richard Smalley’s experiment, Rice University 1985.



Robert F. Curl Jr.

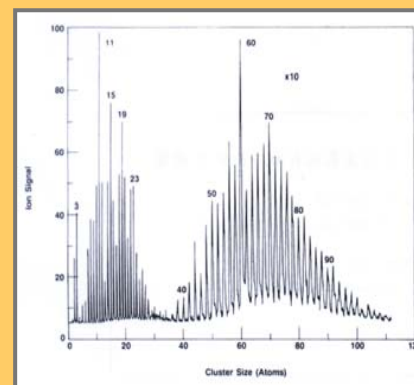
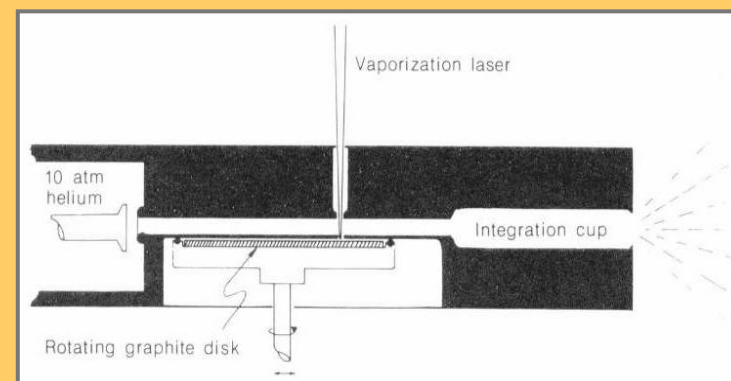
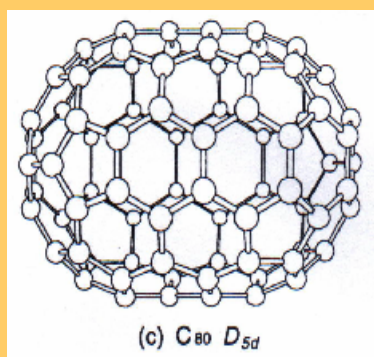
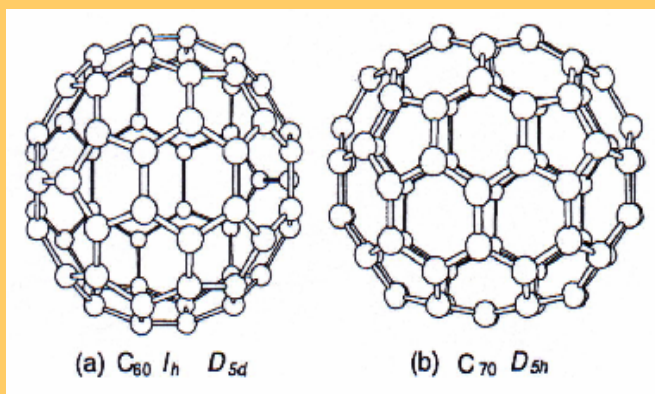


Sir Harold W. Kroto



Richard E. Smalley

**Nobel Prize in Chemistry 1996**



**R. Smalley, “Discovering the Fullerenes”, Nobel Lecture, Dec. 7, 1996.**

# Carbon Nanotube Properties and Applications

**Small sizes**  
 0.4~1.8 nm  
 (E beam Lithography :  
 50 nm Wide, 2~3 nm  
 Thick)

**Low Densities**  
 1.33~1.40 g/cm<sup>3</sup>  
 (Al:2.7 g/cm<sup>3</sup>)

**Tensile Strength**  
 45 GPa  
 (Steel : Broken at 2  
 Gpa.)

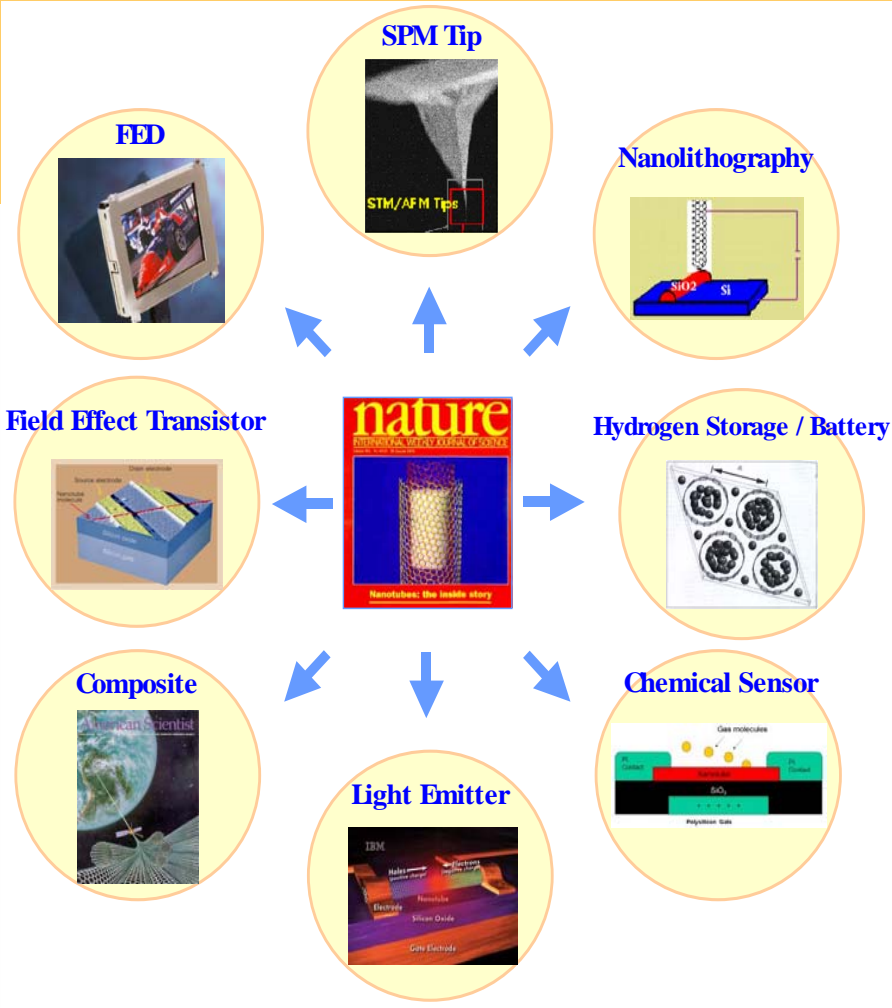
**Elasticity**  
 Bending and Recovery  
 (Metals and carbon fibers  
 are brittle.)

**Electric Currents**  
 Approximaely 1 GA/cm<sup>2</sup>  
 (Cu wires : 1 MA/cm<sup>2</sup>)

**Field Emission of Electrons**  
 1~3 V / μm  
 (Mo tips : 50~100 V / μm. Short  
 life-times)

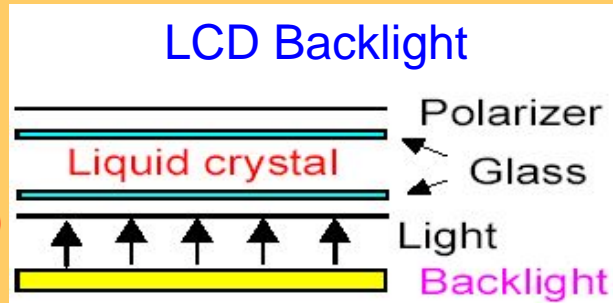
**Thermal Conductivities**  
 6000 W/m · K at Room  
 temperature  
 (Pure diamonds : 3320 W/m · K)

**Thermal Resistivities**  
 2000°C in vacuum. 750°C in Air.  
 (Cu wires in electronic circuits :  
 600~1000°C melting)

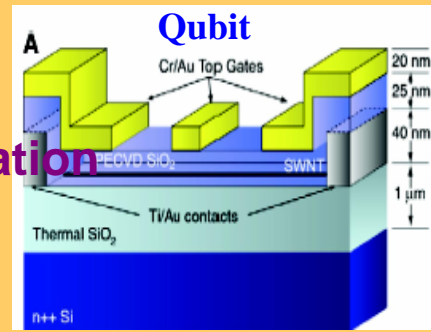


# Carbon Nanotube-based Nano-electronics

## I. Field Emission Electron Source & Devices

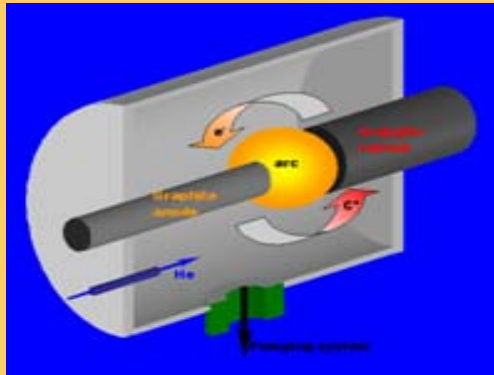


## II. Field Effect Transistor & Devices

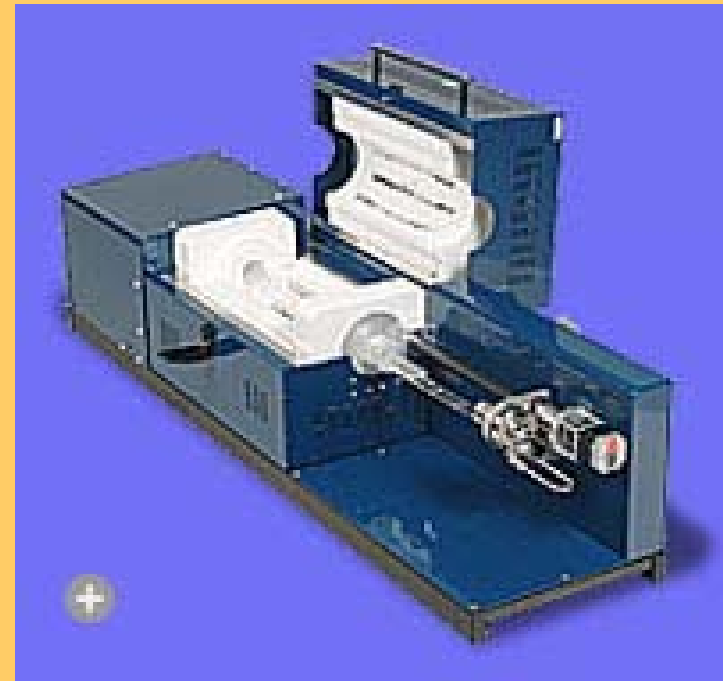


# Fabrication Methods for Carbon Nanotubes

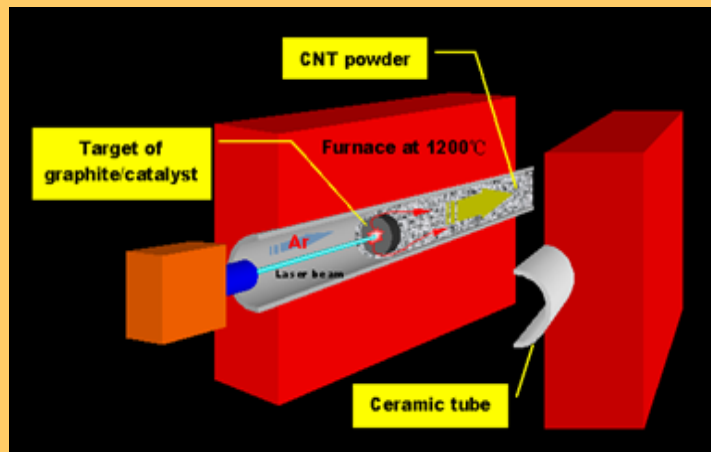
## ◆ Arc Discharge



## ◆ Chemical Vapor Deposition



## ◆ Laser Ablation



# Fabrication of CNT Field Emitters

## Screen Printing

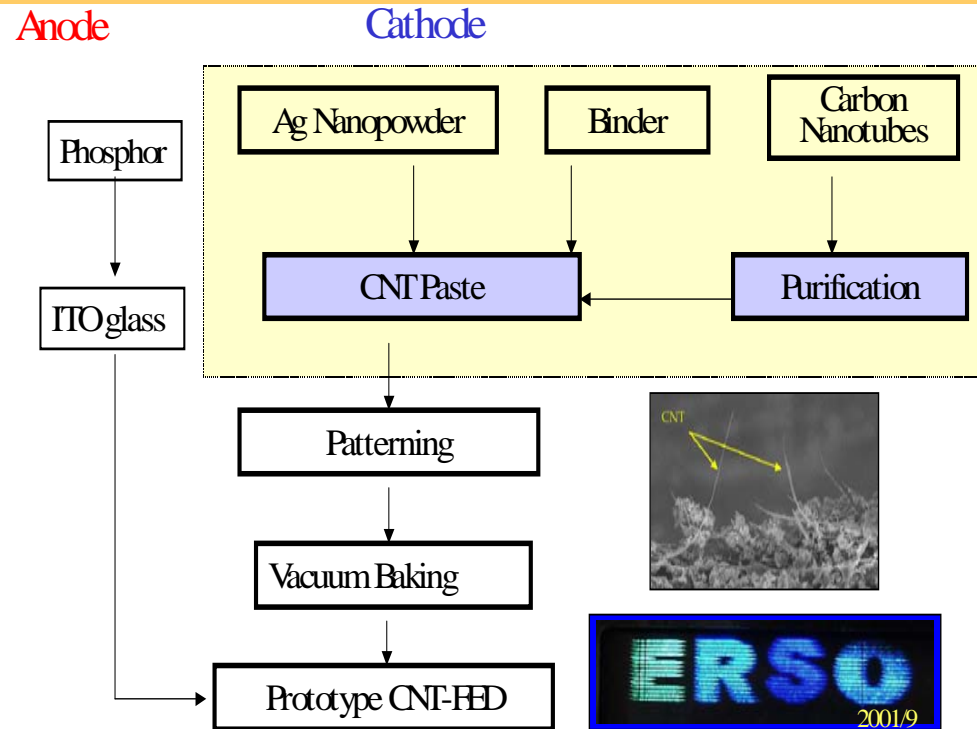
Pre-fabricated CNTs

→ transferred onto substrates  
(unordered films)

## *in-situ* Catalytic CVD Growth

as-grown CNTs on substrates

→ vertically-aligned or unordered



(H.J. Lai, 2002 Hsinchu Materials Nanotechnology Forum)

4" fully-sealed multi-color CNT-FED, Resolution=21(RGB)x256, Vac<220V, Brightness=150nits, Ef.=2 lm/W

## Growth of CNTs by ICP-CVD

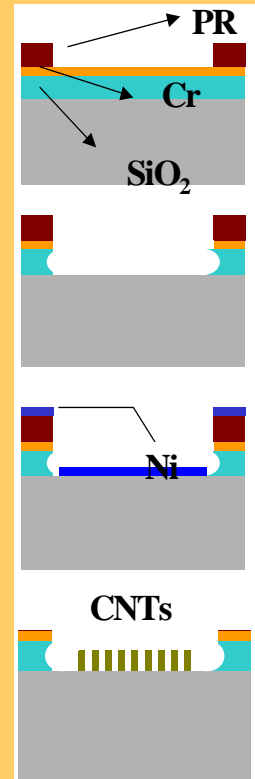
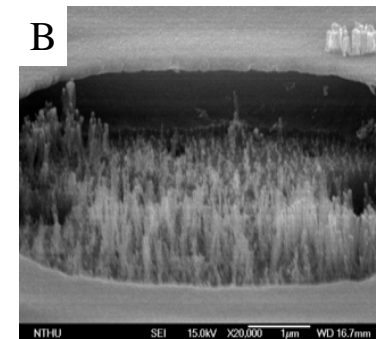
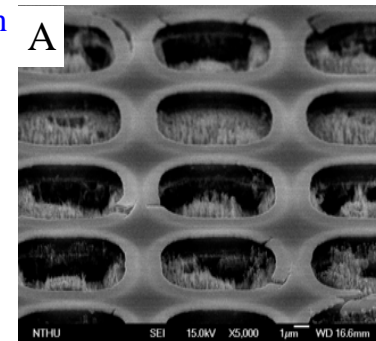
T<sub>g</sub>= 550°C

Gas ratio C<sub>2</sub>H<sub>2</sub>:H<sub>2</sub>:Ar = 8:24:0.8 (scm)

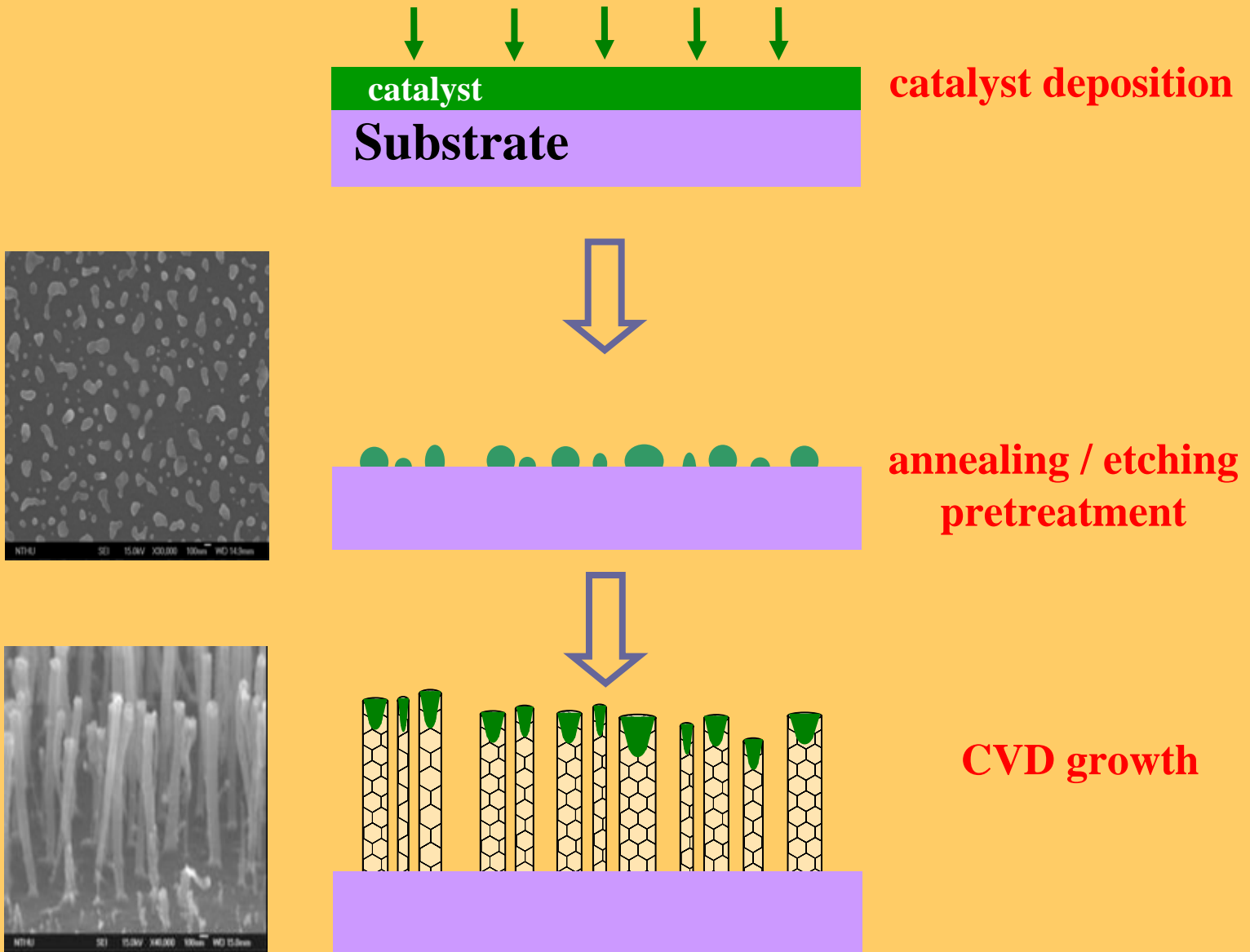
ICP power 1000W

DC bias -400V

t<sub>g</sub>= 5 min



# Growth of Carbon Nanotube by Catalytic CVD

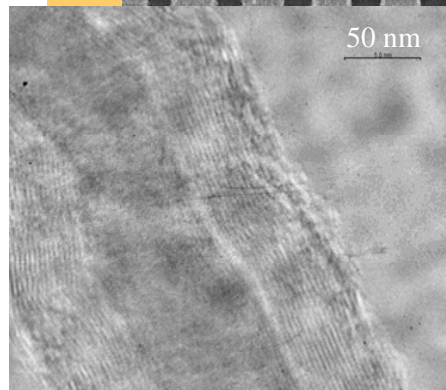
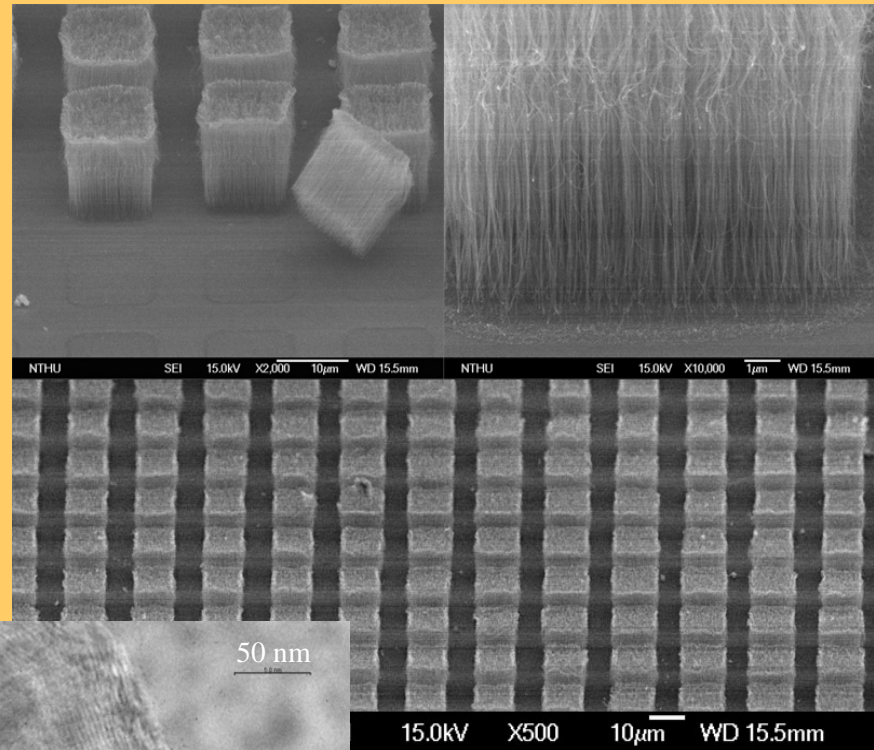




# Synthesis of Carbon Nanotubes by Thermal CVD



Furnace Temperature:  $< 1100\text{ }^{\circ}\text{C}$   
Pressure: 5 torr~1atm  
Gas: Ar,  $\text{NH}_3$ ,  $\text{CH}_4$ ,  $\text{C}_2\text{H}_2$



10 nm Ni / Si(100)  
800°C, 1 atm,  $\text{NH}_3$  pretreated,  
 $\text{C}_2\text{H}_4/\text{NH}_3/\text{Ar}$  (10/20/70 sccm)  
10 mins growth

Z.Y. Juang et al, *Diamond and Related Materials* 13 (2004) 1203.  
W.Y. Lee et al, *Diamond and Related Materials* 13 (2004) 1232.  
Z.Y. Juang et al, *Diamond and Related Materials* 13 (2004) 2140.

# Synthesis of Carbon Nanotubes by Plasma-enhanced CVD

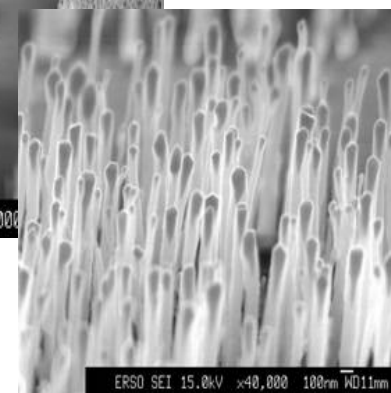
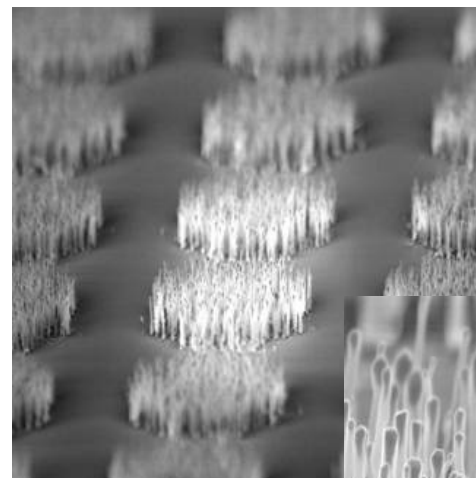
Gas Panel



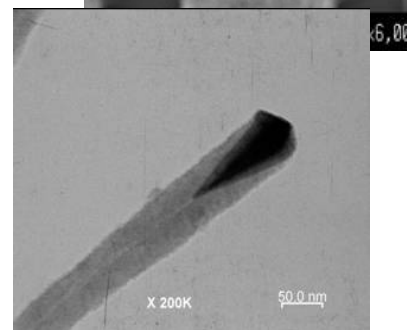
High density plasma  
 RF 13.56 MHz 2500W  
 Pressure 10 ~ 100 mTorr  
 Gas: Ar, H<sub>2</sub>, C<sub>2</sub>H<sub>2</sub>, NH<sub>3</sub>, N<sub>2</sub>  
 DC/RF bias  
 Sub. Temp. (PBN/PG): < 1000 °C

ICP Chamber

Process Chamber

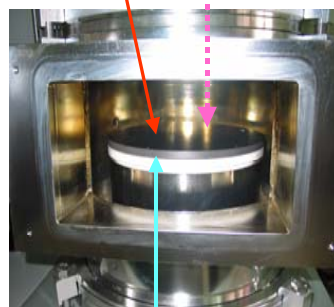


Power supplies  
 Vacuum  
 system  
 controllers



K type TC

IR Pyrometer



R type TC

Automatic Process Control

In situ Diagnostic:

- ◆ Langmuir Probe
- ◆ Optical Emission Spec.
- ◆ Quadruple Mass Spec.
- ◆ Impedance Meter

10 nm Ni /Si (100)  
 ICP 1000 W, 17mTorr, 550 °C  
 C<sub>2</sub>H<sub>2</sub> : H<sub>2</sub> = 8 : 24 sccm, bias -400 V  
 10 min growth

C.H. Weng et al, *Appl. Phys. Lett.* 85 (2004) 4732.

H.W. Wei et al. *J. Appl. Phys.* (2005) in press.

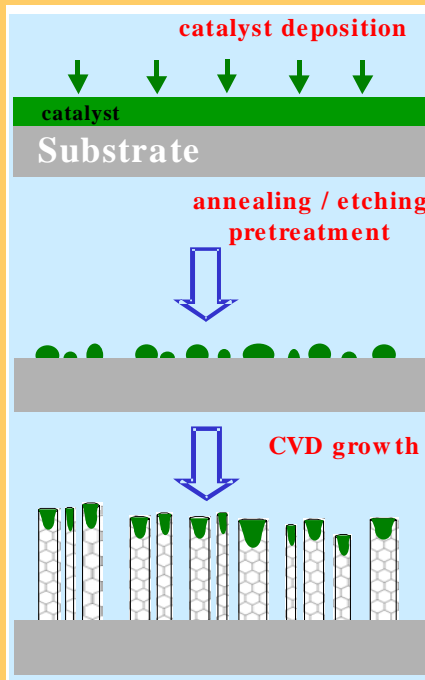
C.H. Tsai et al, *Thin Solid Film* (2005) in press.

# Parametric Study of Catalytic CVD

## Thermal CVD

Effects of:

- ◆ Type of Catalyst
- ◆ Catalyst film thickness
- ◆ Carbon source gas  
( $\text{CH}_4$ ,  $\text{C}_2\text{H}_4$ ,  $\text{C}_2\text{H}_2$ )
- ◆ Feed gas flow rate / ratio
- ◆ Process temperature
- ◆ Pressure



## ICP - CVD

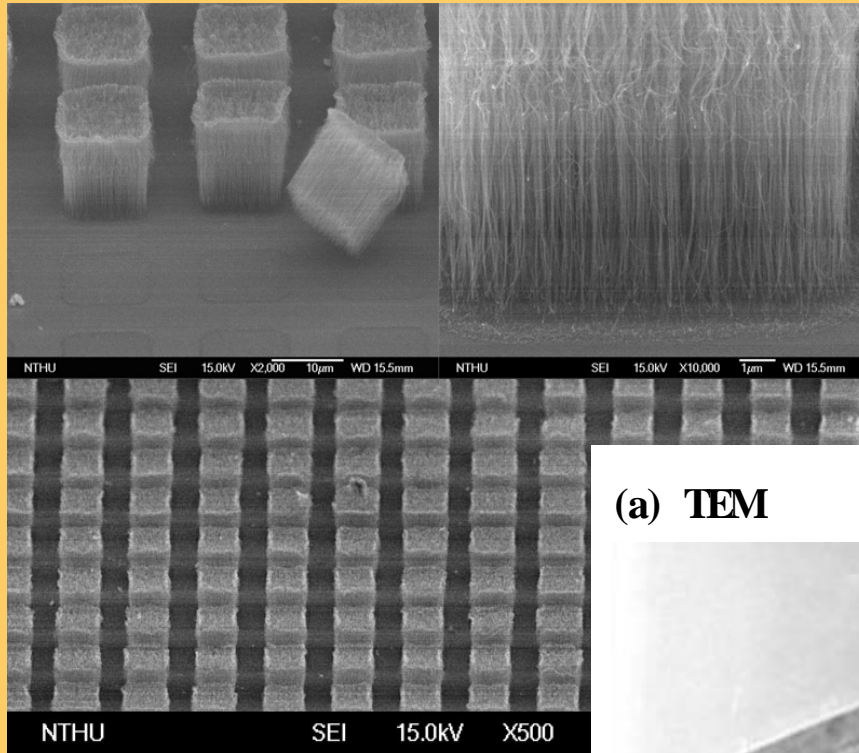
Effects of:

- ◆ Bias voltage / power
- ◆ ICP power
- ◆ Pressure
- ◆ Substrate temperature
- ◆ Feed gas flow rate / ratio

## Objectives:

- ◆ Better understanding of growth mechanisms and growth kinetics
- ◆ Lower the growth temperature to below stress point of glass ( $\sim 570^\circ\text{C}$ )
- ◆ Vertically-aligned and good structure for better field emission
- ◆ Good adhesion to substrate and good conductance

# CNT Growth by Thermal CVD

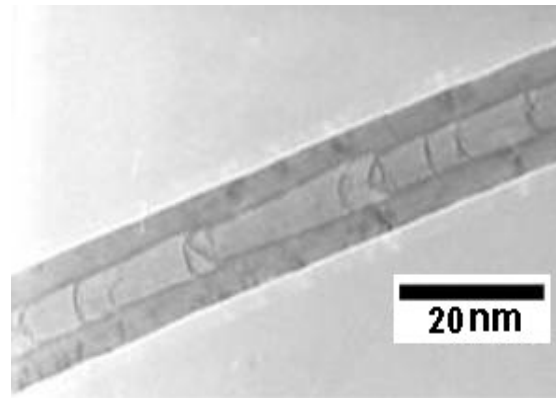


A large area of uniform patterned well-vertically-aligned CNTs were grown on 10 nm Ni/Si with the optimal growth condition:

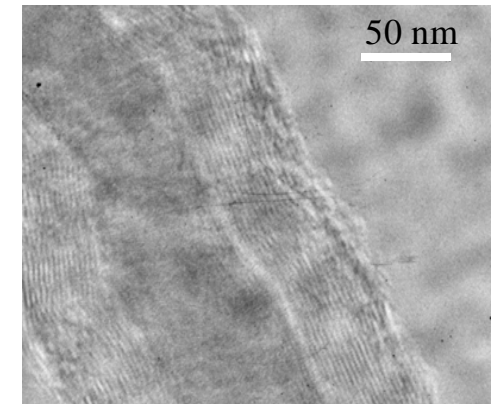
$C_2H_4/NH_3/Ar = 10/20/70$  sccm

800°C, 1 atm, growth time 10 mins

(a) TEM



(b) HR-TEM



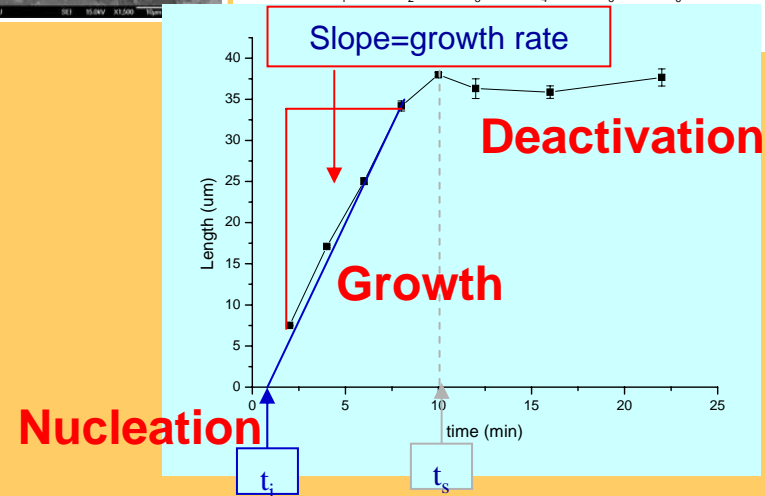
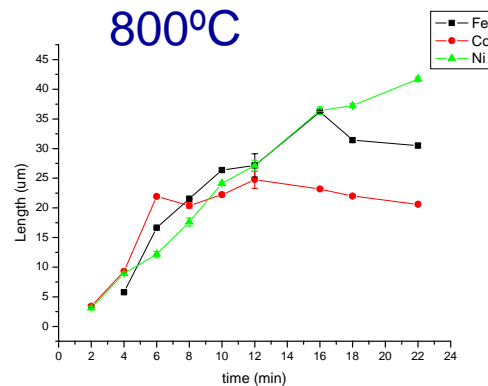
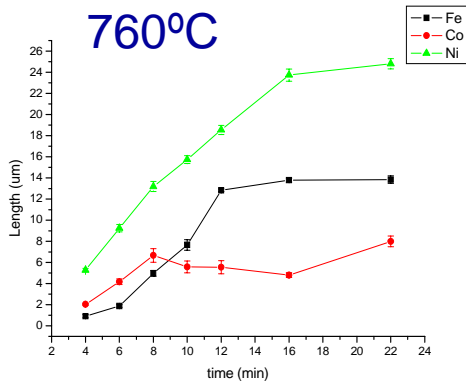
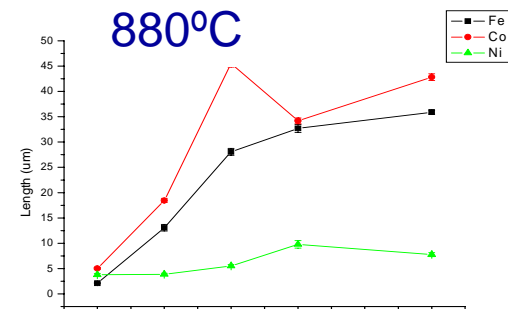
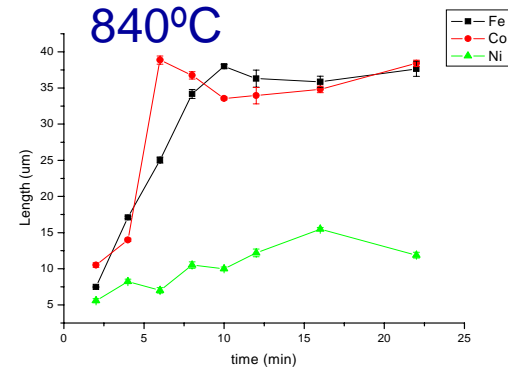
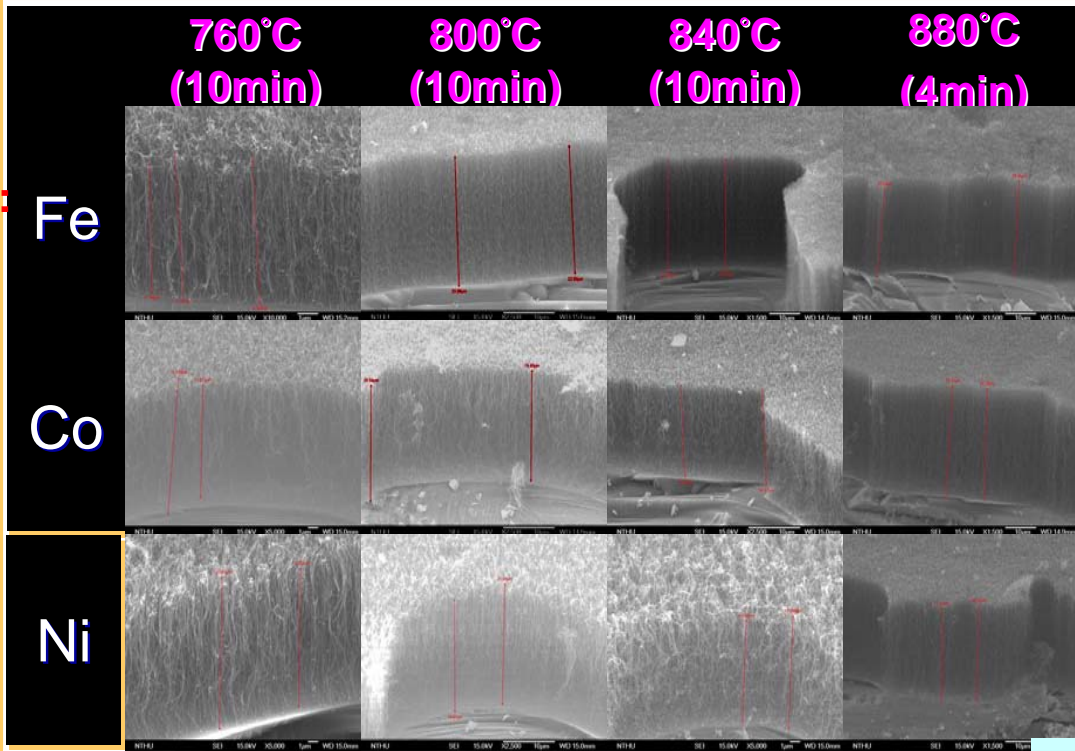
- Inner Diameter: ~7 nm
- Outer Diameter: ~20 nm
- wall thickness: ~18 layers
- Inter-layer spacing: 0.34 nm (graphite)
- Base-growth Mode
- Bamboo-like Structure

# Kinetics Study of MWNT Growth

Catalyst:  
5 nm

Pretreatment:  
NH<sub>3</sub>/Ar 900°C  
5 mins

Growth:  
C<sub>2</sub>H<sub>4</sub>/NH<sub>3</sub>  
(2:3)/Ar



# Nucleation Stage – Arrhenius plot

	Fe	Co-u	Co-d	Ni-l	Ni-r
range (°C)	760-840	760-880	760-880	760-880	760-880
slope	19400.8182	18189.31307	11958.88693	6109.76886	13376.11197
q (kcal/mol)	38.4023	36.004	23.672	12.0938	26.4769
Mean q (Kcal/mol)	38.4023	29.838		19.285	
Mean q (ev)	1.6718	1.299		0.8395	

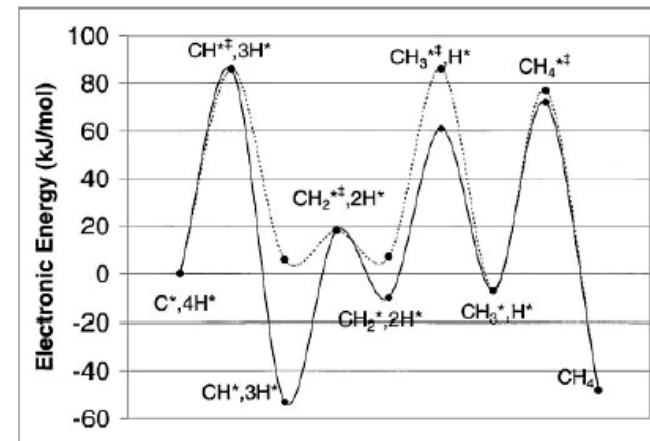
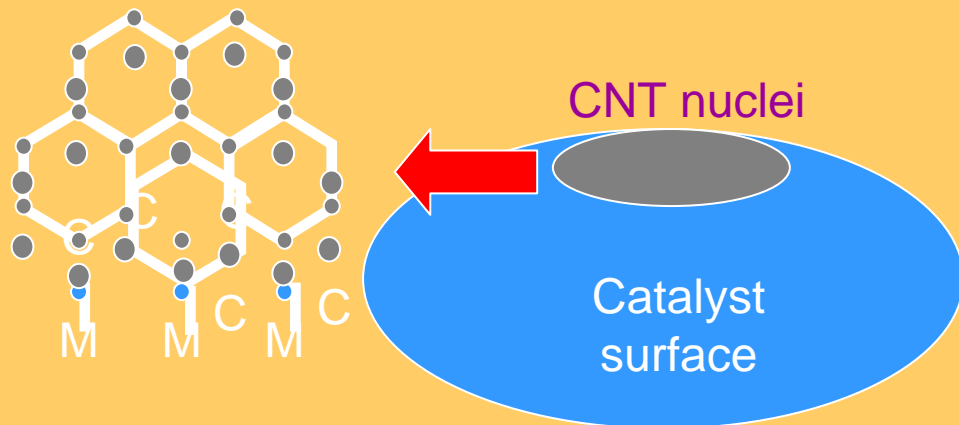


FIG. 6. Electronic energy plot for  $\text{CH}_x$  species on Ni(111), quantum chemical values ( $\blacklozenge$ ) and fitted values ( $\bullet$ ).

R. M. Watwe et al, *Journal of Catalyst* 189 (2000) 16-30

Activation energy  $\cong$  20kcal/mol



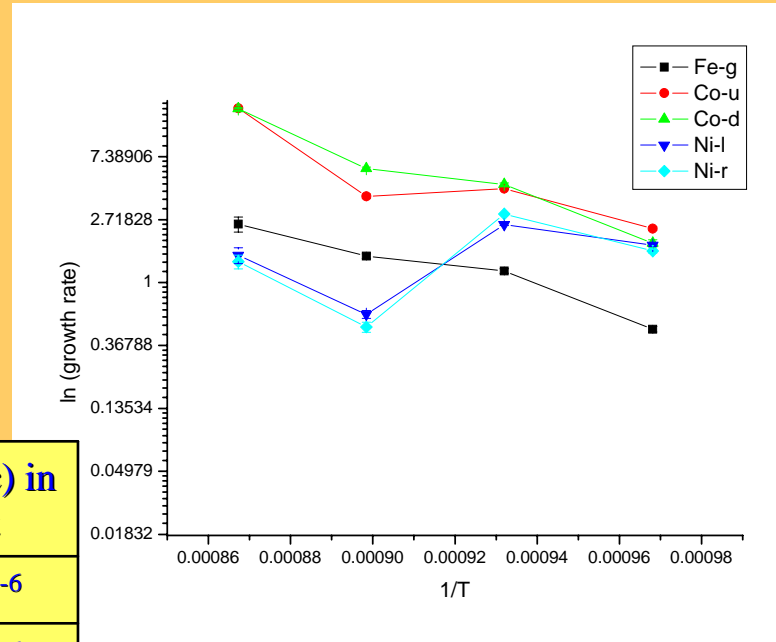
Y.A. Mo et al. *6th Int. Conf. on Sci. and Appl. of Nanotubes*, Jun 26-Jul 1, 2005.

- Nucleation stage:**  
**Process path:** nuclei formed by carbon clustering from dehydrogenation of  $\text{CH}_x$  on catalyst surface.  
**Rate control limit:** carbon species dehydrogenation rate on catalyst

# Growth Stage – Arrhenius plot

## Activation energy

	Fe-g	Co-u	Ni-l	
Temp. range (°C)	760~880	760~880	760~800	840~880
Q(ev)	1.66108	1.57127	1.0991	2.7441



	Q (eV)	D(cm <sup>2</sup> /sec) in 900°C	D(cm <sup>2</sup> /sec) in 1200°C
Ni, Bulk	1.27ev	1.12*10 <sup>-7</sup>	1.44*10 <sup>-6</sup>
polycrystalline Ni, Surface	0.3ev	1.65*10 <sup>-6</sup>	3.07*10 <sup>-6</sup>
Ni(111), Surface	0.5~0.4ev	1.79*10 <sup>-7</sup>	6.19*10 <sup>-7</sup>
Ni(100), Surface	2.1ev		
Ni(110), Surface	0.4ev		
Fe, Bulk	1.3~1.58ev	1*10 <sup>-7</sup>	1~2*10 <sup>-6</sup>
Fe, Surface	0.1 ev	1.1*10 <sup>-3</sup>	1.5*10 <sup>-3</sup>
Co, Bulk	1.54ev		

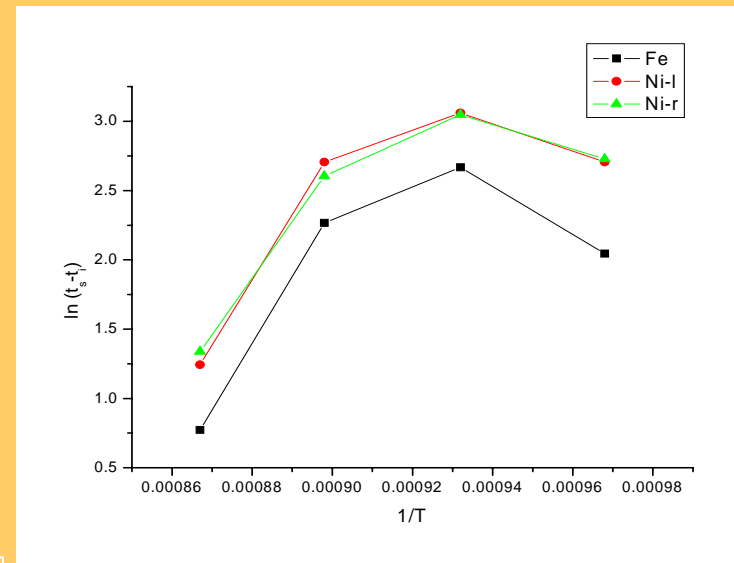
## Steady Growth:

**Process path:** Carbon diffuses through catalyst particle by bulk diffusion, until bond with dangling bond of MWNT graphite layer.

**Rate control limit:**  
carbon bulk diffusion

# Deactivation Stage – Arrhenius plot

catalyst	Fe		Ni	
	range	840-880	760-800	840-880
range	760-800	840-880	760-800	840-880
q(KJ/mol)	-143.76856	400.463322	-77.9052	350.62566
q (Kcal/mol)	-34.23061	95.34841	-18.54886	83.4823
q(ev)	-1.49	4.1508	-0.80748	3.63419



1. In 880~840 °C, the slope is positive, so the carbon which cover the catalyst particle is formed by cracking in gas.
2. In 800~760 °C, the slope is negative, so the carbon which cover the catalyst particle is formed by dehydrogenation on catalyst surface.
3. In 880~840 °C, the slope is much bigger than the slope in 800~760 °C, maybe because the activation energy of formation carbon in gas is large.
4. The ratio of q on Fe to Ni is 1.85 which almost is equal to the ratio of H<sub>2</sub> chemisorption heat on Fe to Ni.

## Deactivation stage:

### Process path:

1. In 880~840°C, active sites covered by carbon formed by cracking in gas adsorbing on catalyst surface.
2. In 800~760°C, active sites covered by the carbon formed by dehydrogenation on catalyst surface.

- Rate control limit:**
1. In 880~840°C, the carbon source species cracking rate.
  2. In 800~760°C, the carbon source species dehydrogenation rate on catalyst.



# Thermal CVD Growth on Glass Substrate

- Synthesis temperature lower than stress point of  $\sim 570^\circ\text{C}$  is required.

- A conducting metal layer on glass is required.
- Cr was chosen for low resistivity and Ni can form nanoparticle on Cr.

## Process Modification:

- (1) Two temperature zone approach: not successful.
- (2) Single temperature:
  - lower temperature: low catalysis efficiency  $\rightarrow$   $\text{C}_2\text{H}_2$  was chosen;
  - low diffusion rate  $\rightarrow$  low  $\text{C}_2\text{H}_2$  flow rate and high  $\text{NH}_3/\text{C}_2\text{H}_2$  ratio
  - A new pumping system was installed to lower the pressure.

Optimal process condition on 10 nm Ni/100 nm Cr/glass:  
 $\text{C}_2\text{H}_2/\text{NH}_3/\text{Ar} = 10/50/430$  sccm  
 $550^\circ\text{C}$ , 8 torr, growth time 10 mins

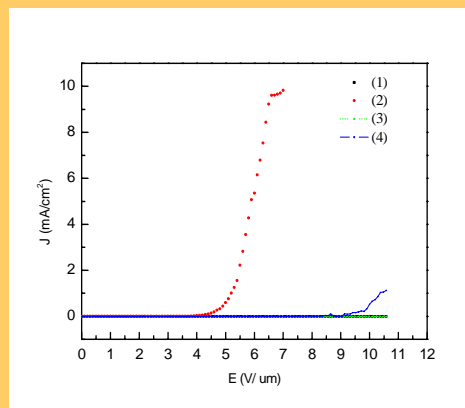
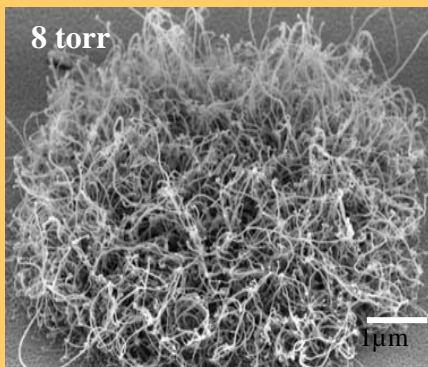
J.H. Lee et al, *Surface and Coating Tech* (2005) in press.



## TECO Nano.

Condition:

pressure  $\sim 2 \times 10^{-5}$  torr  
gap  $\sim 70$   $\mu\text{m}$   
voltage  $\sim 1.1$  kV (DC)  
peak current  $\sim 0.08$  mA



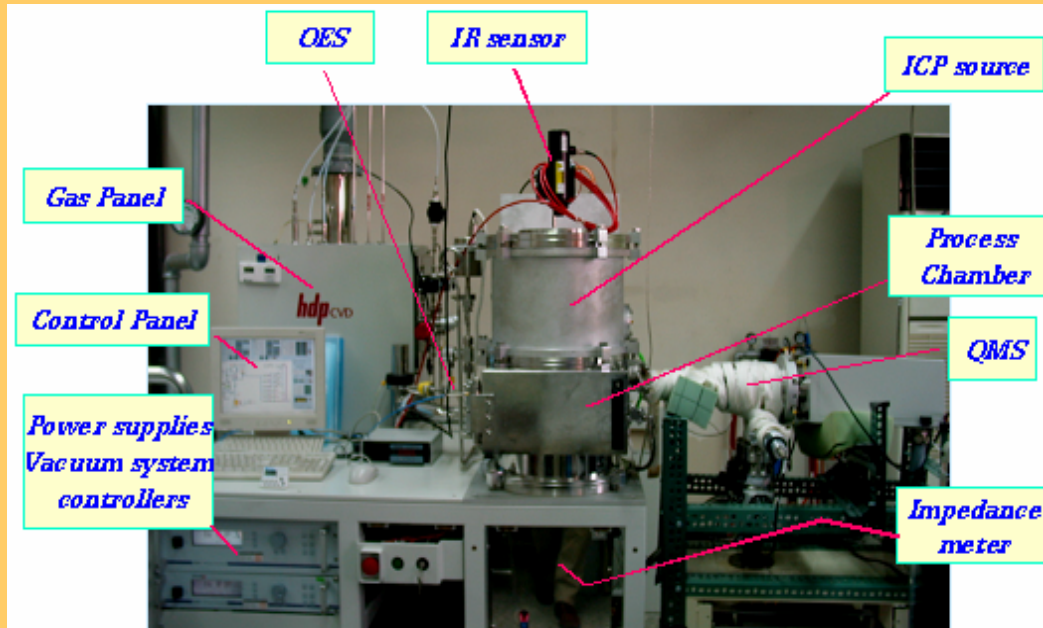
Field Emission:

Turn-on:  $3 \sim 4$  V/ $\mu\text{m}$

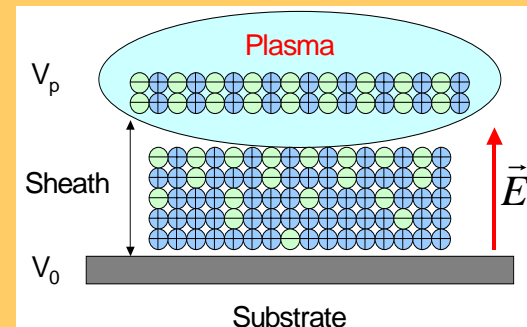
Threshold @  $10$  mA/ $\text{cm}^{-2}$ :  
 $\sim 7$  V/ $\mu\text{m}$

# Controlled Growth of Vertically-aligned Multi-walled Carbon Nanotubes and *in-situ* Pre- / Post- Treatments for Field Emission Enhancement

## ◆ Inductively-Coupled Plasma CVD



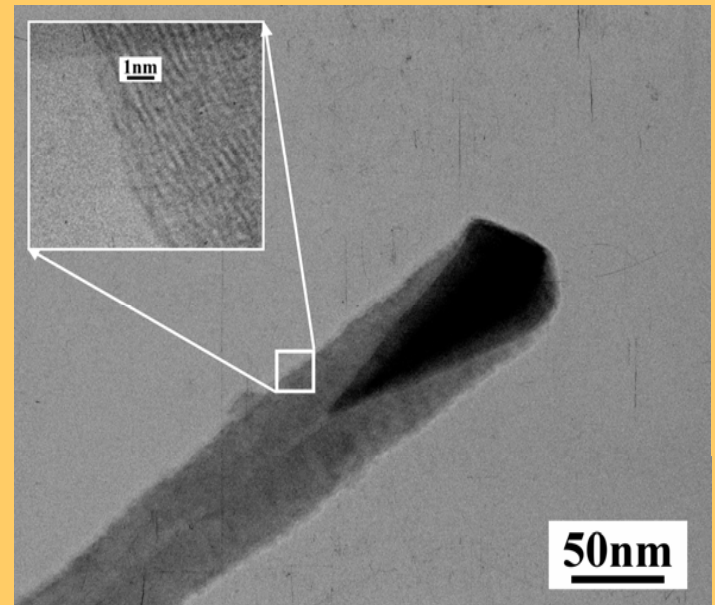
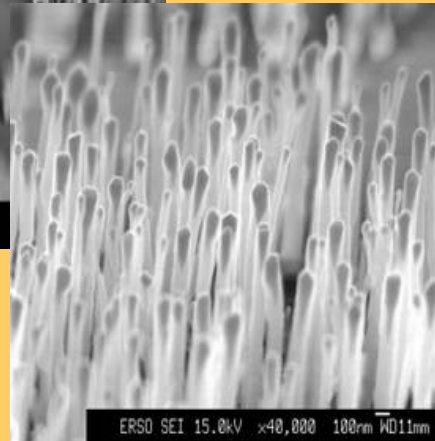
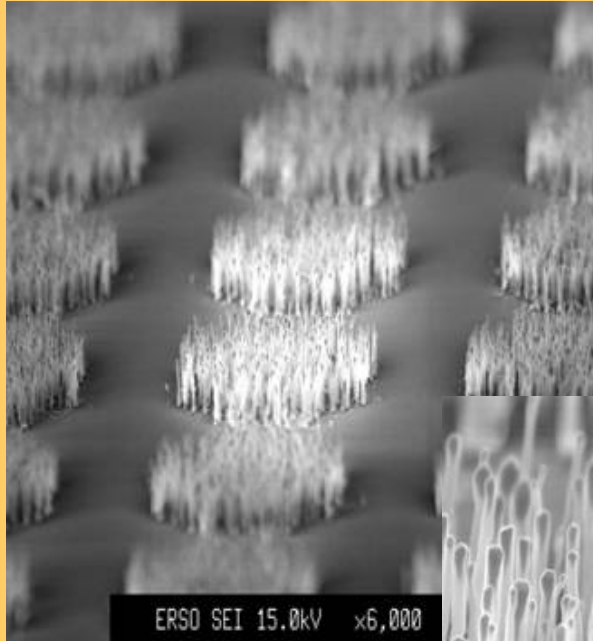
High Density Plasma  
RF 13.56 MHz 2500W max.  
Pressure 10~100 mTorr  
Gas: Ar, H<sub>2</sub>, C<sub>2</sub>H<sub>2</sub>, NH<sub>3</sub>, N<sub>2</sub>  
DC/RF bias: max. 600 V / 600 W  
Sub. Temp. (PBN/PG): < 1000 °C  
Sub. size 150 mm



### Equipment Novelty:

- Developed through Industrial-Cooperative Project with a domestic company, Nano Architect Research Co., in Science Park
- High Plasma Density ( $\sim 10^{12} \text{ cm}^{-3}$ ), Low Pressure ( $\sim \text{mTorr}$ ), Low Temperature ( $400 \sim 550 \text{ }^\circ\text{C}$ )
- Independent control of Ion Density and Energy (through ICP power and Substrate DC / RF bias)
- Automatic Process Control through *in-situ* Diagnostic (Langmuir Probe, Optical Emission, Quadrupole MS, Impedance Meter)
- 2 Patents on Equipment Design, 2 Patents on Process Control and 12 journal/conference papers

# CNT Growth by ICP- CVD



**10 nm Ni/Si**

**ICP power 1000 W, Pressure 17 mTorr**

**$C_2H_2/H_2 = 8/24$  sccm**

**550°C, growth time 10 mins**

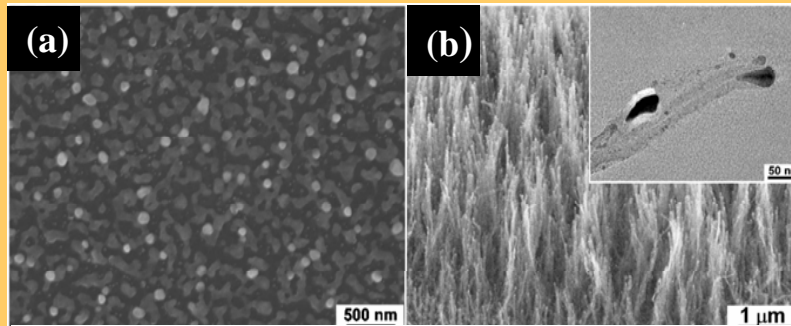
- **Inner Diameter: ~10 nm**
- **Outer Diameter: ~80 nm**
- **wall thickness: ~100 layers**
- **Inter-layer spacing: ~0.4 nm**

- **Tip-growth Mode**
- **Cone-shaped catalyst at tip**
- **Hollow Tube Structure**

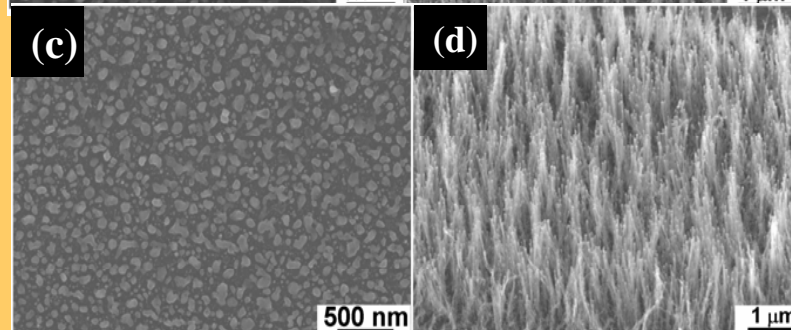
# ICP-CVD Growth on Glass Substrate

- Optimal substrate temperature is already lower than glass stress point.
- Cr was also chosen for conducting metal layer.
- Different Ni thickness was tested (Ni = 20, 30, 40 nm).

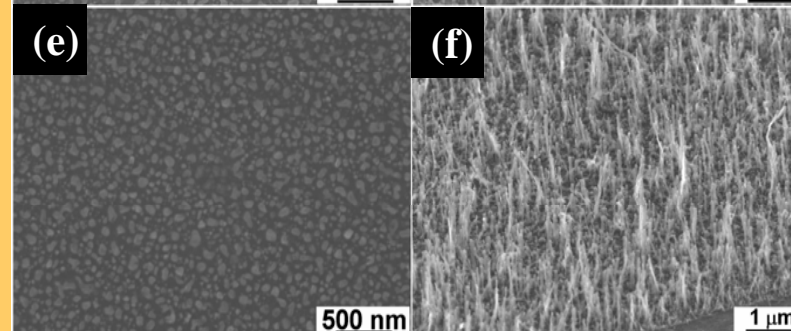
40nmNi/  
60nmCr/  
glass



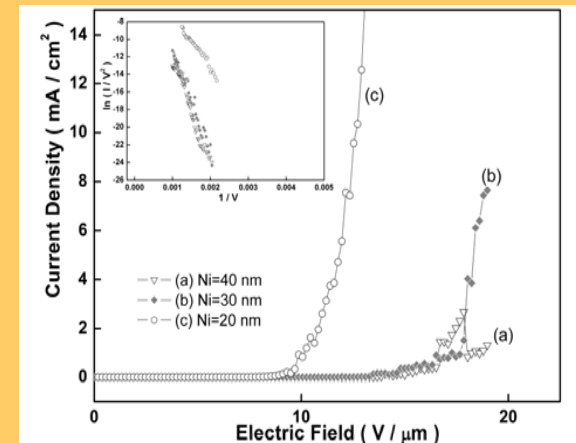
30nmNi/  
60nmCr/  
glass



20nmNi/  
60nmCr/  
glass



Optimal process condition on 20 nm Ni/ 100 nm Cr/glass:  
NH<sub>3</sub> plasma pretreated for 5 mins, ICP 500 W, RF bias 300 W, pressure 20 mTorr, C<sub>2</sub>H<sub>2</sub>/H<sub>2</sub>/Ar = 3/17/0.8 sccm, 500°C, growth time 20 mins



Turn-on: 9~10 V/μm

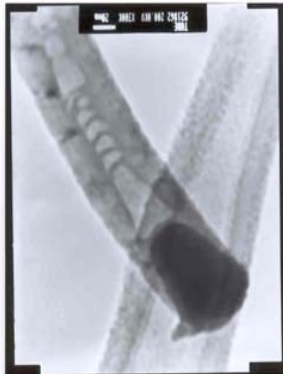
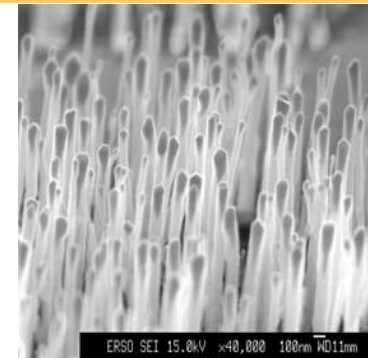
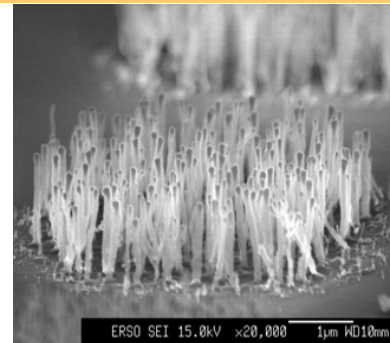
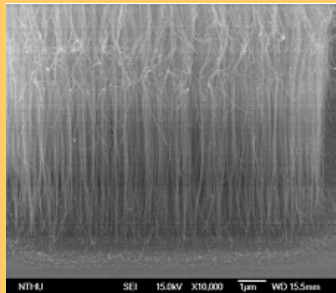
Threshold @ 10 mA/cm<sup>2</sup> ~12 V/μm

C.H.Tung et al. *Thin Solid Film* (2005) in press.

# Carbon Nanotube Growth Mechanisms

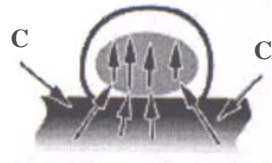
## Base Growth

## Tip Growth

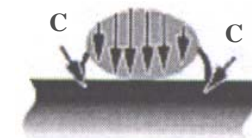
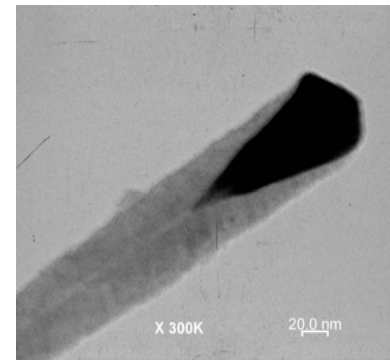


SEM

SEM



carbon film cap on top  
and carbon source at  
bottom



etching at top and carbon  
source at top

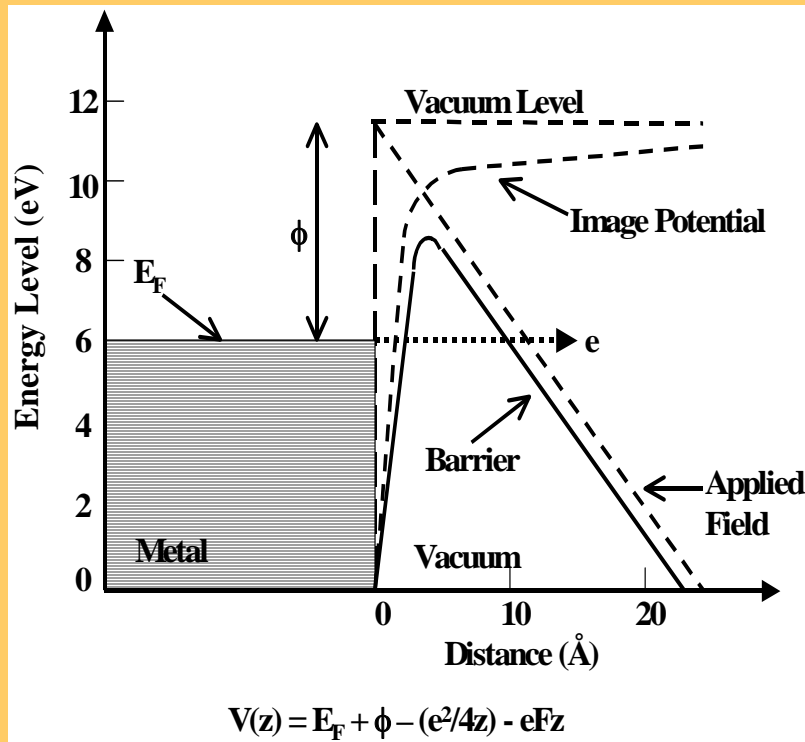
TEM  
bamboo-like structure

TEM  
hollow tube structure

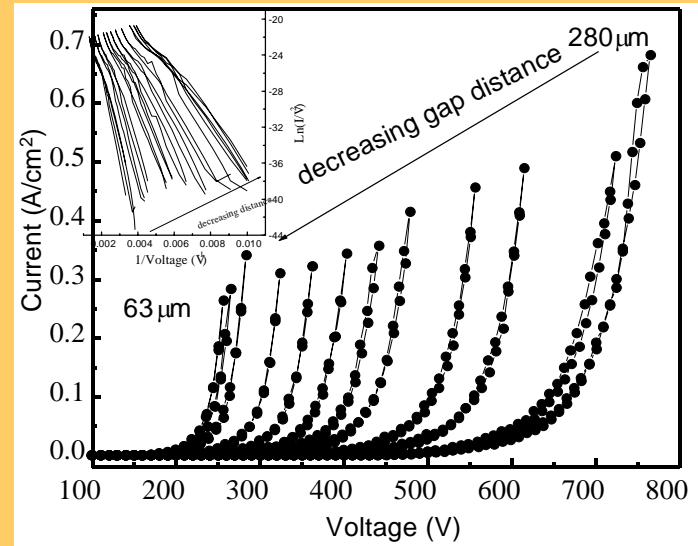
Thermal CVD

ICP-CVD

# Field Emission of Carbon Nanotubes



Electrons quantum mechanically tunnel across the barrier Fowler, R. H. and Nordheim, L. W., *Proc. R. Soc. London A* **119**, 173 (1928).



W.A.de Heer, A. Chatelain, and D. Ugarte, *Science* **270**, 1179 (1995).

$$I = a \frac{V^2}{\phi} \exp\left(-\frac{b \phi^{3/2}}{\beta V}\right)$$

$$\ln\left(\frac{J}{E^2}\right) \approx a' - \frac{b' \phi^{3/2}}{\beta E}$$

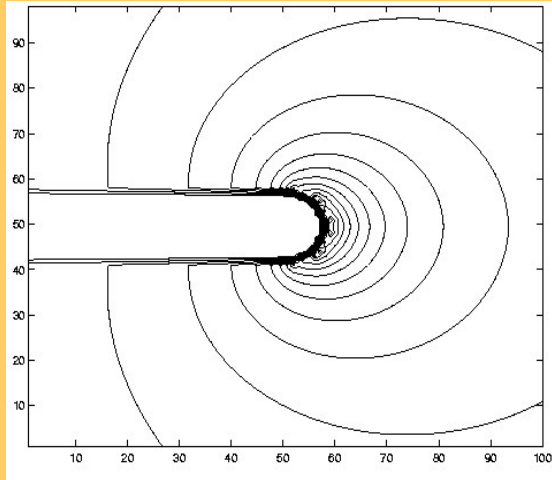
$\phi$  : work function

$\beta$  : field enhancement factor

# Work Function for Electron Emission from CNTs

Type of CNT	Diameter (nm)	Measurement Method	Work Function (eV)	Reference
SWNT	1.0~1.4	Energy Spectrum of Photoelectrons	<b>4.65 ± 0.1</b>	Liu X et al., AIP conf. Proc. Vol. 544, 288 (2000)
SWNT	1.4	Energy Spectrum of Photoelectrons	<b>4.8</b>	Suzuki S et al., APL 76, 4007 (2000)
SWNT	1.4	Fowler-Nordheim and measured I-V	<b>5.1</b>	Bonard J-M et al., APL 73, 918 (1998)
SWNT		Fowler-Nordheim and measured I-V (field emission microscopy)	<b>4.76~4.88</b>	Sun JP et al., Appl. Phys. A 75, 479 (2002)
SWNT (armchair)	0.8~8.15	First principle calculation	<b>6.75~7.05</b>	Zhou G et al., APL 79, 836 (2001)
MWNT	14~55 (single)	Fowler-Nordheim and measured I-V (in-situ TEM)	<b>4.6~4.8 (some~5.6)</b>	Gao R et al., APL 78, 1757 (2001)
MWNT	44	Fowler-Nordheim and measured I-V	<b>7.3 ± 0.7</b>	Fransen MJ et al., Appl. Surf. Sci. 146, 312 (1999)
MWNT		Energy Spectrum of Photoelectrons	<b>5.7</b>	Chen P et al., PRL 82, 2548 (1999)
MWNT		Energy Spectrum of Photoelectrons	<b>4.3</b>	Ago H et al., Phys. Chem. B 103, 8116 (1999)
MWNT	10	Energy Spectrum of Photoelectrons	<b>4.95</b>	Shiraishi M. et al., AIP Conf. Proc. Vol. 544, 359 (2000)

# Field Enhancement Factor



◆ Main features affecting the field emission characteristics:

\* Microstructure / Physical property:

- SWNT or MWNT
- electrical conductivity
- good graphitic structure

\* Geometrical features:

- aligned or non-aligned
- closed or open-ended
- tip curvature
- diameter and length (aspect ratio)
- density

- ◆ Electron emission is driven by the local electrical field strength
- ◆ The electrical field strength in the vicinity of a nanotube is hundreds times higher than the volumetrically averaged value  $V/d$



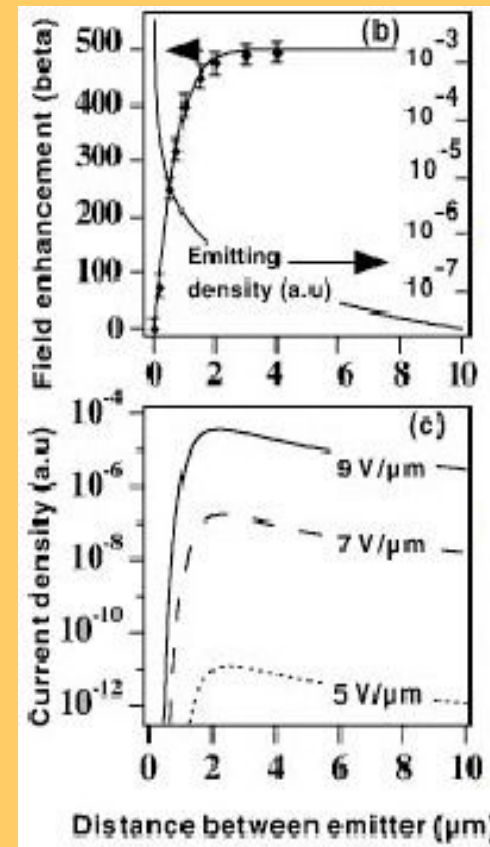
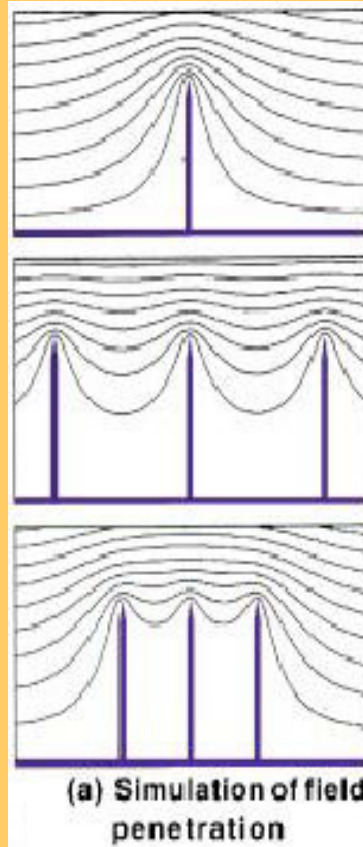
# CNT Field Emission of Different Densities

distance between tubes  
(density)

$4 \mu\text{m}$   
( $6 \times 10^6 \text{ cm}^{-2}$ )

$1 \mu\text{m}$   
( $10^8 \text{ cm}^{-2}$ )

$0.5 \mu\text{m}$   
( $4 \times 10^8 \text{ cm}^{-2}$ )

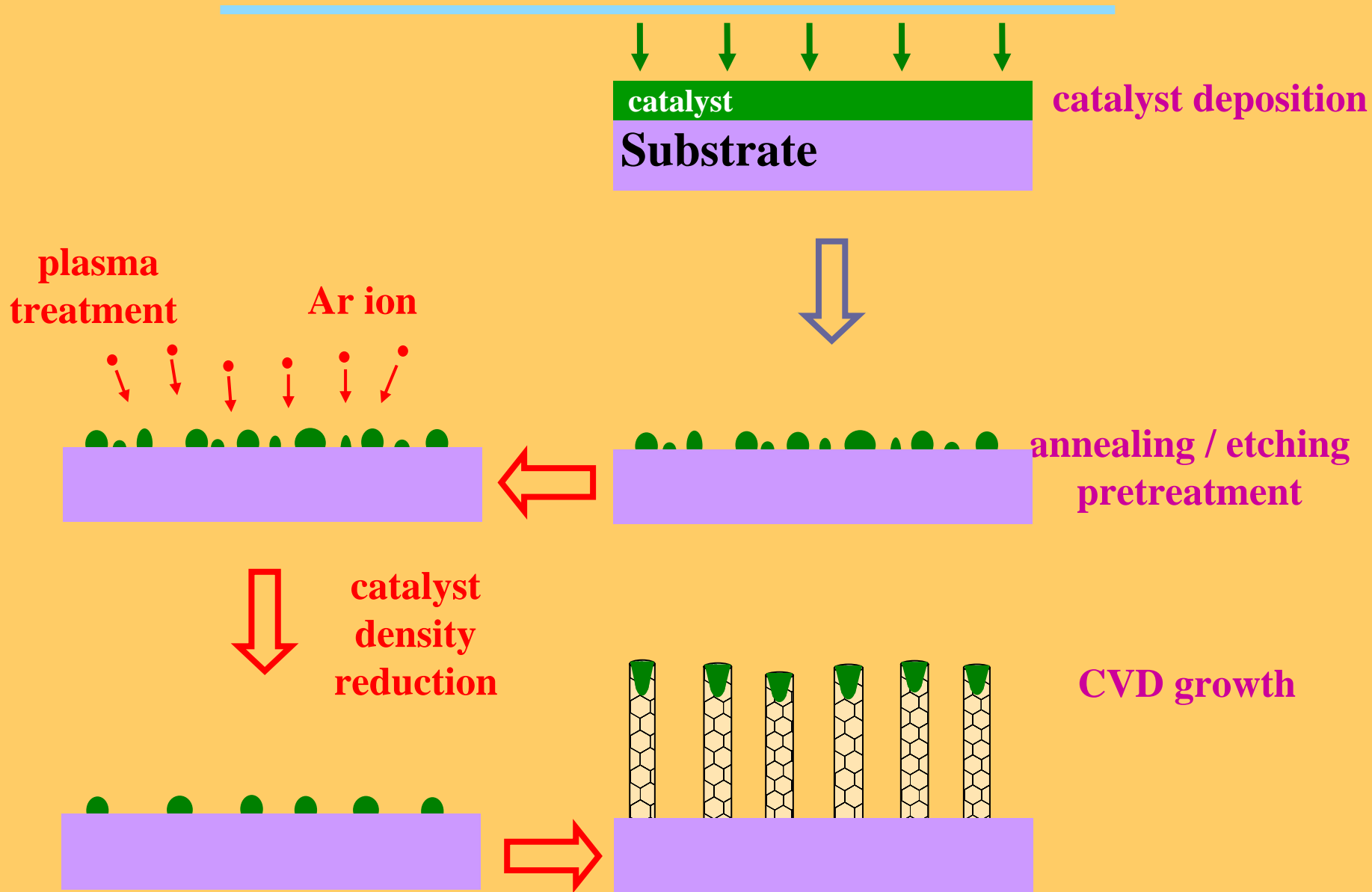


CNTs height  $1 \mu\text{m}$ , tip apex  $2 \text{ nm}$  (electrostatic calculation)

L. Nilsson, O. Groening, C. Emmenegger, O. Kuettel, E. Schaller, L. Schlapbach, H. Kind, J-M. Bonard and K. Kern, *Appl. Phys. Lett.* **76**, 2071 (2000).

# Process Modification for Field Enhancement

## - Plasma Pre-treatment



# Control of Nanocatalyst Size / Density by Ar Sputtering

## Pretreatment: ICP CVD

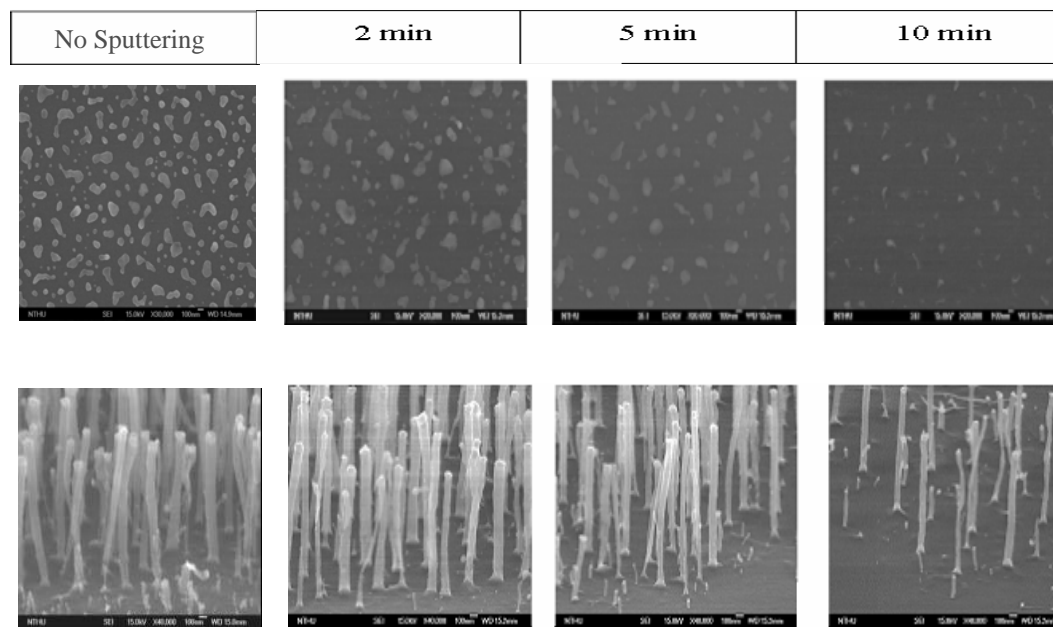
Parameters	
Gas	Ar: 10sccm
Pressure	40mTorr
RF Power	1000 W
Time	2, 5, 10 min
Bias	-400V

## CNT Growth: ICP CVD

Parameters	
Gas	C <sub>2</sub> H <sub>2</sub> : 10sccm H <sub>2</sub> : 20sccm
Pressure	17mTorr
RF Power	1000 W
Time	10 min

## Catalyst: Electron Gun

Ni 100 Å  
Si substrate



With Ar plasma sputtering under  $-400$  V bias for 10 min, the catalyst particle density was obviously reduced.

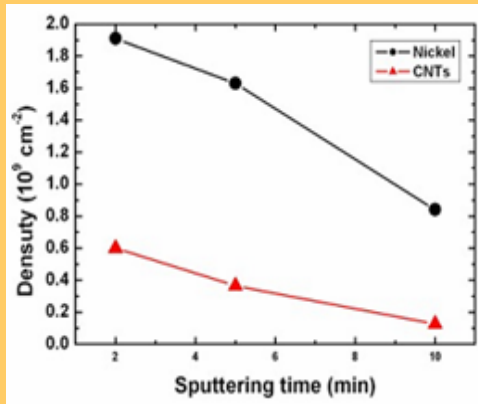


CNT density was drastically reduced for those pretreated under  $-400$  V bias consistent with the change of particle density, and good vertical alignment was kept even at low density ( $\sim 10^8$  cm<sup>-2</sup>).

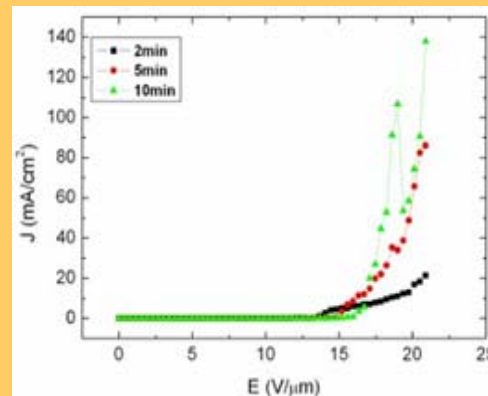
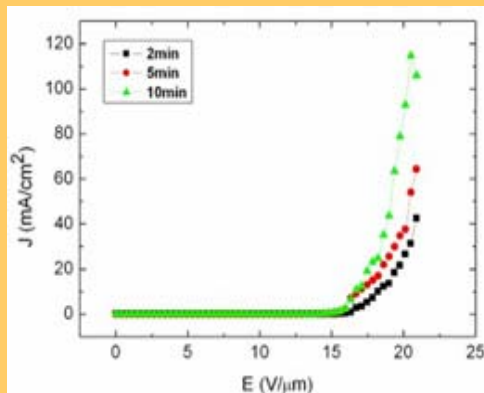
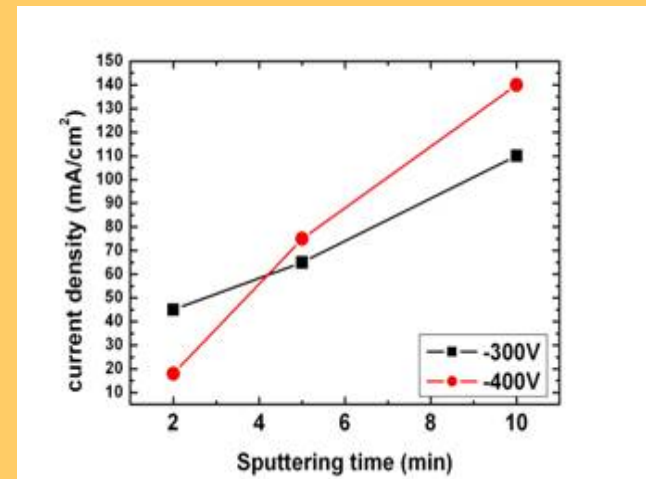
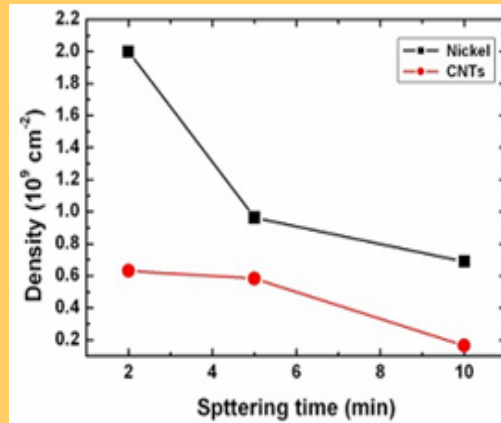
# Effects of Ar Sputtering on CNT Density and Field Emission

Ar plasma sputtering, ICP power 1000 W  
Ar flow rate 10 sccm, pressure 40 mTorr

Bias -300 V



Bias -400 V

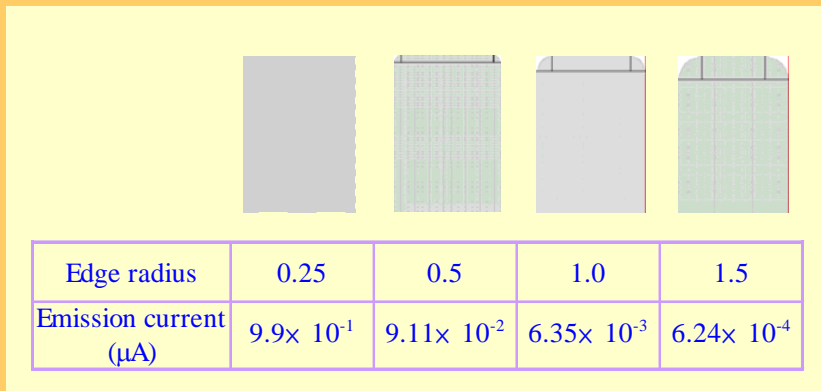


C.T. Lin et al, 9th International Conference on New Diamond Science and Technology (ICNDST-9) Mar. 26-29, 2004, Tokyo, Japan.

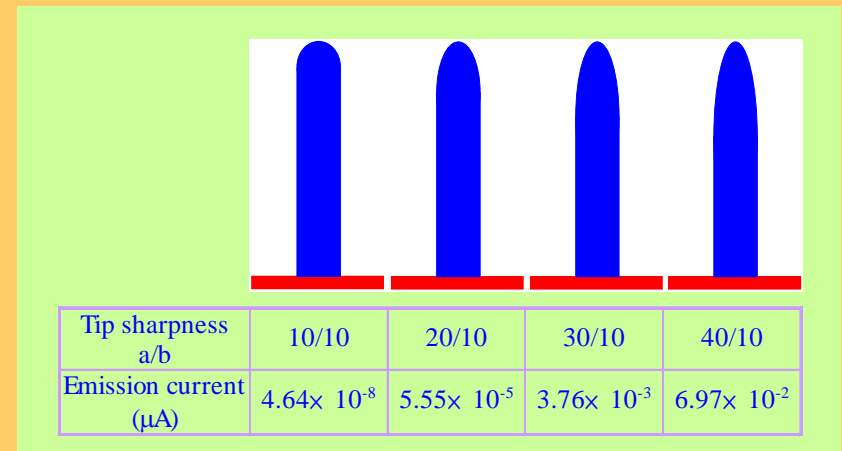
# Field Emission from a Single MWNT (simulation)

Applied voltage 40V, cathode-to-anode distance 2 $\mu$ m  
 MWNT height 100nm, radius 10nm, work function 1eV

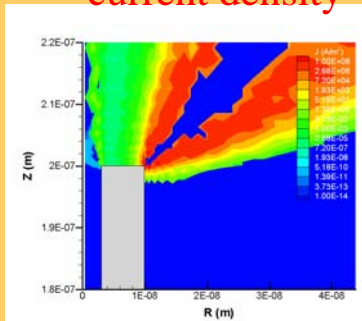
Open-ended  
 Effect of Edge Sharpness



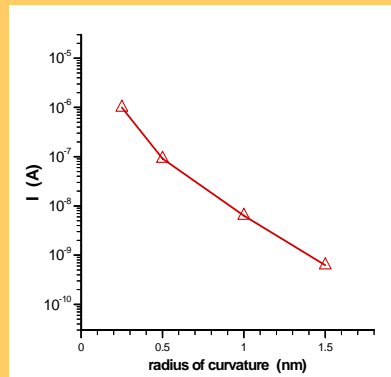
Closed-caped  
 Effect of Tip Sharpness



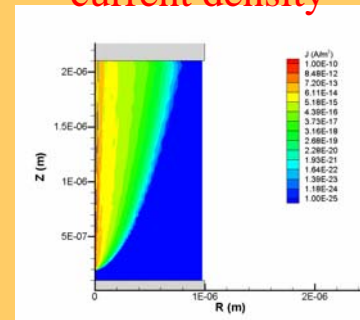
current density



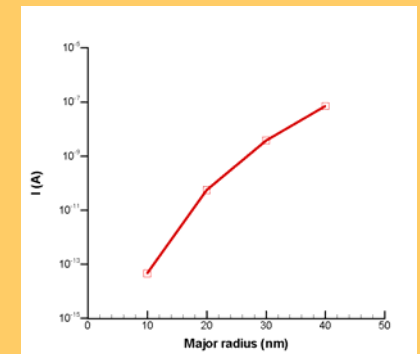
(edge radius=0.25nm)



current density

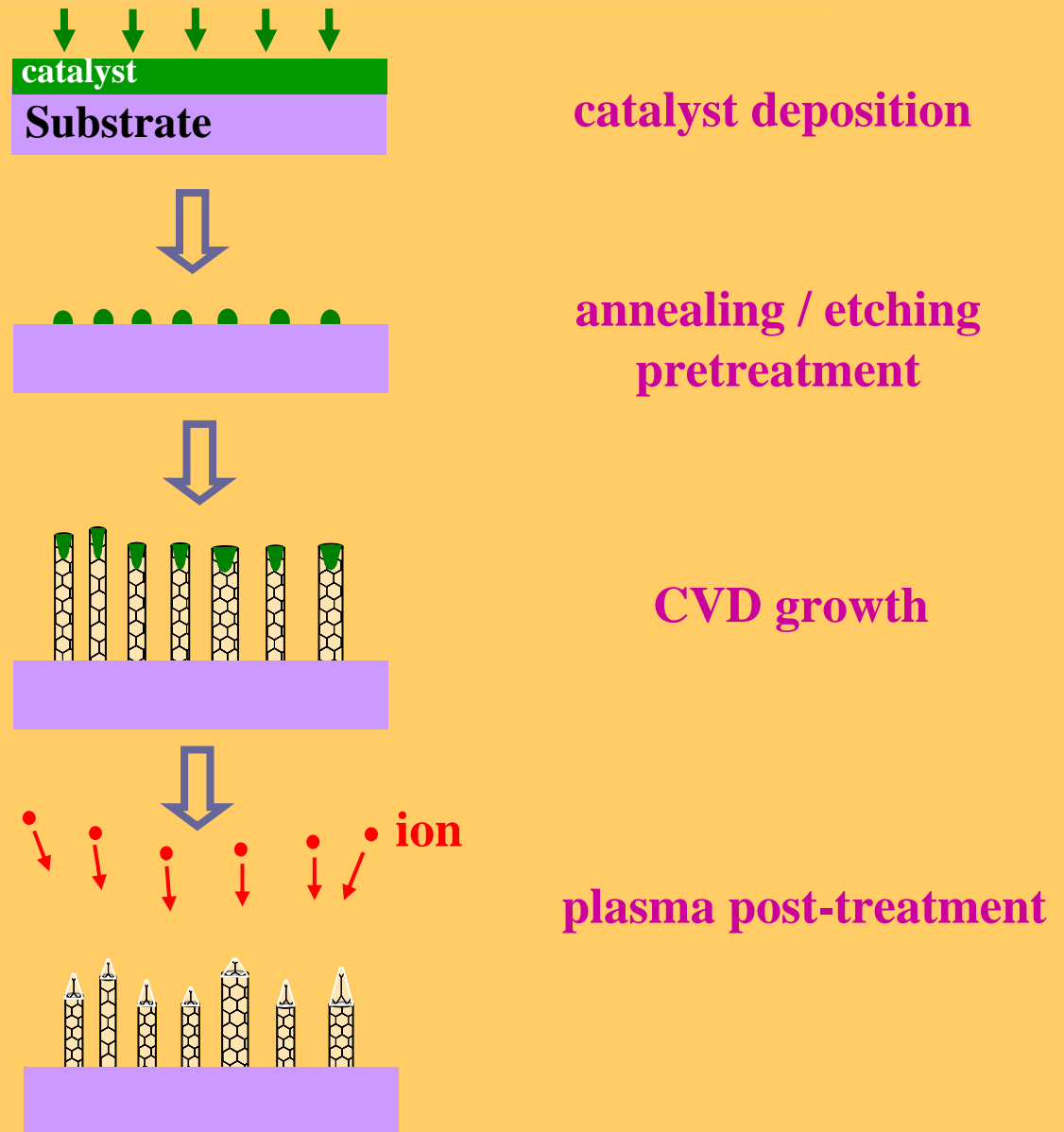


(a/b=10nm/10nm)



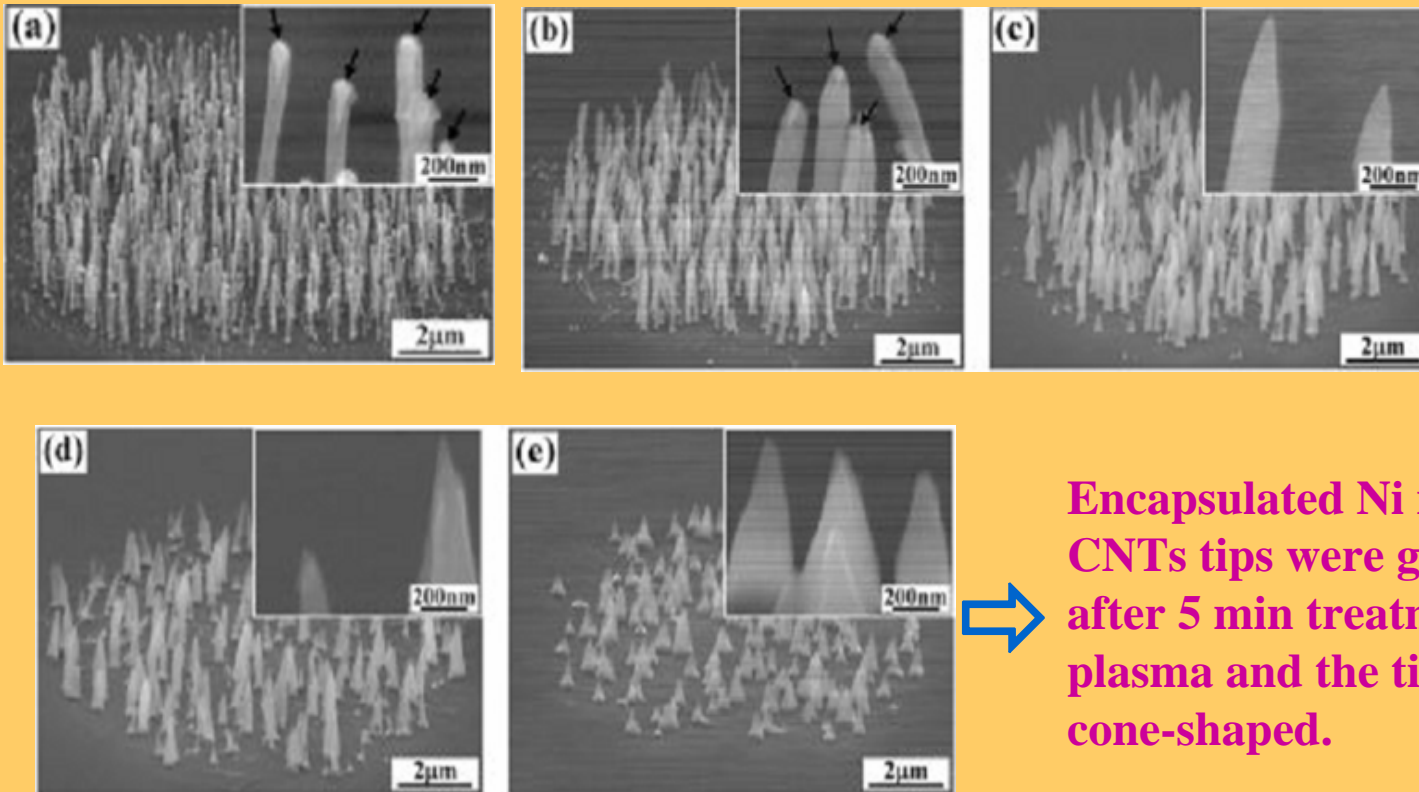
# Process Modification for Field Enhancement

## - Plasma Post-treatment



# Plasma Post-treatment of ICP-CVD grown CNTs

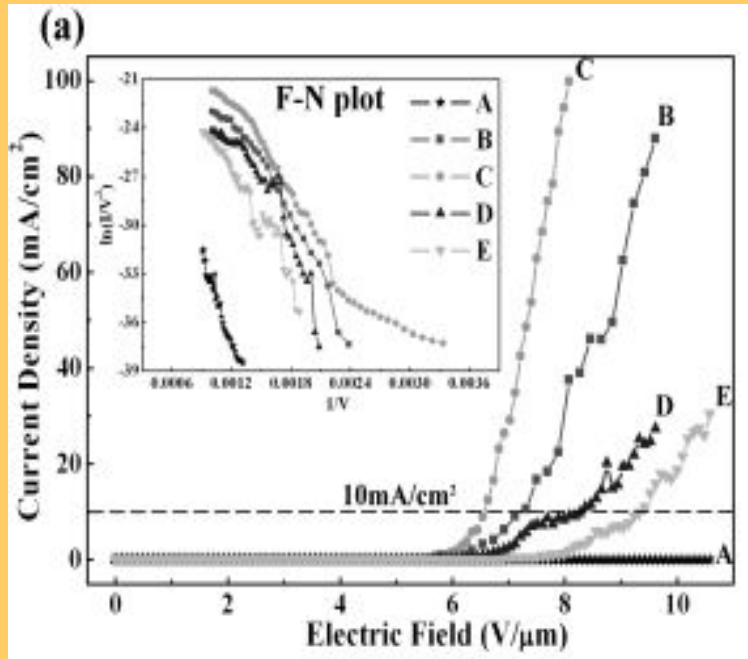
Ar plasma sputtering, ICP power 1000 W  
RF bias power 300 W, pressure 20 mTorr



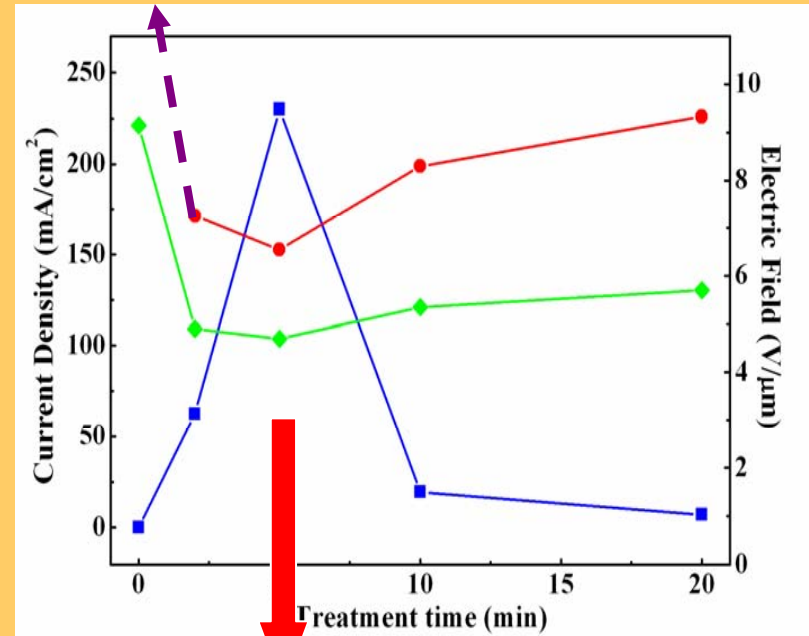
Encapsulated Ni nanoparticles at CNTs tips were gradually removed after 5 min treatment with Ar plasma and the tips became cone-shaped.

C.H. Weng et al. *Appl. Phys. Lett.* 85, 4732 (2004).

# Field Emission Characteristics of CNTs after Plasma Post-treatment



A: as grown      B: 2 min      C: 5 min  
D: 10 min      E: 20 min



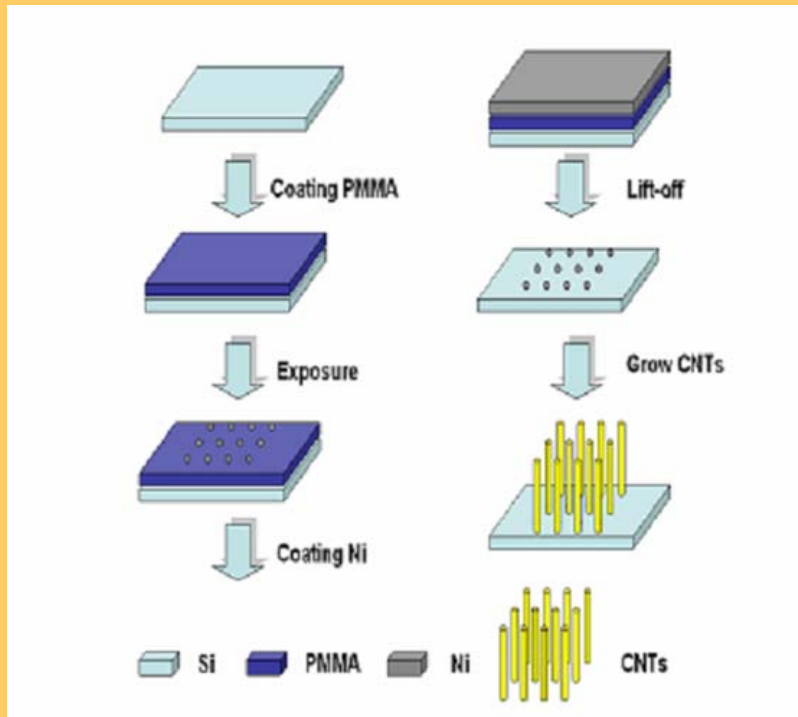
C.H. Weng et al. *Appl. Phys. Lett.* 85, 4732 (2004).

➡ Best field emission property at 5 min post-treatment

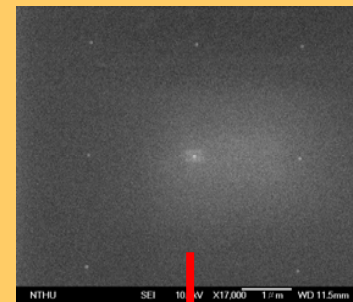


# Controlled Growth of Single Free-standing MWNT

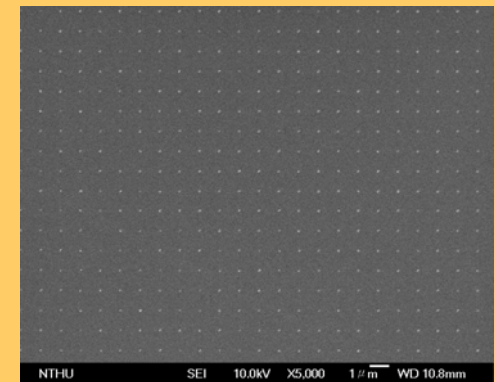
## • Catalyst Definition by E-Beam Lithography



After development



After lift-off



Dot distance 1 $\mu$ m

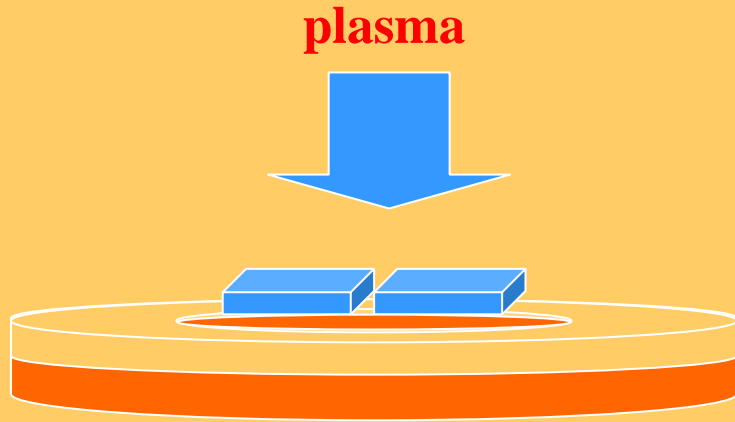
EBL conditions

Acceleration voltage 20KV

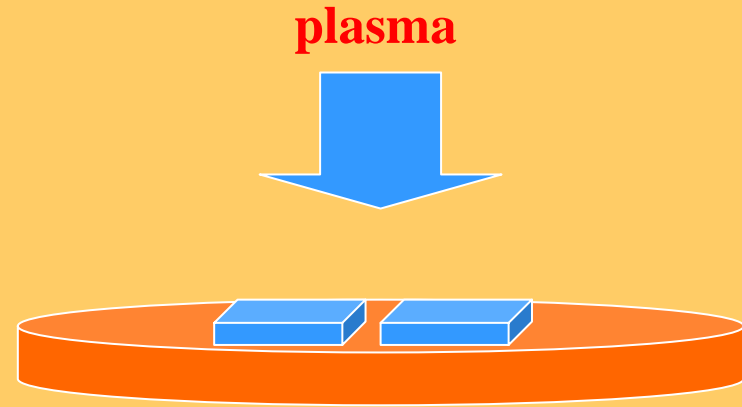
Probe current 6

Exposure time 8 ms

# CNTs growth with different substrates by ICP-CVD



**condition 1: small graphite electrode**



**condition 2: large graphite electrode**



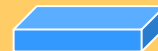
**Graphite electrode substrate**  
(Diameter~21.5 cm)



**Small electrode graphite**  
(Diameter~2.5 cm)



**Quartz**



**specimen**

# condition 1: small graphite electrode

## ICP Conditions

$C_2H_2 / H_2 / Ar = 8 / 24 / 0.5$  sccm

$T_s = 610$  °C

ICP Power = 1000W

RF Bias = 300W

Pressure = 20mTorr

Time = 10min

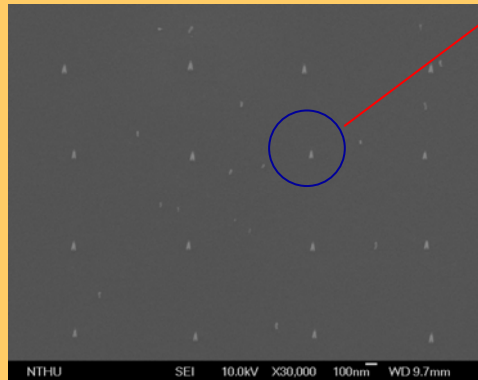
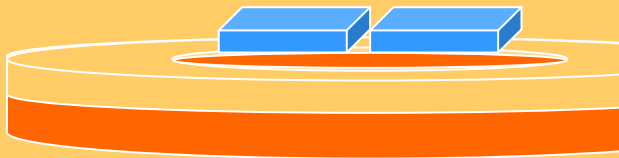
Thickness = 10 nm

## ICP conditions

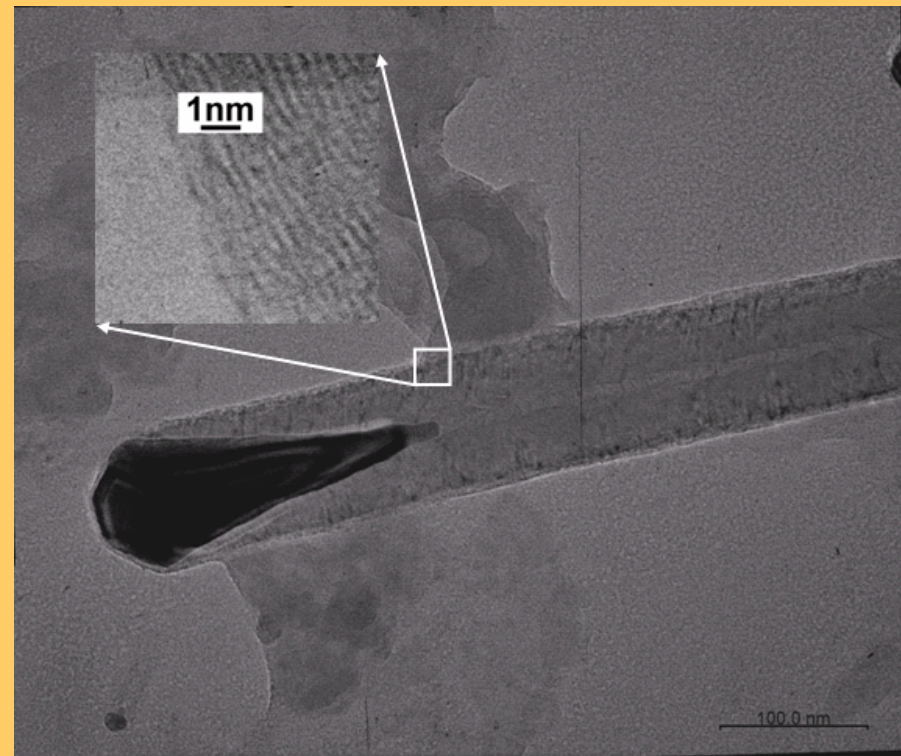
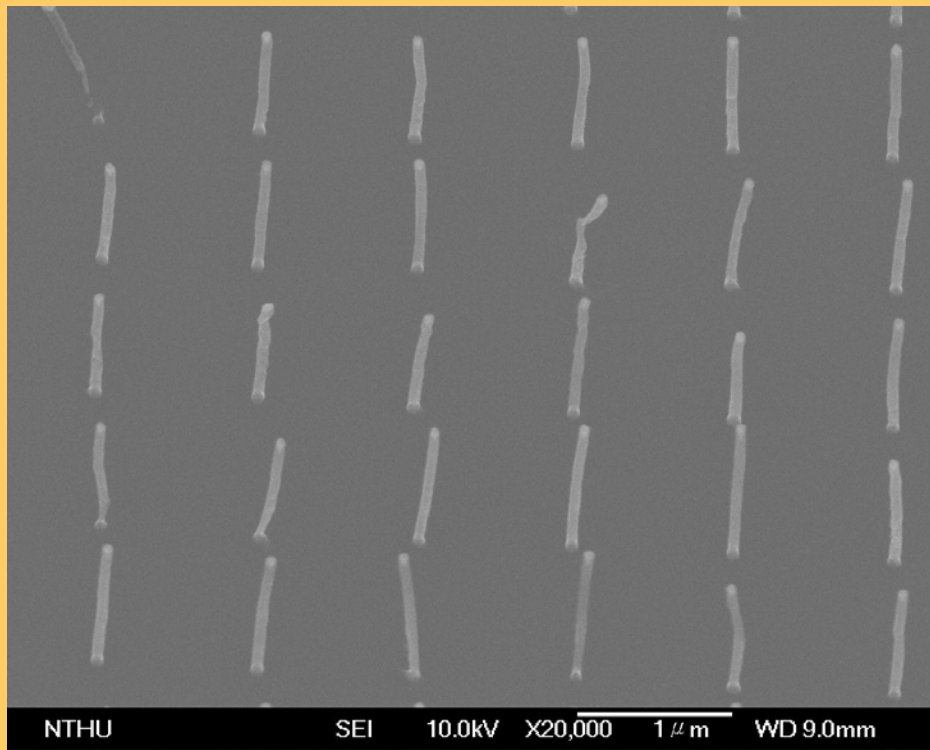
Acceleration voltage 20 KV

Beam current 6

plasma



Dwelltime	Length	diameter
5 ms	80.6 nm	15.6 nm
8 ms	77.7 nm	17.2 nm
9 ms	98.4 nm	18.8 nm
10 ms	100 nm	25.5 nm



Probe current 6

Dwelltime 5ms



Dwelltime 8ms



Dwelltime 6ms



Dwelltime 9ms

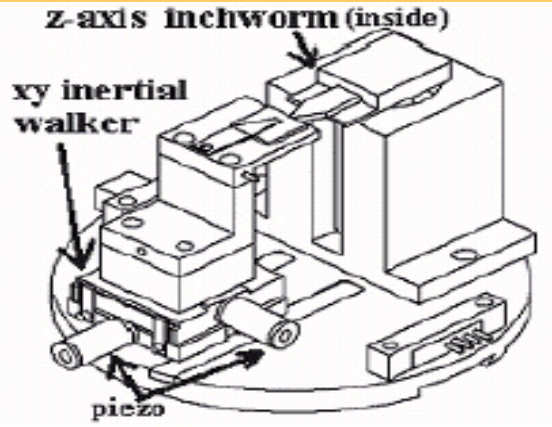


Dwelltime 7ms

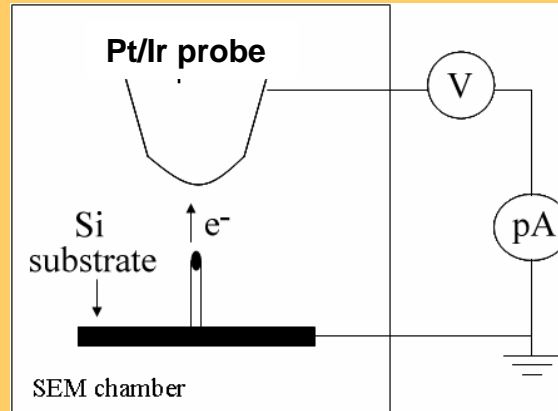
Dwelltime 10ms

Dwelltime	length	diameter
5 ms	453 nm	31.1 nm
6 ms	552 nm	34.4 nm
7 ms	709 nm	33.3 nm
8 ms	788 nm	37.5 nm
9 ms	837 nm	41.7 nm
10 ms	800 nm	44.8 nm

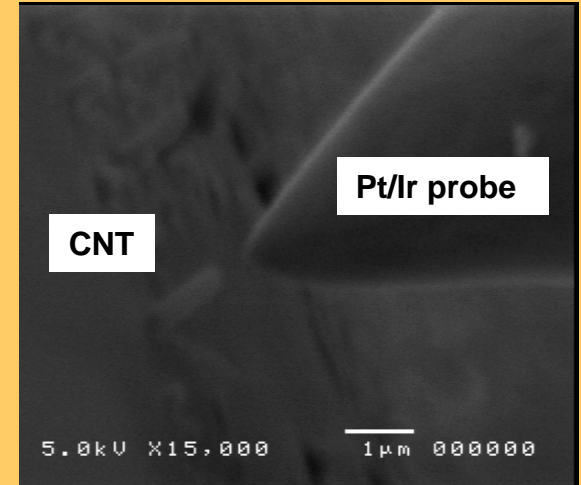
# Field emission characterization of single CNT



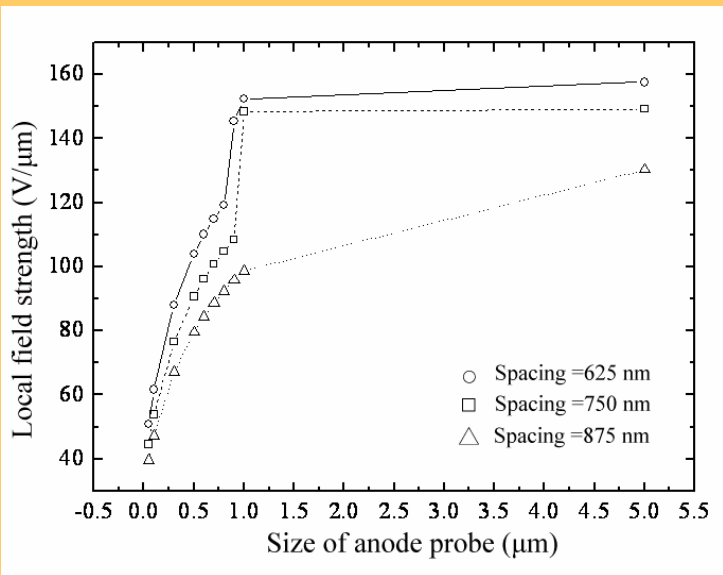
Carbon nano tip assembler  
inertial walker for x- and y-axis.  
inchworm unit for z-axis.



Schematic of a probe-type anode diode structure for field emission measurement (title angle of the specimen is  $\sim 85^\circ$ , and the angle between probe and CNT tip is  $135^\circ$ )



The image of CNT(cathode) and probe (anode)



**Relation between local peak field strength and anode probe size**

Code : SIMION 7.0  
Length of CNT : 800 nm  
Diameter of CNT : 50 nm  
Anode voltage : 12 V

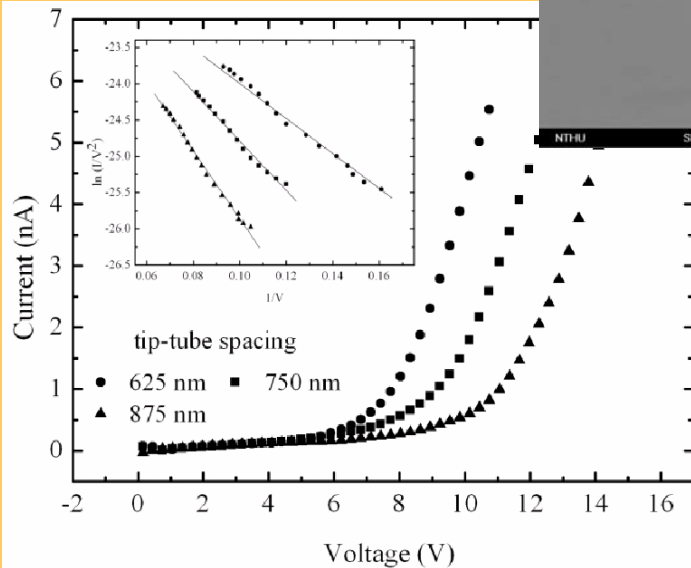


As the diameter of anode probe is higher than  $1 \mu\text{m}$ , the local peak field strength is equal to a planar anode.

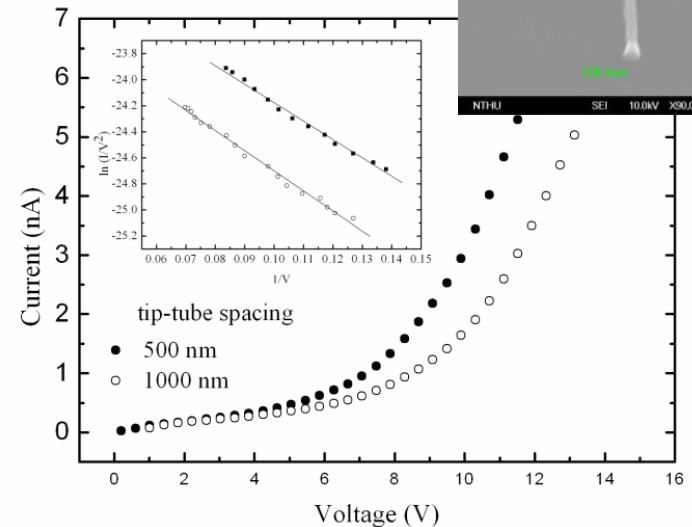
# Field emission characteristics of single CNT

I-V emission characteristic of single VACNT as a function of the spacing between CNT and Pt/Ir probe

## Conical CNT

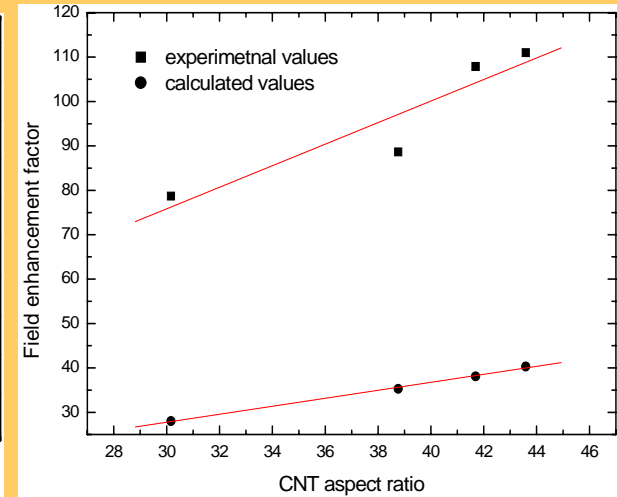
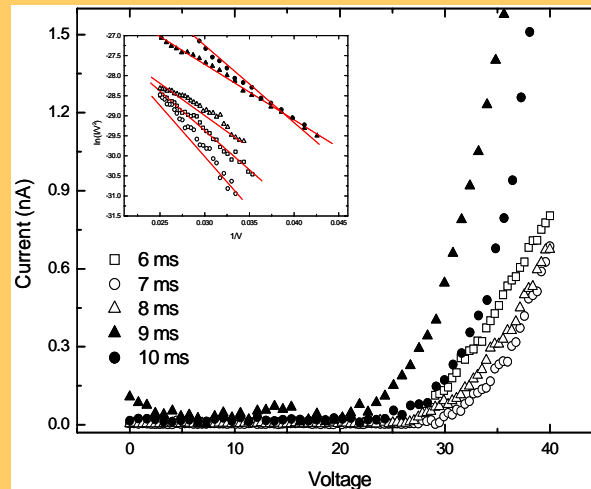
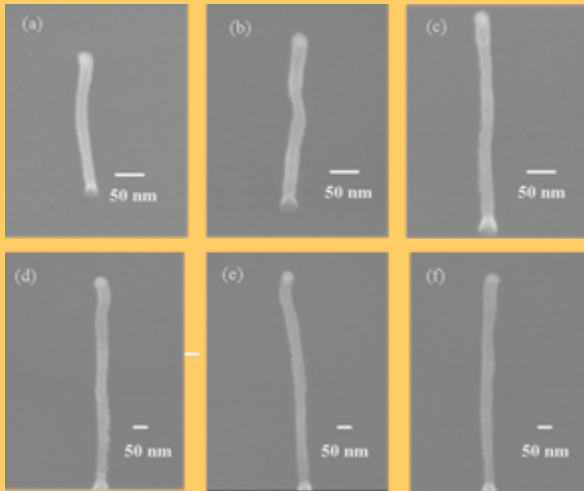


## Tubular CNT



- Results of Field emission measurement on single CNTs revealed Fowler-Nordheim characteristics.
- The field enhancement factor increases with the anode-CNT spacing.

# Field emission characteristics of single CNT



Dwell times (ms)	radius (nm)	CNT length (nm)	aspect ratio	experimental values ( $\beta$ )	calculated* values ( $\beta$ )
6	18.3	552	30.16	78.71	28.04
7	18.35	709	38.76	88.66	35.32
8	18.9	788	41.69	107.89	38.12
9	19.2	837	43.59	110.99	40.34

## \*Theoretical calculation:

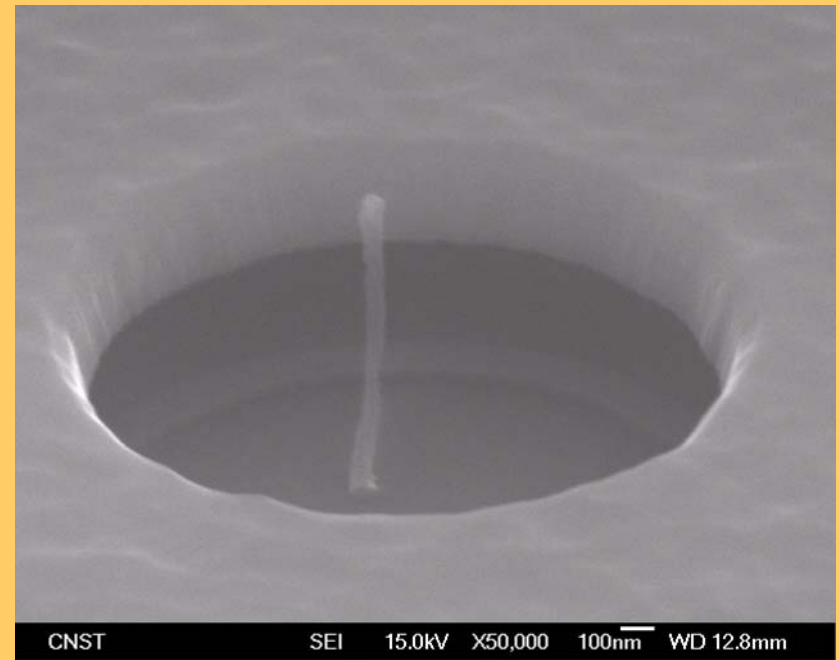
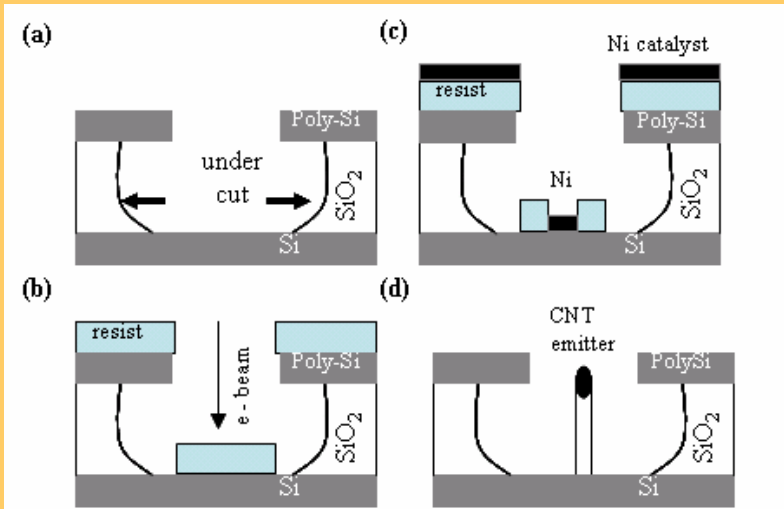
$$\beta = 1.2 \left[ 2.5 + \frac{h}{r} \right]^{0.9} \left[ 1 + 0.013 \left( \frac{d-h}{d} \right) \right]^{-1} - 0.033 \left( \frac{d-h}{d} \right)$$

J. M. Bonard, etc. *Phy.Rev.Lett.* **89**, 197602 (2002).



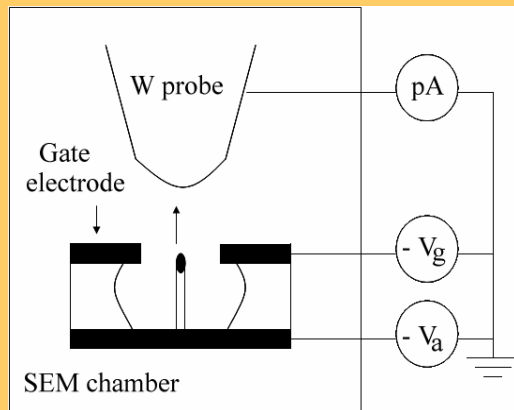
- The field enhancement factors of CNTs increased with the tube aspect ratio.
- However, the experimental values were 2~3 times higher than the theoretical calculations based on literature, which needs further investigation.

# Triode structure device with single CNT

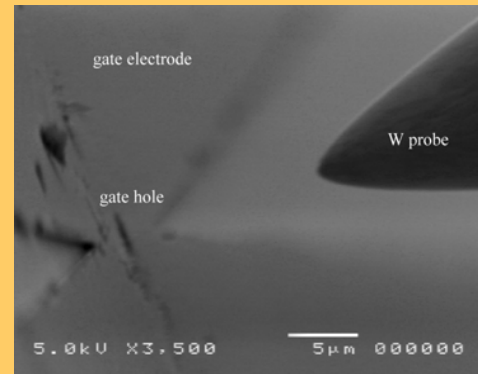


Gated CNT structure with a 800 nm height and 54 nm diameter nanotube (gate hole size = 1.5  $\mu\text{m}$ )

Process for fabricating CNT microcathode gated structure: (a) Deposition of SiO<sub>2</sub> insulator and poly-Si electrode, followed by optical lithography and etching, (b) Resist (PMMA) coating and E-beam lithography, (c) Sputter deposition of Ni catalyst, and (d) Lift off and CNT growth by ICP-CVD.



Schematics of the field emission measurement system used to examine a single gated device.

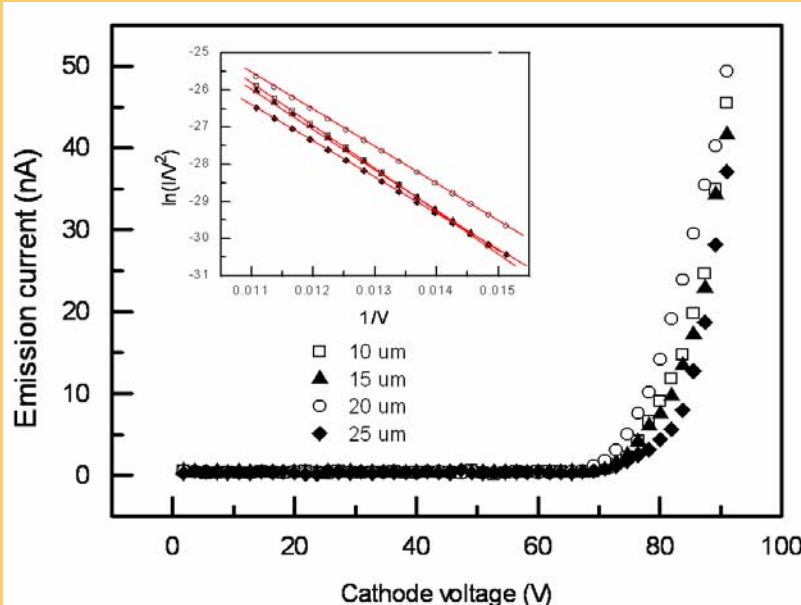


SEM images of spacing between CNT and gate electrode. The spacing is about 10  $\mu\text{m}$ .

S.C. Tseng et al. *Diamond and Related Materials*, 14 (2005) 2064.

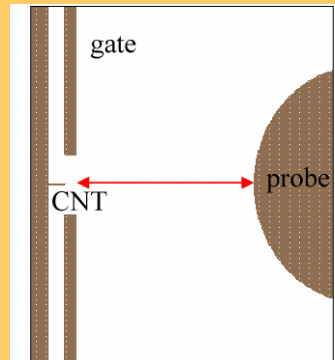


# The relation between the gate electrode-to-probe spacing and field emission characteristics



I-V emission characteristics with different spacing between anode-to-gate.

The gate size is  $1.5 \mu\text{m}$ ; height of CNT is 530 nm. The inset shows the data plotted in Fowler-Nordheim form.



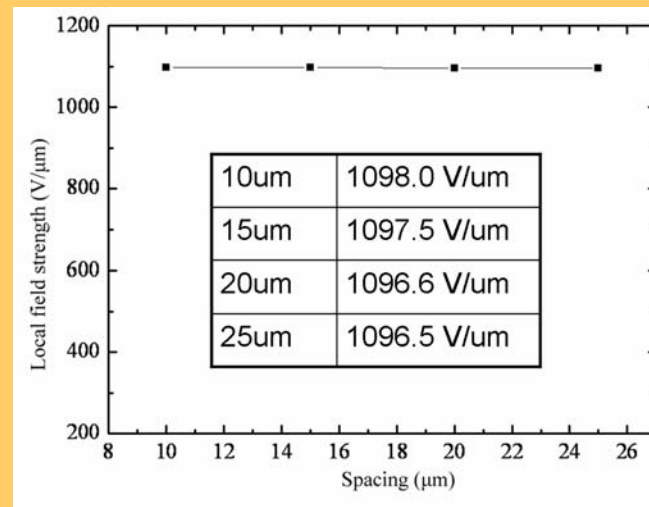
To simulate the relation between spacing (gate electrode-to-probe) and local field strength at the apex of CNT.

Simulation conditions:

Aperture size :  $1.5 \mu\text{m}$  ; The height of the CNT :  $\sim 530 \text{ nm}$

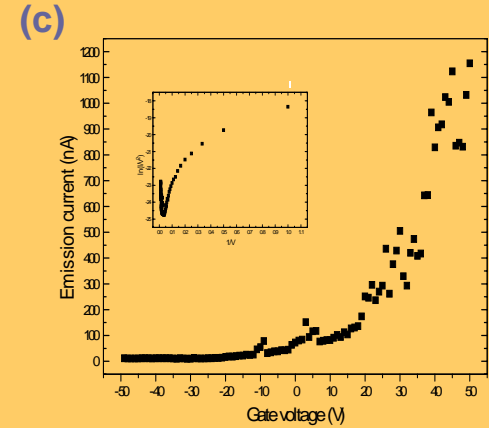
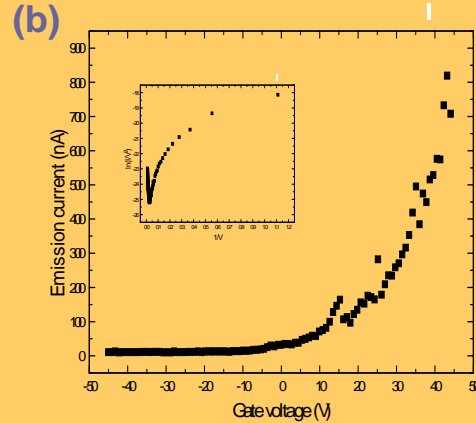
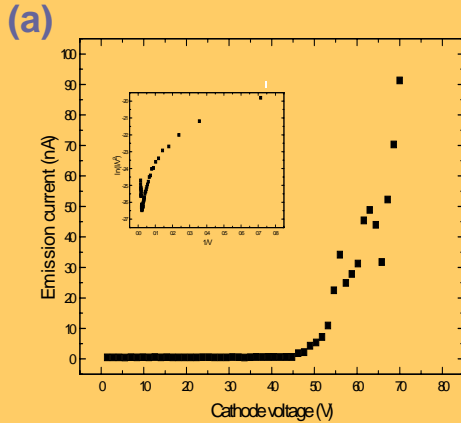
The voltage of the gate :  $-10 \text{ V}$  ;

The voltage of the probe :  $0 \text{ V}$

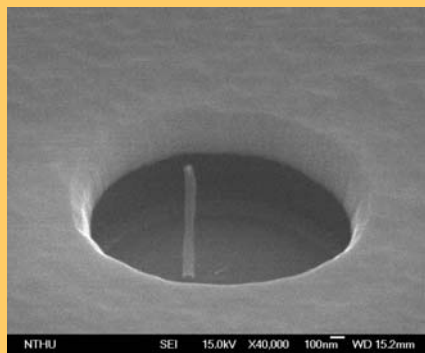
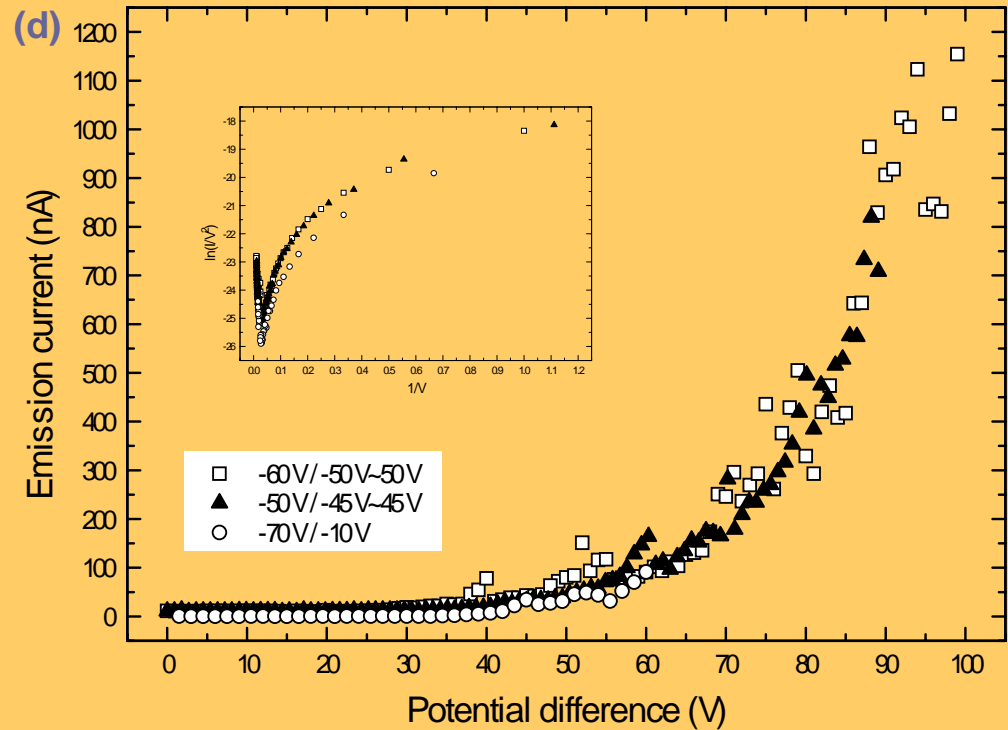


The relation between spacing (gate electrode-to-probe) and local field strength at the apex of CNT (Simulation by Simion 7.0)

# Field emission characteristics with different control scheme



(a) constant gate voltage (-10 V) and scanning cathode voltage (0~ -70 V).  
(b) scanning gate voltage (-45 V~45 V) and constant cathode voltage (-50 V).  
(c) scanning gate voltage (-50 V~50 V) and constant cathode voltage (-60 V).  
(d) combine (a)~(c) into one figure.

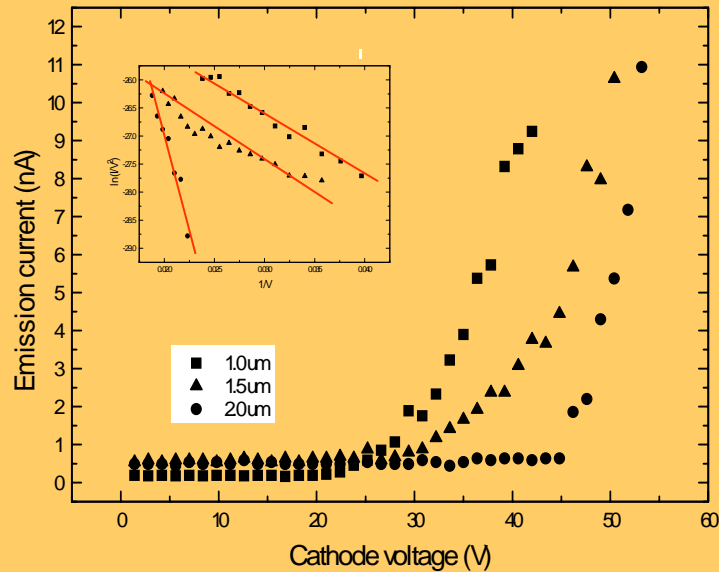
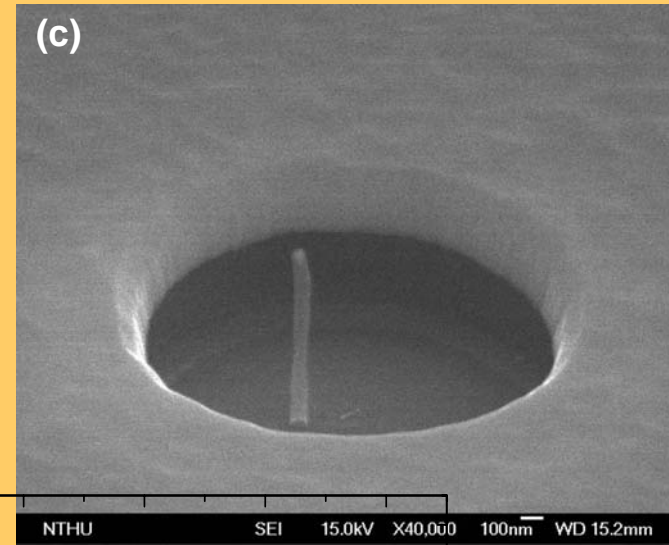
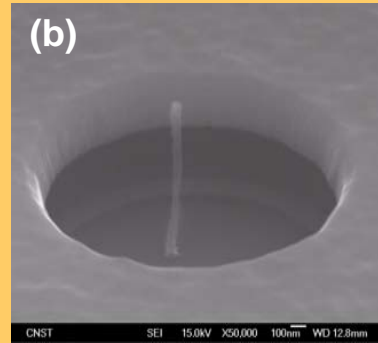
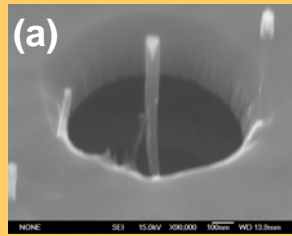


Aperture size : 2.0  $\mu\text{m}$   
The height of the CNT : ~800 nm

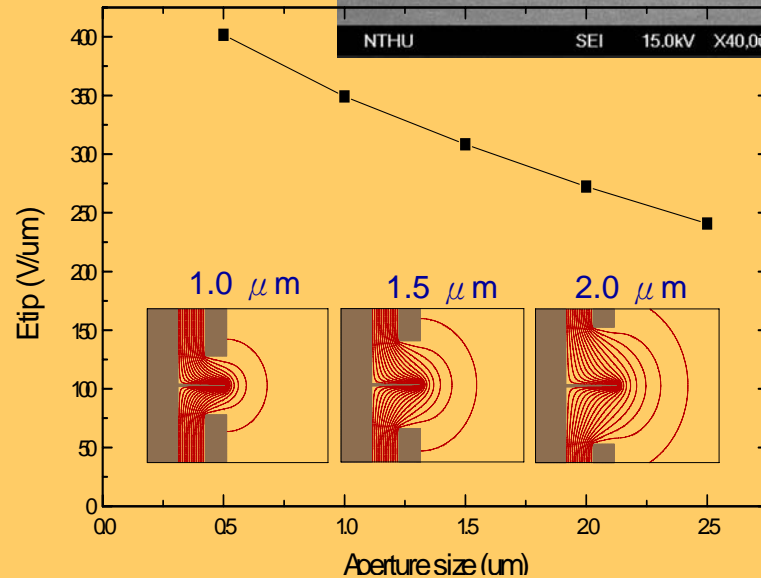
# Field emission characteristics with various gate hole size

CNT gated structure with different hole size of gate  
(a)  $1.0\ \mu\text{m}$  (b)  $1.5\ \mu\text{m}$  (c)  $2.0\ \mu\text{m}$ .

The height of single vertically aligned CNT is about 800 nm.



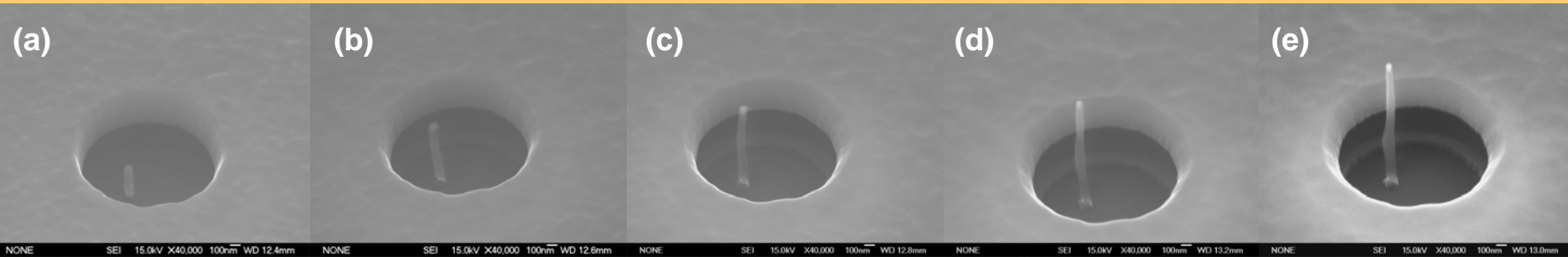
I-V emission characteristics with different gate hole size. The inset shows the data plotted in Fowler-Nordheim form.



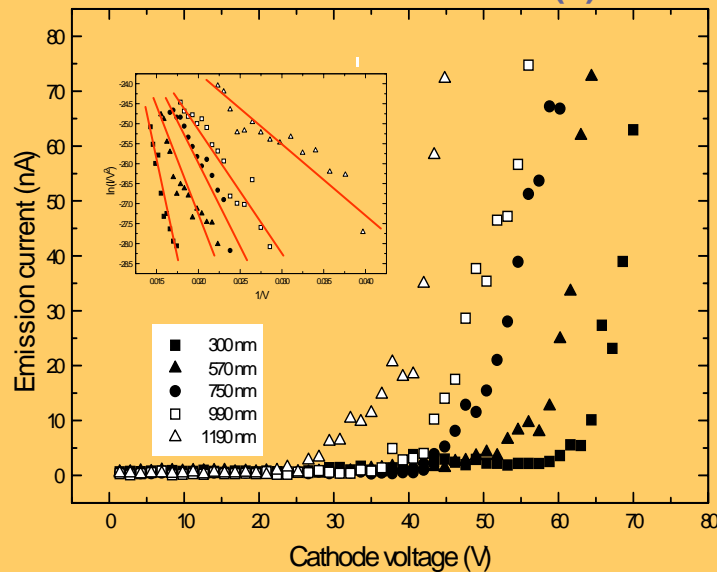
Calculated tip peak field strength (field enhancement) with various gate hole size.

(Simulation by Simion 7.0)

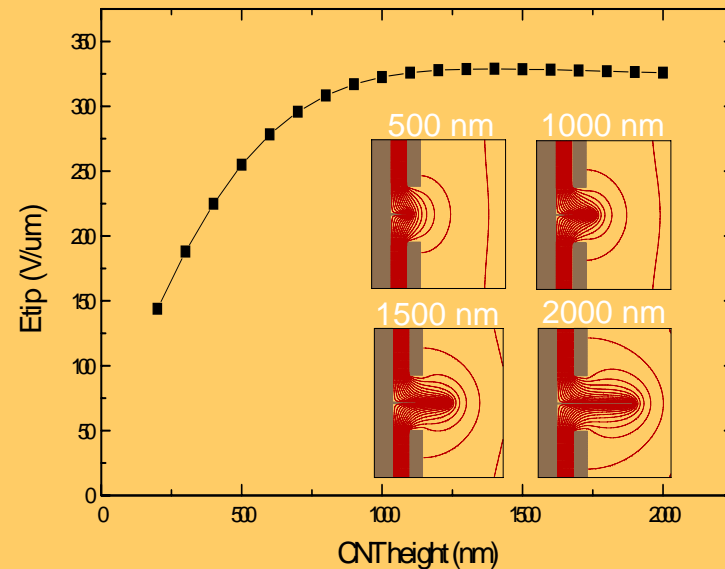
# Field emission characteristics with various CNT height



CNT Gated structure with different height of CNT (a) 300 nm (b) 570 nm (c) 750nm (d) 990 nm (e) 1190 nm. The gate hole size is 1.5  $\mu$  m.



I-V emission characteristics from gate electrode device (gate hole size 1.5  $\mu$  m) with different height of single vertically aligned CNT. The inset shows the data plotted in Fowler-Nordheim form.



Calculated tip peak field strength (field enhancement) with various CNT height.

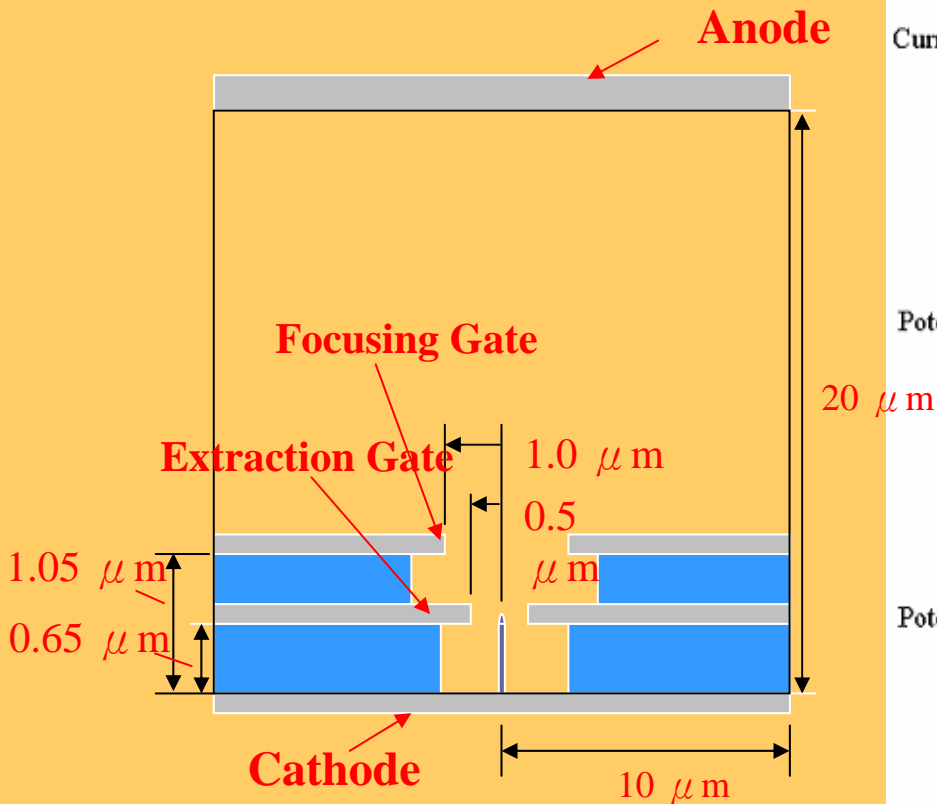
(Simulation by Simion 7.0)

# Double-gated Triode Field Emitter Design & Simulation

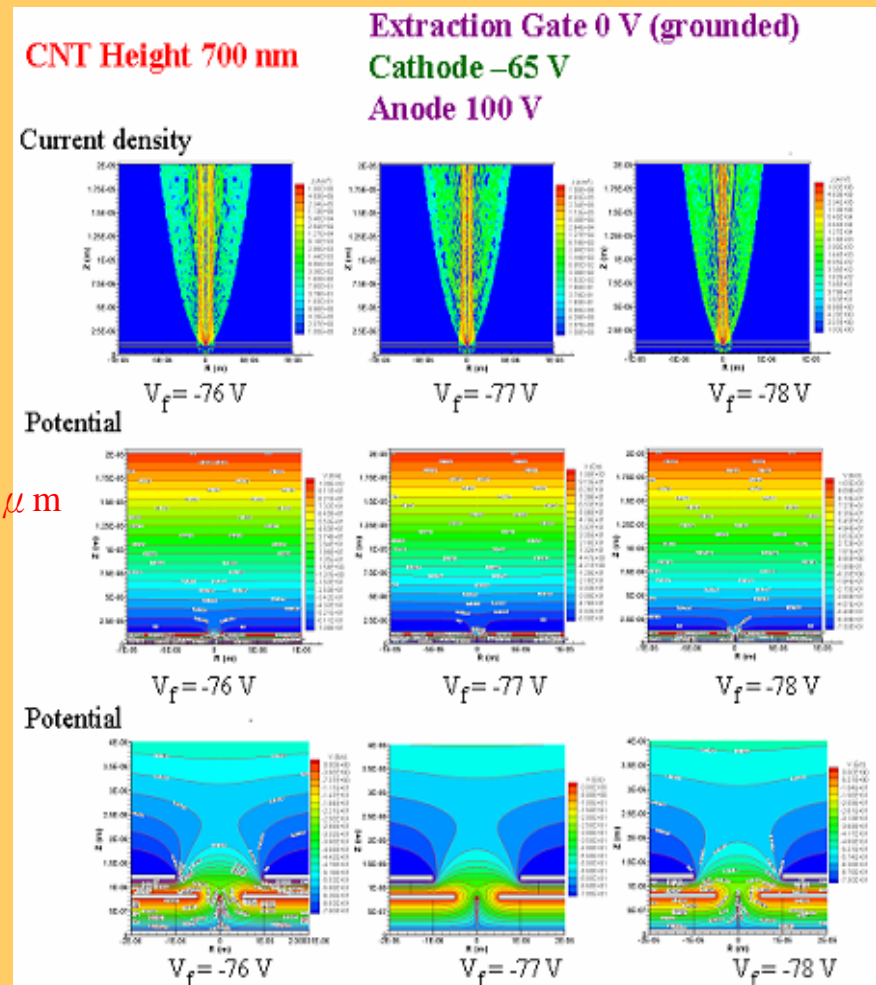
Extraction gate hole radius:  $0.5 \mu\text{m}$

Focusing gate hole radius:  $1.0 \mu\text{m}$

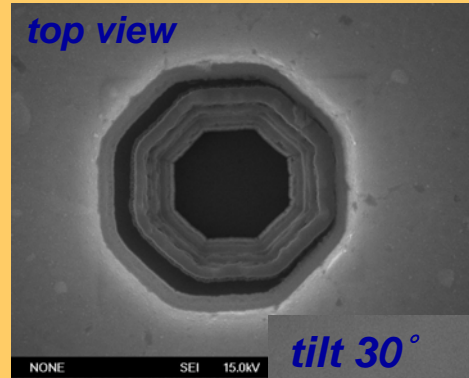
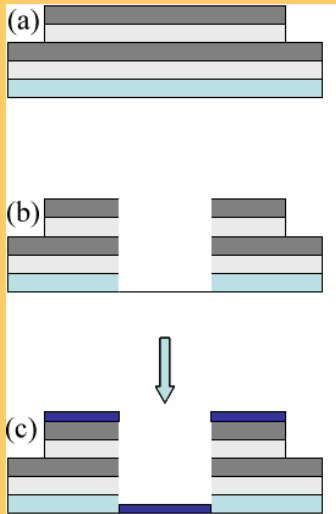
Half-ellipsoid tip MWCNT, minor radius  $10 \text{ nm}$ , major radius  $40 \text{ nm}$



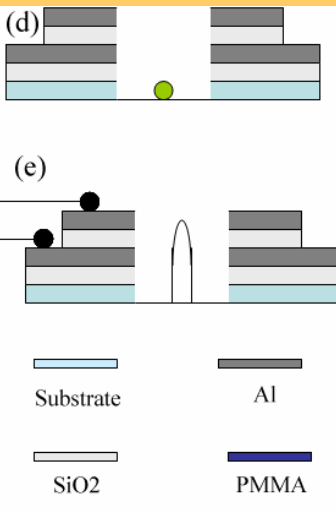
Y. Hu et al. (2004)



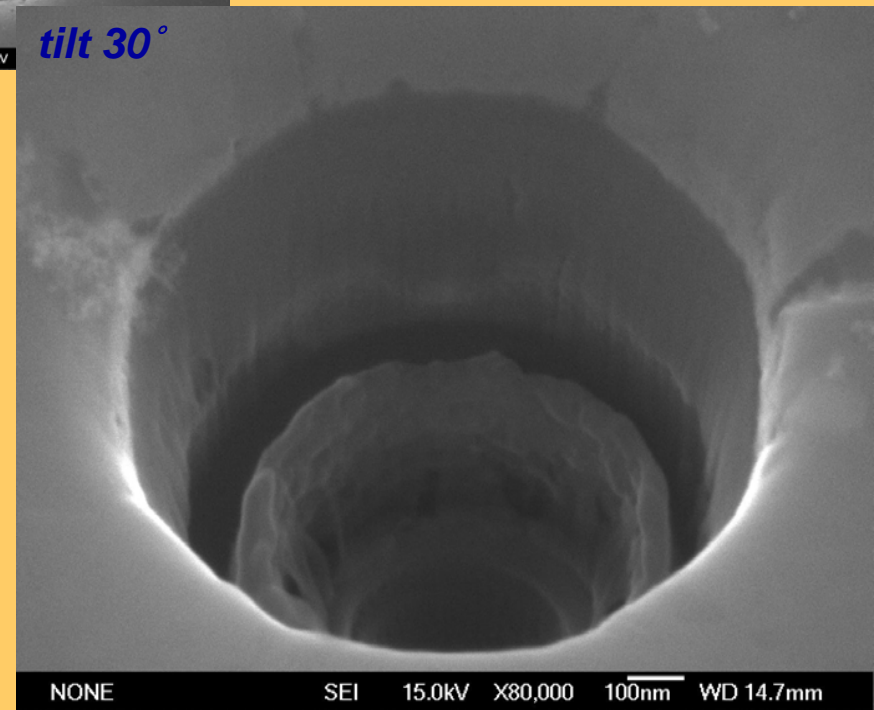
# Double gated electrode device



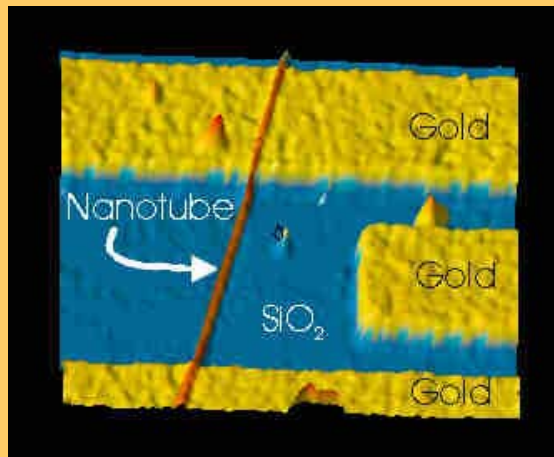
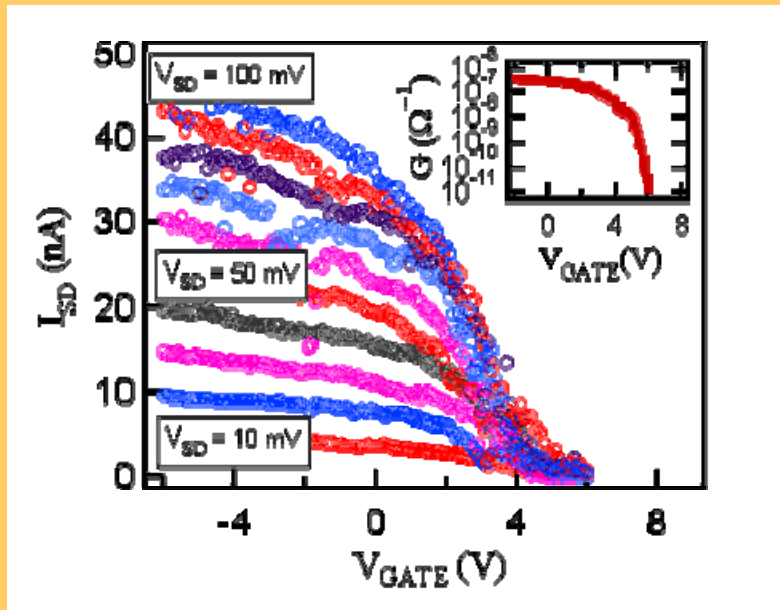
SEM images of double gate electrode device before CNT growth. The aperture size is 1.0 μm.



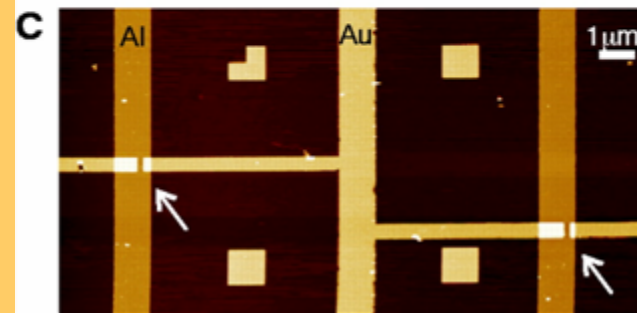
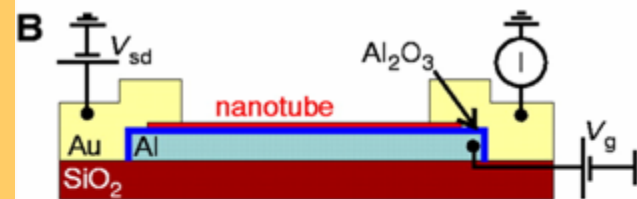
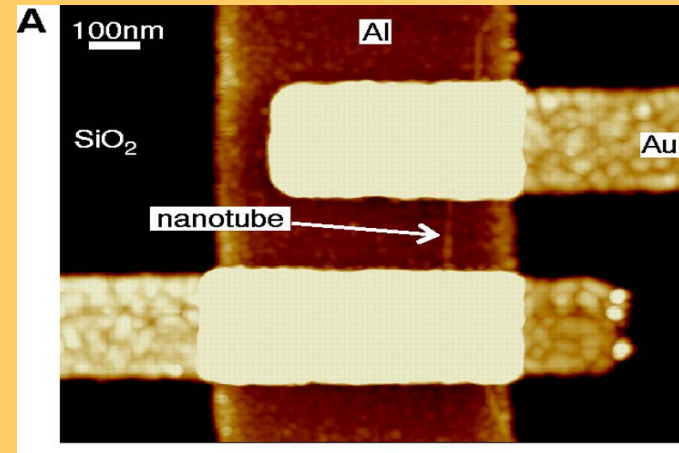
Process for fabricating double gate CNT electrode device : (a) deposition of SiO<sub>2</sub> insulator and Al electrode, (b) gate hole fabricated by optical lithography and etching, (c) Resist (PMMA) coating and E-beam lithography, (d) deposition of Ni catalyst followed by lift off, (e) CNT growth by ICP-CVD.



# SWNT-based Field Effect Transistor



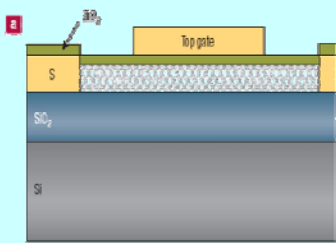
R. Martel, T. Schmidt, H. R. Shea, T. Hertel and Ph. Avouris, *Appl. Phys. Lett.* 73 (1998)



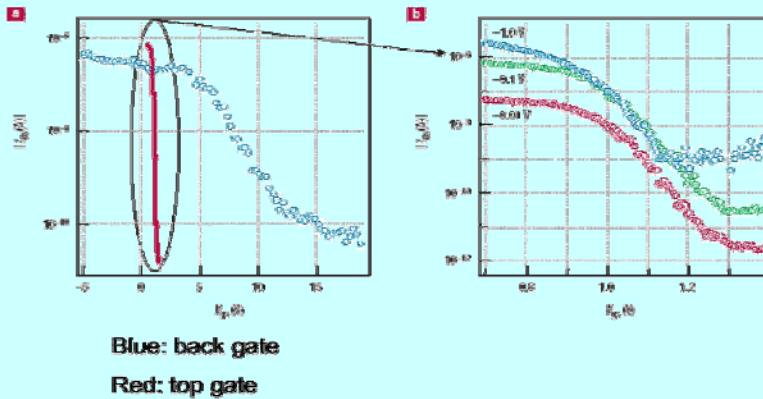
Adrian Bachtold et al, *Science* 294, 2001

# SWNT-based FET and Inverter

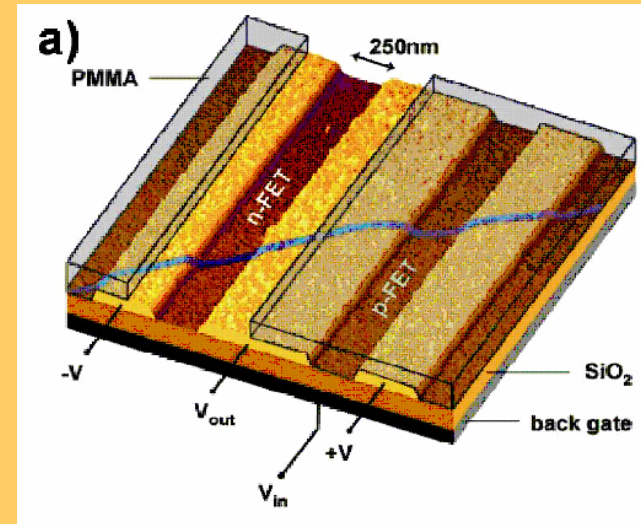
## High-performance p-type CNT-based FET



SiO<sub>2</sub>: 500 nm  
ZrO<sub>2</sub> ~8 nm by ALD

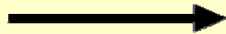


- Subthreshold swing: 70 mV/dec  $\longleftrightarrow$  limit ( $k_B T/e \ln 10$ ) ~ 60 mV/dec at RT
- Transconductance: 6000 S m<sup>-1</sup>
- Hole mobility: 3000 cm<sup>2</sup> V<sup>-1</sup> S<sup>-1</sup>  $\longleftrightarrow$  Hole mobility in Si: 505 cm<sup>2</sup> V<sup>-1</sup> S<sup>-1</sup>

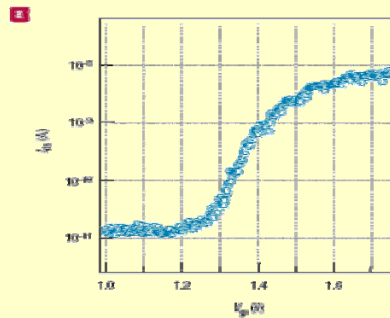


## Conversion of p-type to n-type

When heating in H<sub>2</sub>  
at 400 °C

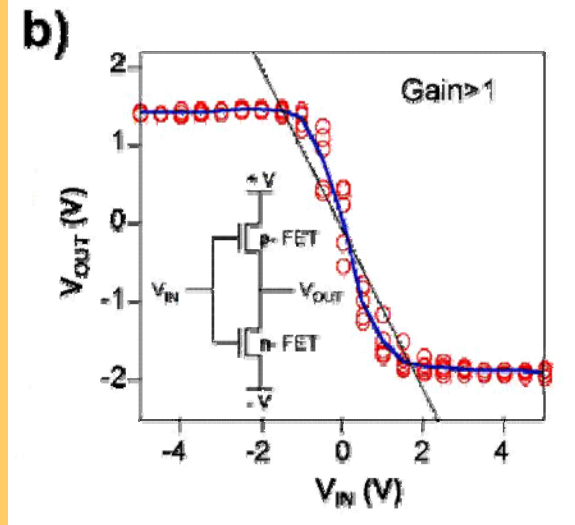


Possible mechanism:  
vary metal work function  
at the contacts of CNT/metal



Electron mobility in Si: 1450 cm<sup>2</sup> V<sup>-1</sup> S<sup>-1</sup>  $\longleftrightarrow$  Electron mobility: 1000 cm<sup>2</sup> V<sup>-1</sup> S<sup>-1</sup>

Subthreshold swing: 90-100 mV/dec  
Transconductance: 600 S m<sup>-1</sup>





# Challenges for Commercial Applications

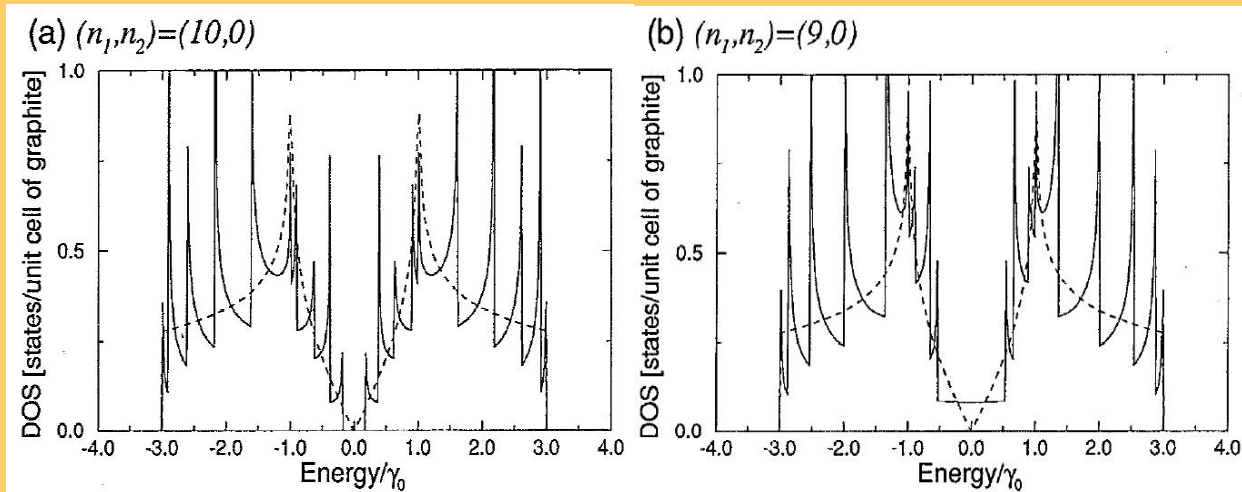
- **Performance Challenges:**

- (1) Ambipolar behavior or p-n (n-p) transition due to environment
- (2) Strong dependence on the drain voltage
- (3) Electron mobility in long channel
- (4) Subthreshold slope to thermal limit  
~ 60 mV/dec at RT ( $kT/e \ln 10$ )

- SWNT diameter  $d_1$  (bandgap  $\sim 1/d_1$ )
- Contact metal (Ti, Pd, Al, etc.)
- Gate dielectric thickness &  $\kappa$

- **Process Challenges:**

- (1) **Positioning** of the SWNTs on the designated locations / direction by *in-situ* catalytic CVD
- (2) **Controllability** of desired chirality or **semiconducting** properties of SWNTs
- (3) **Low temperature synthesis** techniques for high purity SWNTs
- (4) **Low resistance** for SWNTs/metal contacts and controllability on SWNTs/metal Schottky barrier height



R. Saito et al.  
*APL* 60 (1992)

# In-situ Growth of SWNTs by Catalytic CVD

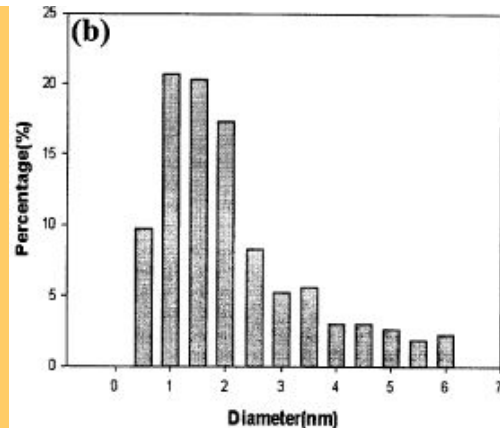
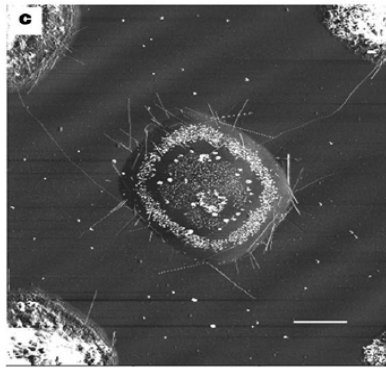
## Discrete particles by support materials

\* Supported catalyst prepared by impregnation method of metal nitrate followed by baking and mechanical grinding.

\* CVD: methane, 1000°C., min.

Summary of results of methane CVD experiments using supported metal-oxide catalysts

Catalyst composition	Support material	SWNTs?	Description of synthesized material
Fe <sub>2</sub> O <sub>3</sub>	alumina	yes	abundant individual SWNTs; some bundles; occasional double-walled tubes
Fe <sub>2</sub> O <sub>3</sub>	silica	yes	abundant SWNT bundles
CoO	alumina	yes	some SWNT bundles and individual SWNTs
CoO	silica	no	no tubular materials synthesized
NiO	alumina	no	mainly defective multi-walled structures with partial metal filling
NiO	silica	no	no tubular materials synthesized
NiO/CoO	alumina	no	no tubular materials synthesized
NiO/CoO	silica	yes	some SWNT bundles

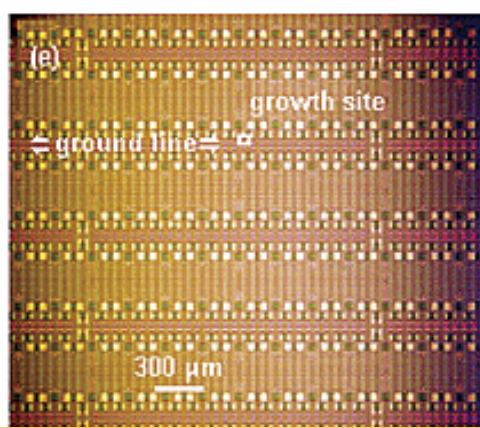


➤ Large diameter dispersion from 0.7 to 6 nm was observed.

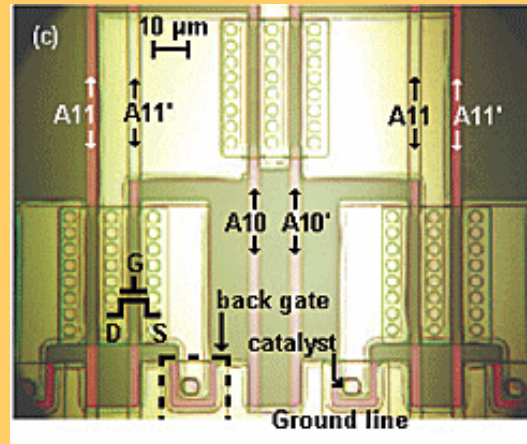
Hongjie Dai et al., *Nature* **395**, 878 - 881 (1998)

Jing Kong, Alan M. Cassell, Hongjie Dai, *Chem. Phys. Lett.* **292**, 567 (1998)

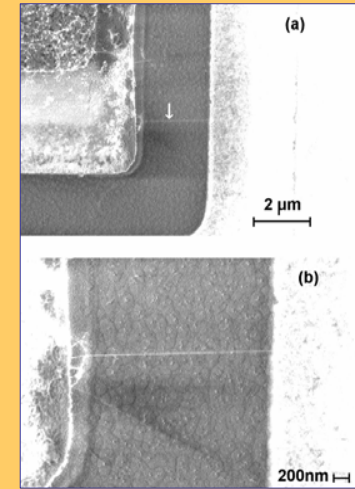
# Carbon Nanotube MOSFETs in The Circuit



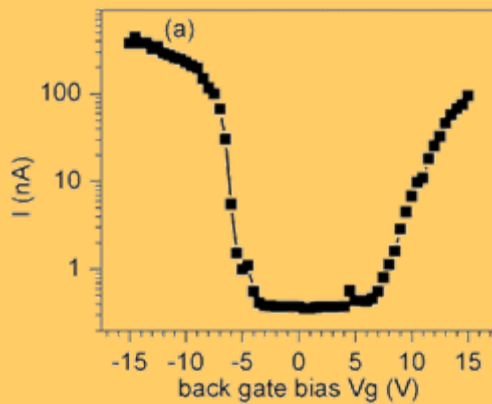
Expanded view of the circuit



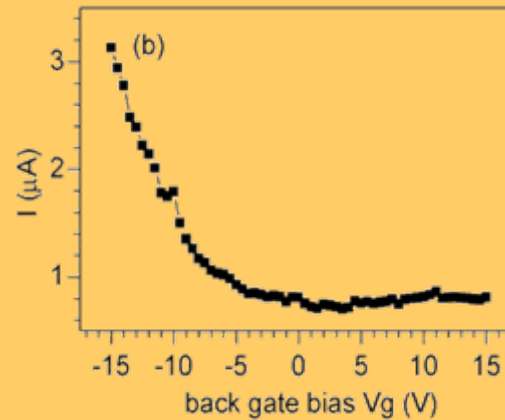
Optical micrograph of part of the circuit



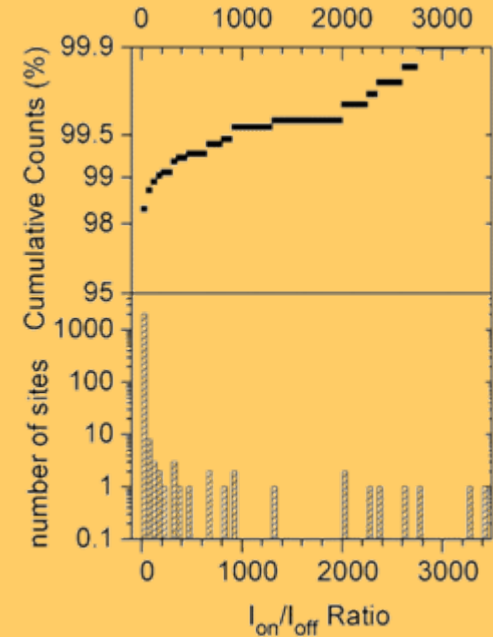
SEM image of a CNT bridging the gap



Ambipolar  $I$ - $V_g$  characteristic, at growth site 125.



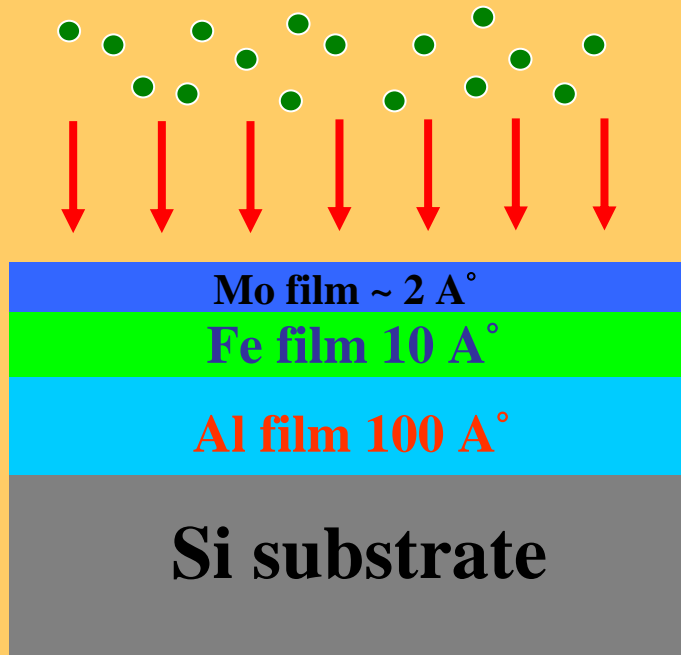
CNT device exhibiting weak dependence on back gate bias (site 7).



Statistics of electrical measurements on 2048 growth sites.

Yu-Chih Tseng, Hongjie Dai, et al., *Nano Letters* 4 (2004)

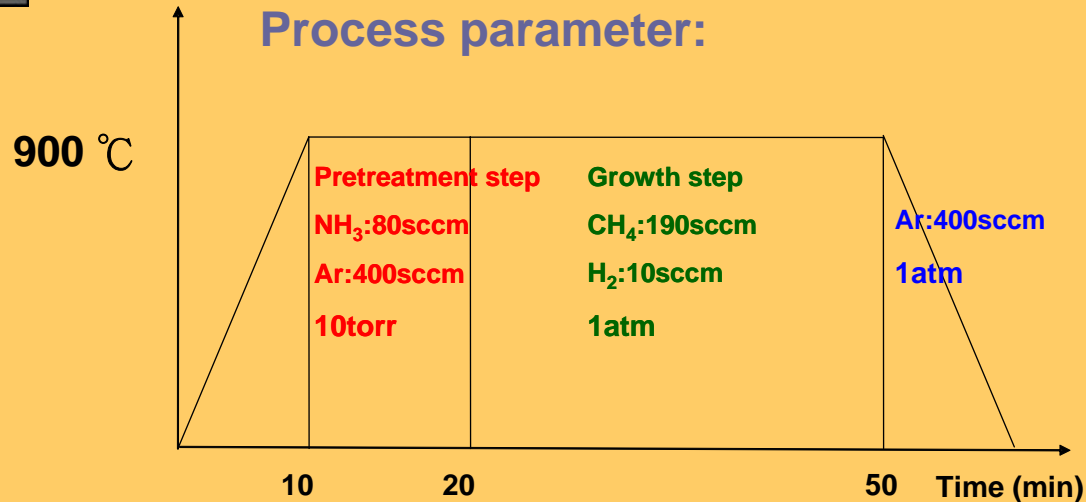
# SWNTs Growth by Multilayered Metal Catalysts



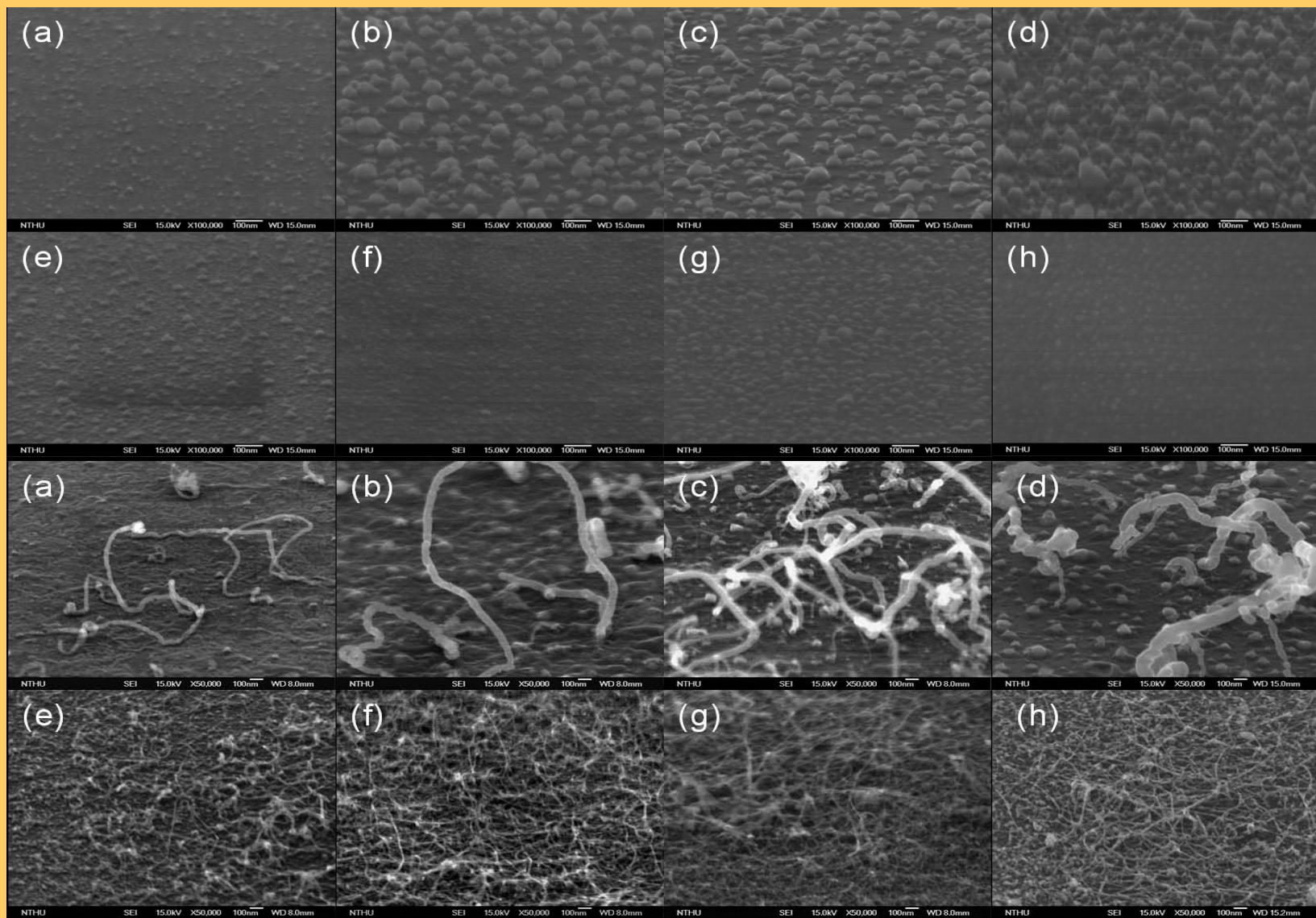
Eight samples:

- (a) Fe1/Si
- (b) Fe1/SiO<sub>2</sub>
- (c) Mo0.2/Fe1/Si
- (d) Mo0.2/Fe1/SiO<sub>2</sub>
- (e) Fe1/Al10/Si
- (f) Fe1/Al10/SiO<sub>2</sub>
- (g) Mo0.2/Fe1/Al10/Si
- (h) Mo0.2/Fe1/Al10/SiO<sub>2</sub>

➤ Thermal CVD



# SWNTs Growth by Multilayered Metal Catalysts

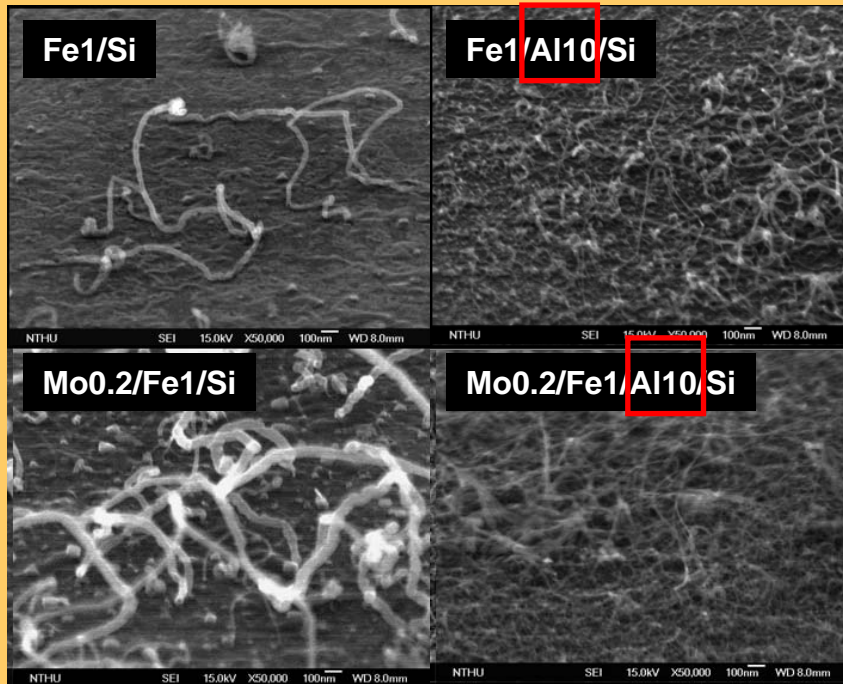


SEM  
100K

SEM  
50K

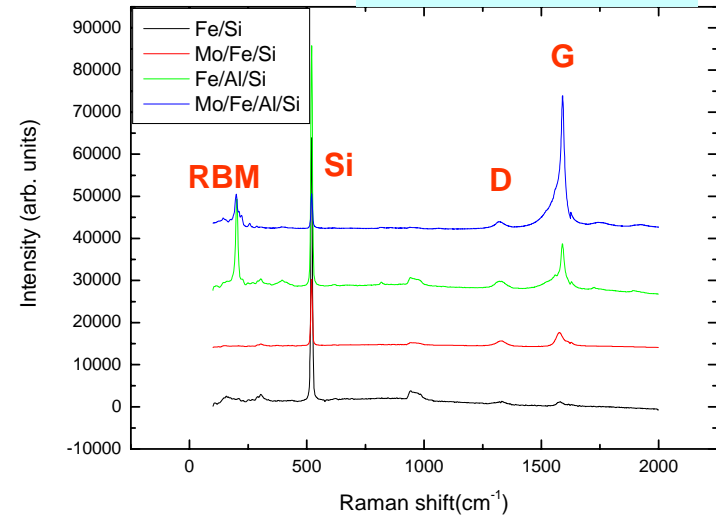
(a)Fe1/Si、(b)Fe1/SiO<sub>2</sub>、(c)Mo0.2/Fe1/Si、(d)Mo0.2/Fe1/SiO<sub>2</sub>、(e)Fe1/Al10/Si、(f)Fe1/Al10/SiO<sub>2</sub>、  
(g)Mo0.2/Fe1/Al10/Si、(h)Mo0.2/Fe1/Al10/SiO<sub>2</sub>

# SWNTs growth by multilayered metal catalysts



## Micro-Raman

\*Laser 632.8 nm

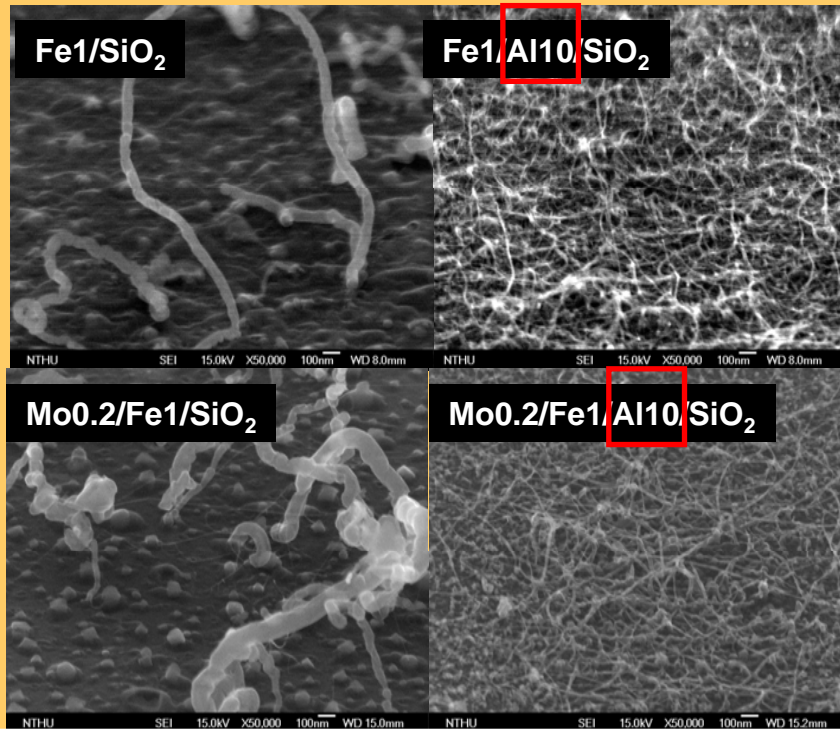


➤  $D \text{ (nm)} = 248 / \Omega \text{ (cm}^{-1}\text{)}$

## Summary of the process parameters

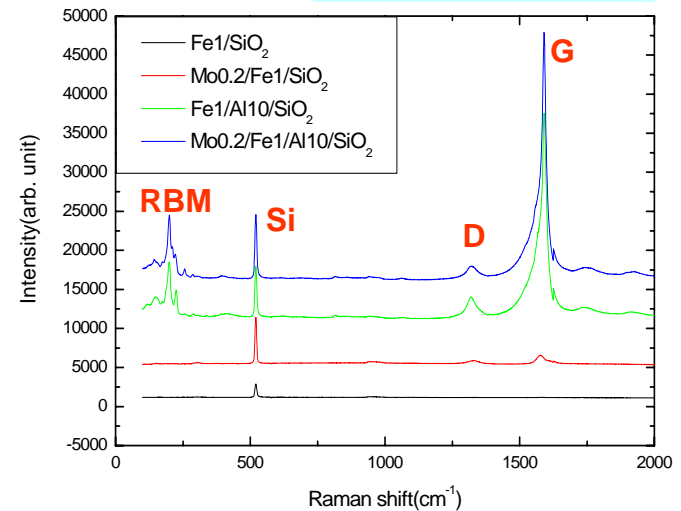
Sample	Method	Standard Process	Shorter Growth time 5min	Longer Growth time 30min	Lower pressure 100 torr	Lower temperature 800°C	Dilution of hydrocarbon	SWNTs diameter range
Fe1/Si		Rare MWNTs	MWNTs	MWNTs	N/A	None	N/A	None
Mo0.2/Fe1/Si		Rare SWNTs & MWNTs	Mix. SWNTs & MWNTs	Mix. SWNTs & MWNTs	N/A	None	N/A	None
Fe1/Al10/Si		Abundant SWNTs	Rare SWNTs	Abundant SWNTs	Rare SWNTs	None	None	1.265~1.252
Mo0.2/Fe1/Al10/Si		Abundant SWNTs	Abundant SWNTs	Abundant SWNTs	Rare SWNTs	Rare SWNTs	Rare SWNTs	1.258~1.246

# SWNTs growth by multilayered metal catalysts



## Micro-Raman

\*Laser 632.8 nm



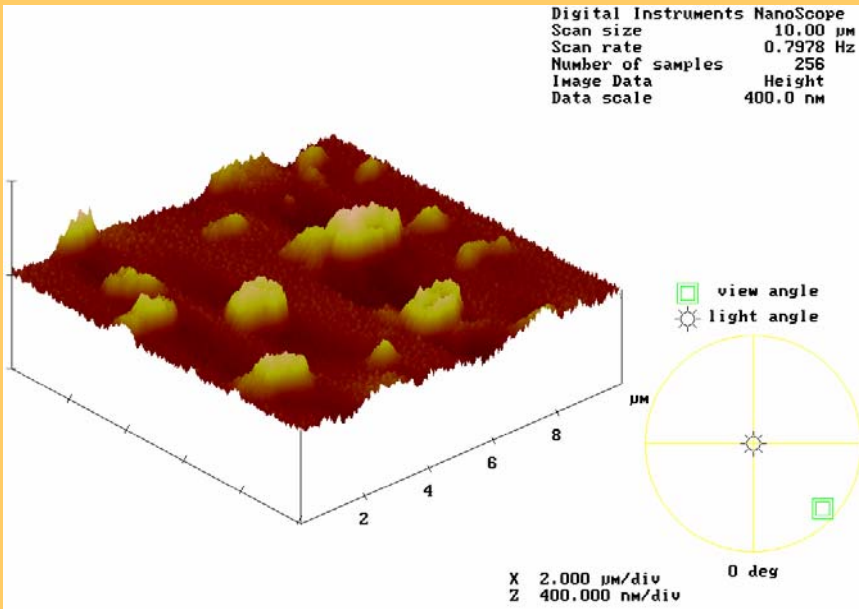
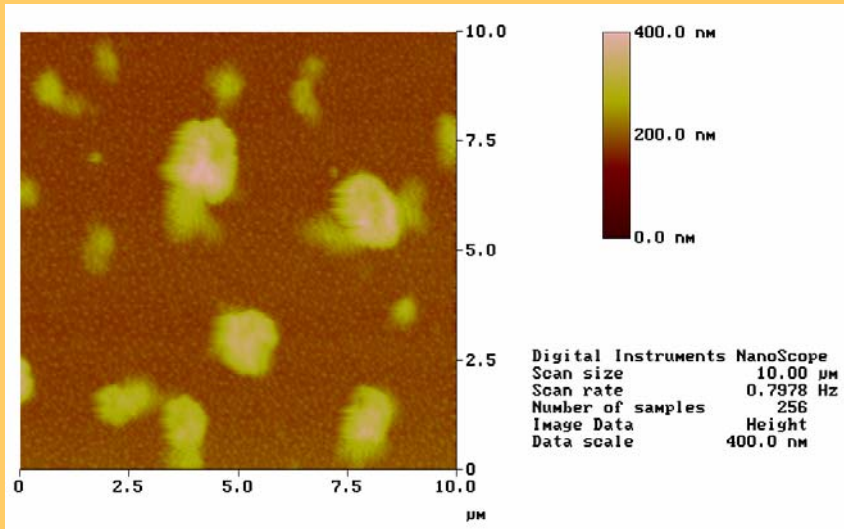
$$\text{D (nm)} = 248 / \Omega \text{ (cm}^{-1}\text{)}$$

## Summary of the process parameters

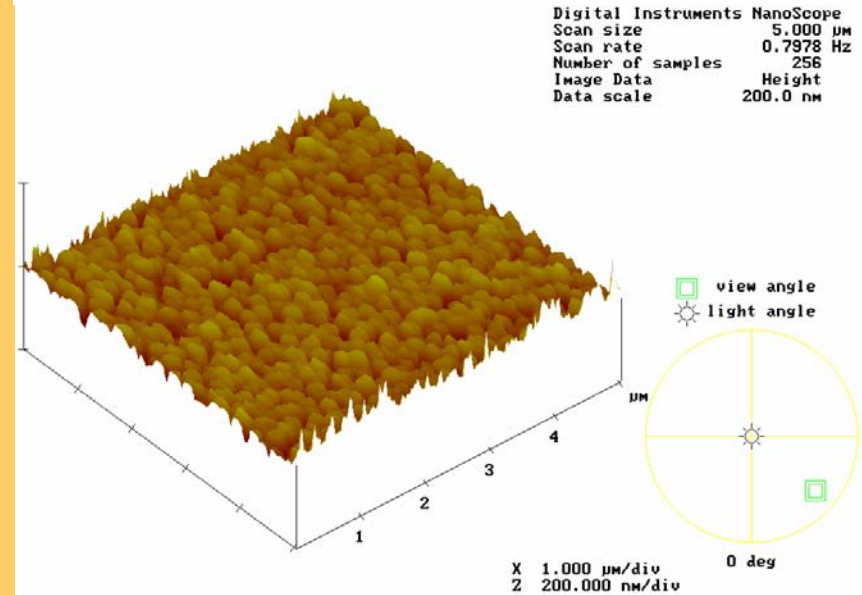
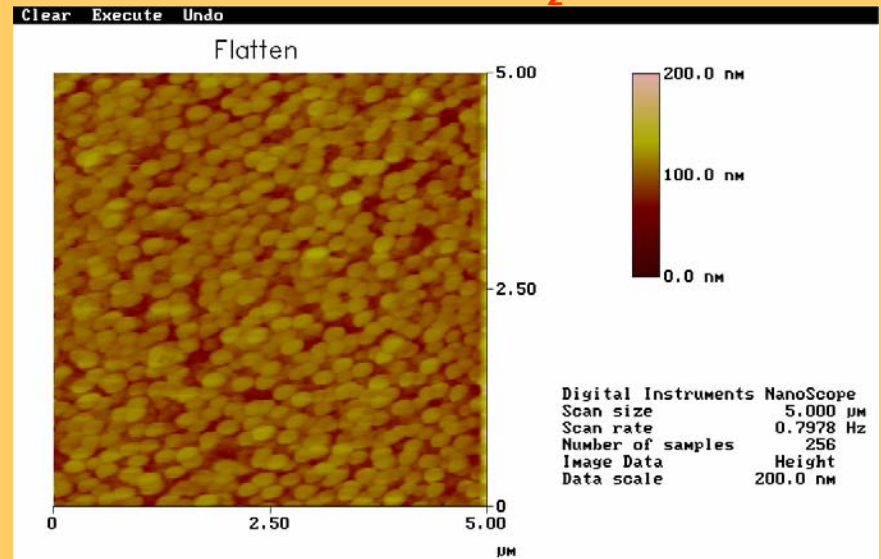
Sample	Method	Standard Process	Shorter Growth time 5min	Longer Growth time 30min	Lower pressure 100 torr	Lower temperature 800°C	Dilution of hydrocarbon	SWNTs diameter range
Fe1/SiO <sub>2</sub>		Rare MWNTs	MWNTs	MWNTs	N/A	Rare MWNTs	N/A	None
Mo0.2/Fe1/SiO <sub>2</sub>		Rare SWNTs & MWNTs	Mix. SWNTs & MWNTs	Mix. SWNTs & MWNTs	N/A	Rare MWNTs	N/A	None
Fe1/Al10/SiO <sub>2</sub>		Abundant SWNTs	Rare SWNTs	Abundant SWNTs	Rare SWNTs	None	None	1.265~1.252
Mo0.2/Fe1/Al10/SiO <sub>2</sub>		Abundant SWNTs	Abundant SWNTs	Abundant SWNTs	Rare SWNTs	Rare SWNTs	Rare SWNTs	1.265~1.246

# Atomic Force Microscope (AFM) Analysis

## Mo<sub>0.2</sub>/Fe<sub>1</sub>/Al<sub>10</sub>/Si



## Mo<sub>0.2</sub>/Fe<sub>1</sub>/Al<sub>10</sub>/SiO<sub>2</sub>

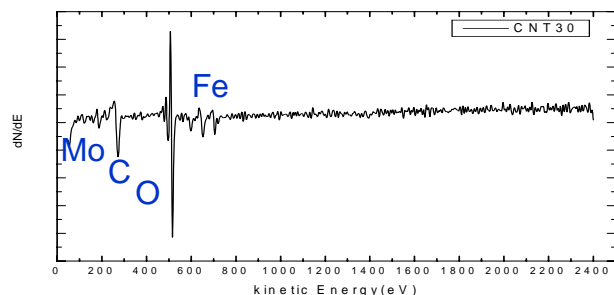




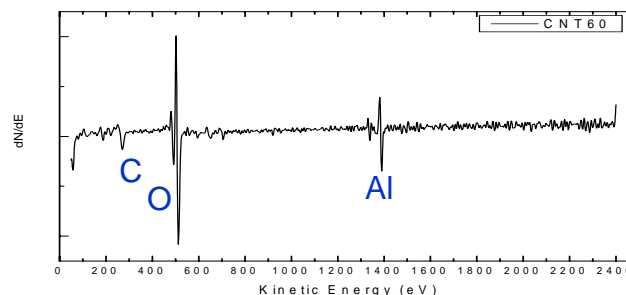
# Auger electron spectrometer (AES) analysis

Mo<sub>0.2</sub>/Fe<sub>1</sub>/Al<sub>10</sub>/SiO<sub>2</sub> sample

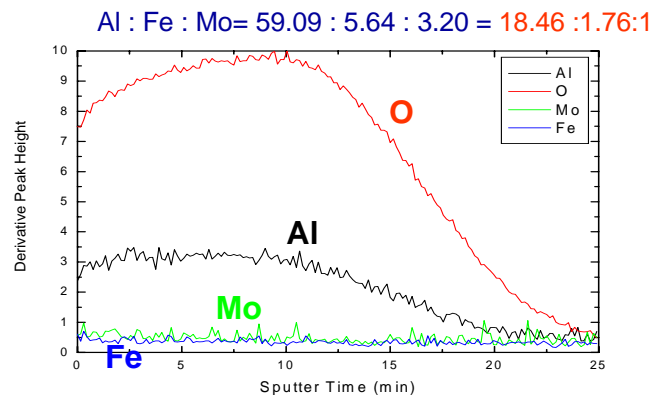
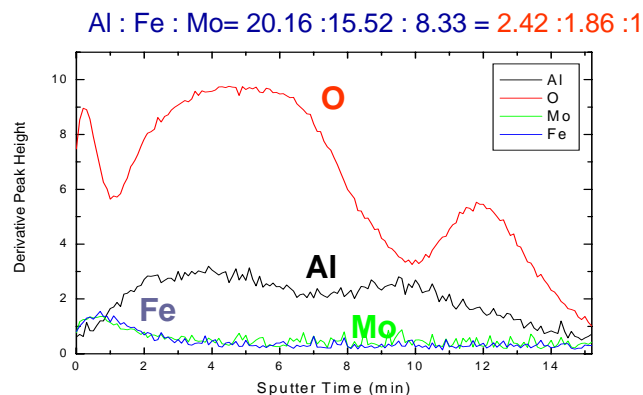
As-deposited



after heat treatment



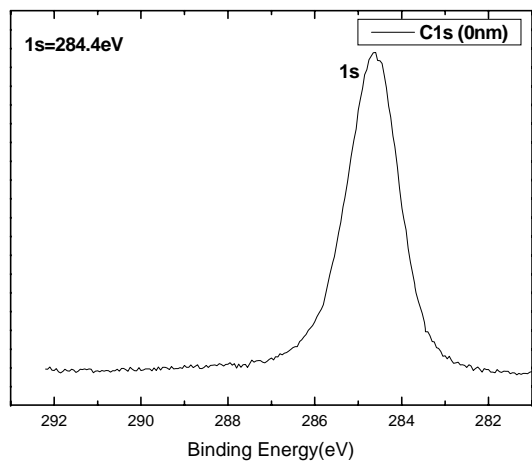
Depth profile



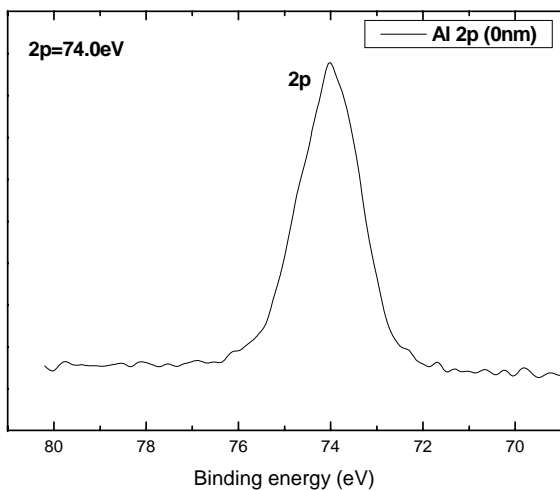
- Al transformed to aluminum oxide (Al<sub>x</sub>O<sub>y</sub>) and retained oxide in the reducing environment which provided a good support material for the catalyst particles.
- Fe and Mo were oxidized by the atmosphere before the pretreatment, but the iron oxide and molybdenum oxide were reduced during the pretreatment and retained activity to catalyze the dissociation of hydrocarbon.

# X-Ray Photoelectron Spectroscopy (XPS) Analysis

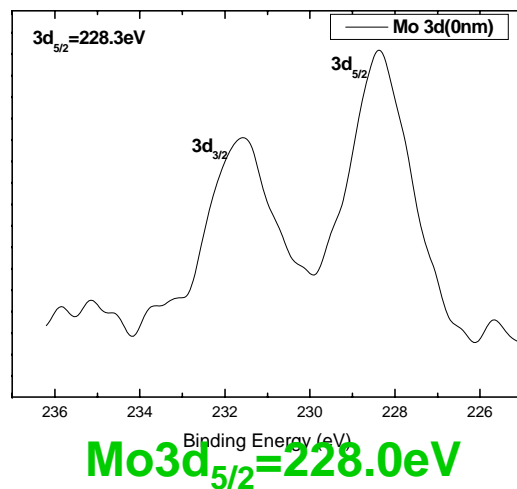
Surface: after heat treatment



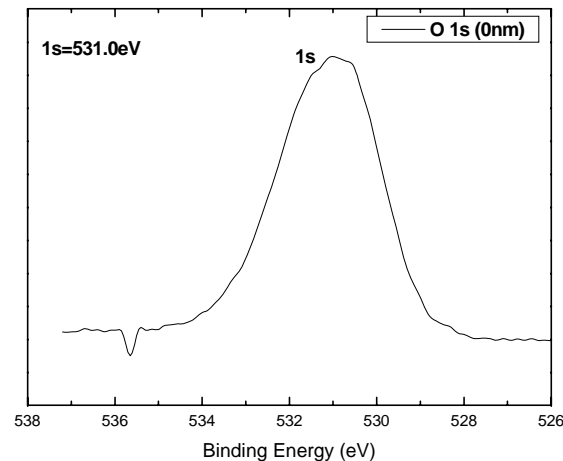
**C1s=284.5eV (calibrate)**



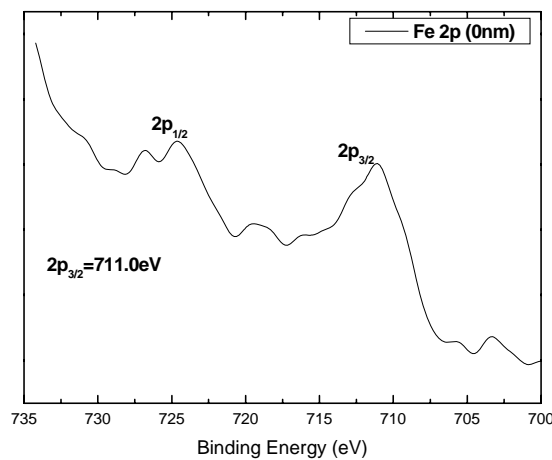
**Al2p=72.9eV → Al<sub>2</sub>O<sub>3</sub>2p=74.4eV**



**Mo3d<sub>5/2</sub>=228.0eV**



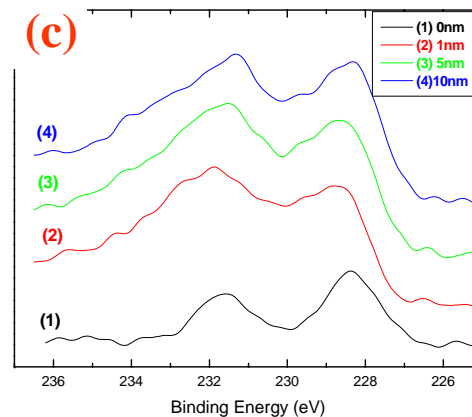
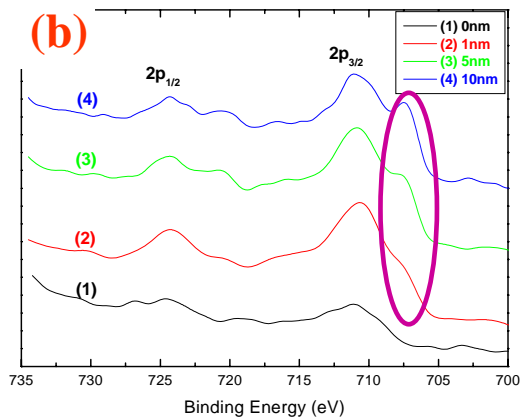
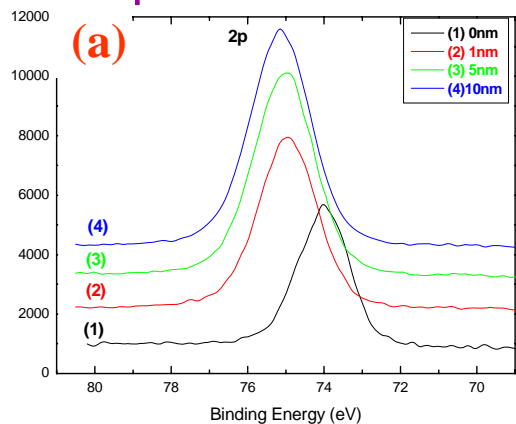
**O1s=531.0eV**



**Fe2p<sub>3/2</sub>=707.0eV → Fe<sub>2</sub>O<sub>3</sub>2p<sub>3/2</sub>=710.9eV**

# X-Ray photoelectron spectroscopy (XPS) analysis

Depth: after heat treatment



➤  $\text{Al}_2\text{O}_3, \text{Al}2p = 74.4\text{eV}$

(1).  $2p = 74.0\text{eV}$  (2).  $2p = 74.6\text{ eV}$  (3).  $2p = 74.6\text{ eV}$  (4).  $2p = 74.9\text{eV}$

➤  $\text{Fe}_2\text{O}_3, \text{Fe}2p_{3/2} = 710.9\text{eV}$  →  $\text{Fe}2p_{3/2} = 707.0\text{eV}$

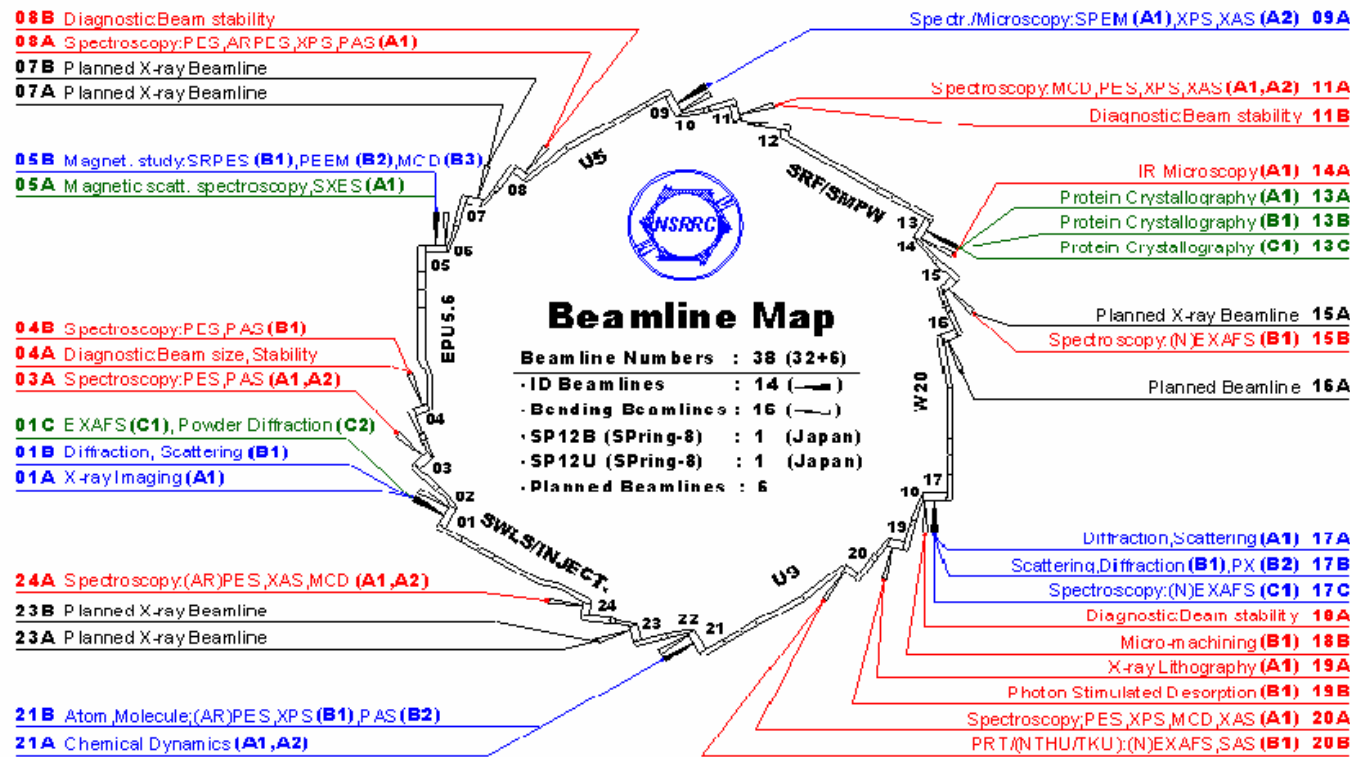
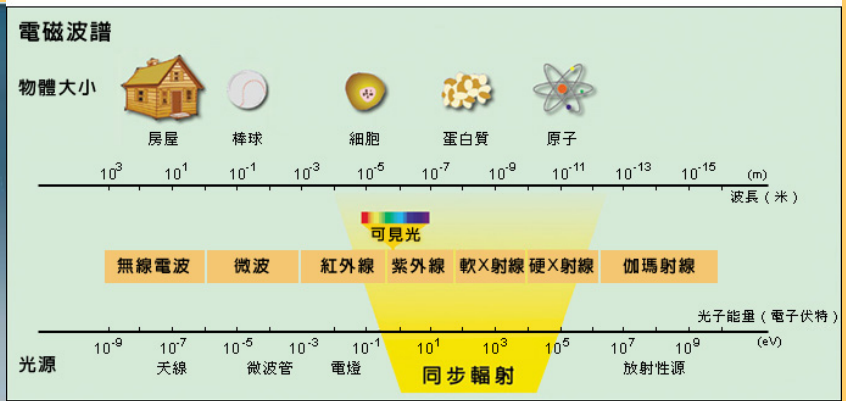
(1).  $2p_{3/2} = 711.0\text{eV}$  (2).  $2p_{3/2} = 710.9\text{eV}$  (3).  $2p_{3/2} = 710.9\text{eV}$  (4).  $2p_{3/2} = 710.9\text{eV}$

➤  $\text{Mo}3d_{5/2} = 228.0\text{eV}$

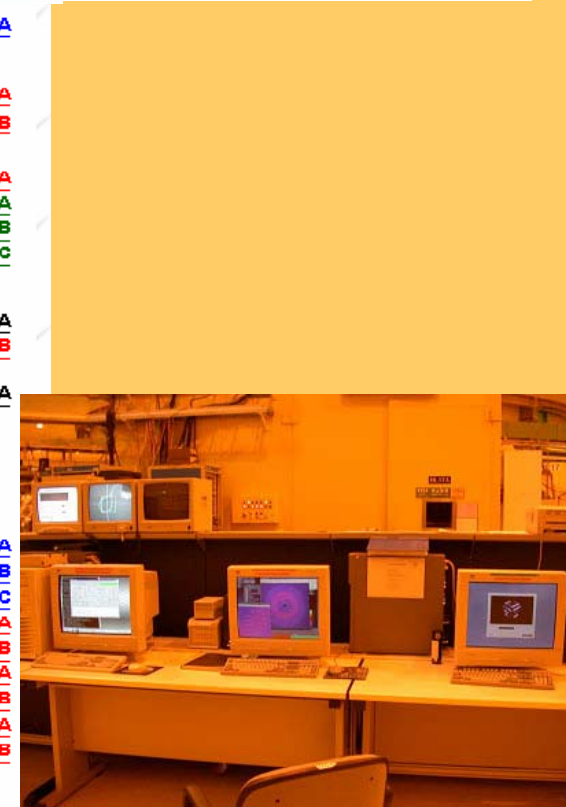
(1).  $3d_{5/2} = 228.3\text{eV}$  (2).  $3d_{5/2} = 228.6\text{eV}$  (3).  $3d_{5/2} = 228.5\text{eV}$  (4).  $3d_{5/2} = 228.3\text{eV}$

- To prove the aluminum oxide ( $\text{Al}_x\text{O}_y$ ) is  $\text{Al}_2\text{O}_3$  and to show the iron oxide and molybdenum oxide were reduced.
- There appeared reduced Fe at ~ 1 nm under surface, therefore the  $\text{Fe}_2\text{O}_3$  observed on the sample surface after pretreatment was believed due to sample exposure to the atmosphere before the XPS analysis.

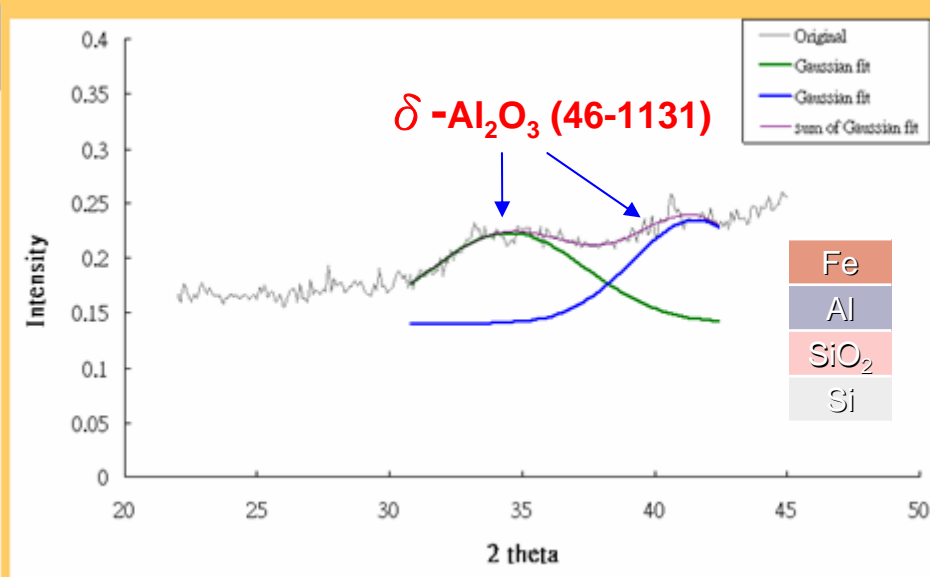
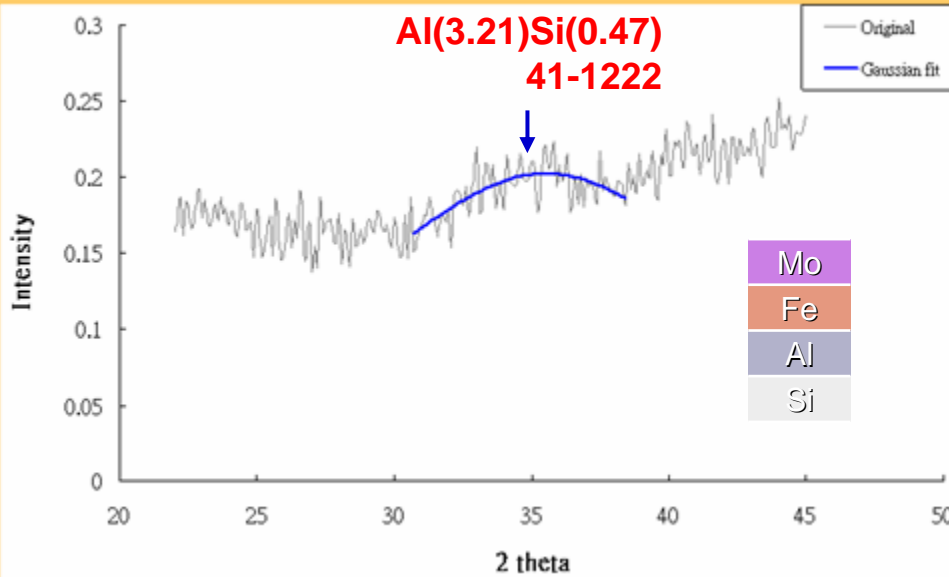
# NSRRC 17B2 Beam Line



— Bending beamlines in operation   
 — Under construction   
 (A1, ...) End-station  
— ID beam lines in operation   
 — Planned beamlines



# NSRRC 17B2 Analysis



**PCPDFWIN - [PDF # 411222, Wavelength = 1.3778 (Å)]**

PDFnumber Search Print View Data Conversion Window Clear Help

41-1222 (Deleted) Al<sub>3.21</sub>Si<sub>0.47</sub>  
 CAS Number: Aluminum Silicon  
 Molecular Weight: 99.81  
 Volume[CD]:  
 Dx: Dm:  
 S.G.:  
 Cell Parameters:  
 a b c  
 α β γ  
 SS/FOM: F = ( , )  
 I/cor:  
 Rad: CuKα1  
 Lambda: 1.54056  
 Filter: Graph  
 d-sp: diffractometer

**PCPDFWIN - [PDF # 461131, Wavelength = 1.3778 (Å)]**

PDFnumber Search Print View Data Conversion Window Clear Help

46-1131 Quality: 5-Al<sub>2</sub>O<sub>3</sub>  
 CAS Number: 1344-28-1  
 Molecular Weight: 101.96  
 Volume[CD]: 741.62  
 Dx: 2.740 Dm:  
 S.G.: P4m2 (115)  
 Cell Parameters:  
 a 5.599 b c 23.65  
 α β γ  
 SS/FOM: F30=5(0.090, 69)  
 I/cor:  
 Rad: CuKα  
 Lambda: 1.5418  
 Filter:  
 d-sp: diffractometer

2θ	Int-f	h	k	l	2θ	Int-f	h	k	l	2θ	Int-f	h	k	l
25.328	11				42.001	9				60.903	2			
34.195	100				49.690	5				67.076	2			
39.714	35				57.450	18				68.618	25			

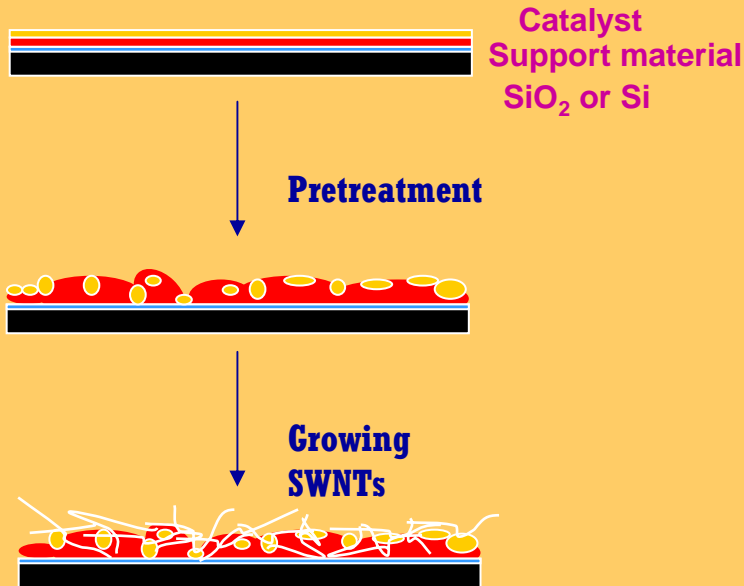
Fixed Slit Intensity vs 2θ

Fixed Slit Intensity vs 2θ

2θ	Int-f	h	k	l	2θ	Int-f	h	k	l	2θ	Int-f	h	k	l
14.479	3	0	1	1	41.839	<1	2	2	3	74.023	10	2	3	14
15.640	2	0	1	2	42.210	16	2	0	9	74.349	5	0	4	12
17.423	15	0	1	3	44.540	2	0	3	3	74.678	4	1	3	16
19.474	<1	0	1	4	44.847	4b	2	0	10	76.496	1	0	5	2
22.003	<1	0	1	5	45.383	4	0	3	4	76.659	1	0	4	13
24.636	2	0	1	6	45.783	4	1	3	0	76.659	1	0	5	3
26.112	6	1	1	5	45.783	4	2	2	6	76.954	3	2	4	10
27.675	29	0	1	7	50.055	3	1	2	11	76.954	3	2	3	15
28.367	32	0	2	0	50.664	4	2	0	12	77.484	2	0	5	4
28.633	30	0	2	1	53.217	19	2	3	2	77.812	1	1	5	0
29.254	71	0	2	2	54.013	16	1	3	8	82.224	3b	0	5	8
30.850	22	1	1	7	54.013	16	2	2	10	82.224	3b	0	4	15
32.090	37	1	2	1	56.482	17	2	2	11	82.560	4	1	5	7
32.762	56	1	2	2	56.929	16	0	2	14	82.986	3b	3	3	14
33.239	43	0	2	5	58.972	56	0	4	0	82.986	3b	2	5	0
33.540	38	1	2	3	59.144	90	0	4	1	83.398	5	2	5	2
33.753	34	1	0	9	59.144	90	2	2	12	83.954	3	2	4	2
34.619	37	1	2	4	59.368	100	0	4	2	86.374	8	2	4	14
35.183	50	0	2	6	64.456	4	0	4	7	86.374	8	2	5	6
37.195	3	0	2	7	64.912	4	2	2	14	87.130	7	1	4	16
40.013	45	1	2	7	66.354	5	1	4	7	87.469	8	1	5	10
40.171	60	0	1	11	66.354	5	2	3	11	87.879	7	0	5	11
40.593	70	2	2	0	68.344	2	3	3	7	89.971	3	3	4	12
40.963	30	2	2	1	68.946	<1	2	3	12					
41.436	36	2	2	2	73.558	9	2	4	8					

PCPDFWIN Table

# The Growth Model of SWNTs



1. Multilayered catalysts were oxidized by the atmosphere.
2.  $\text{Al}_2\text{O}_3$  was retained oxide and the  $\text{Fe}_2\text{O}_3$  was reduced to Iron by the pretreatment.
3.  $\text{Al}_2\text{O}_3$  acted the role of support material and prevented the catalyst particles to aggregate.
4. SWNTs grown on small catalyst particles.

## Function of Al :

Aluminum oxide acts as a good support material for the catalyst

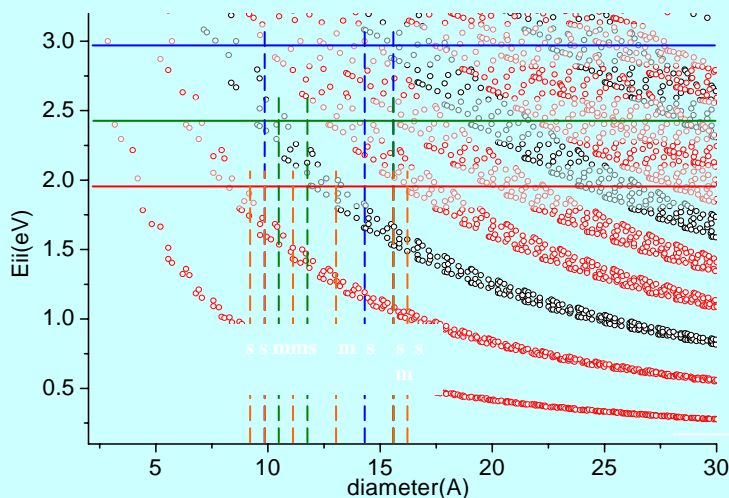
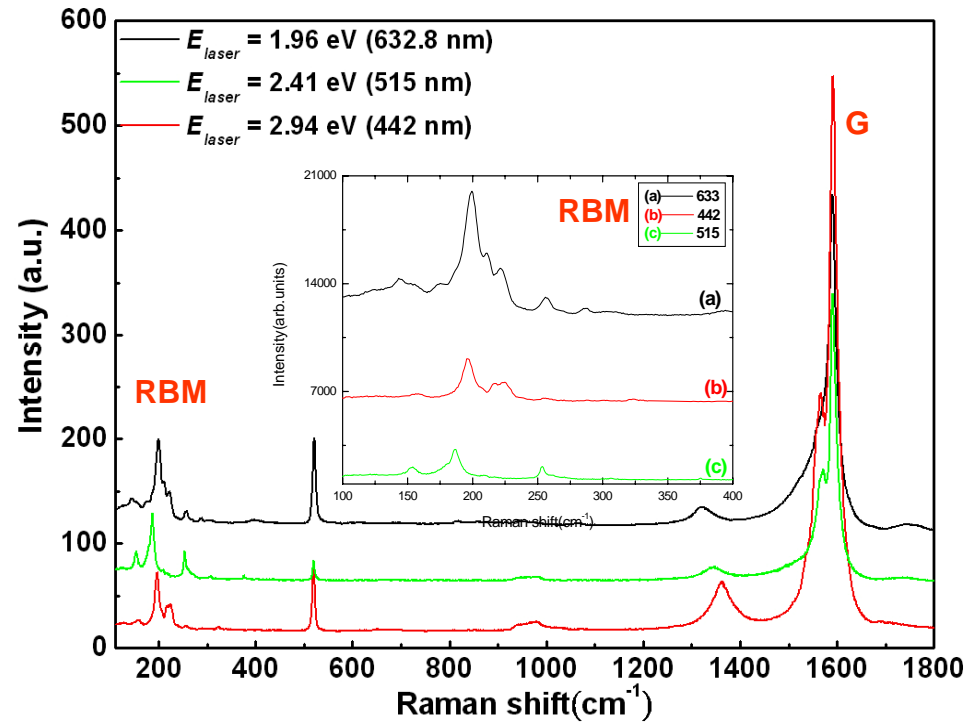
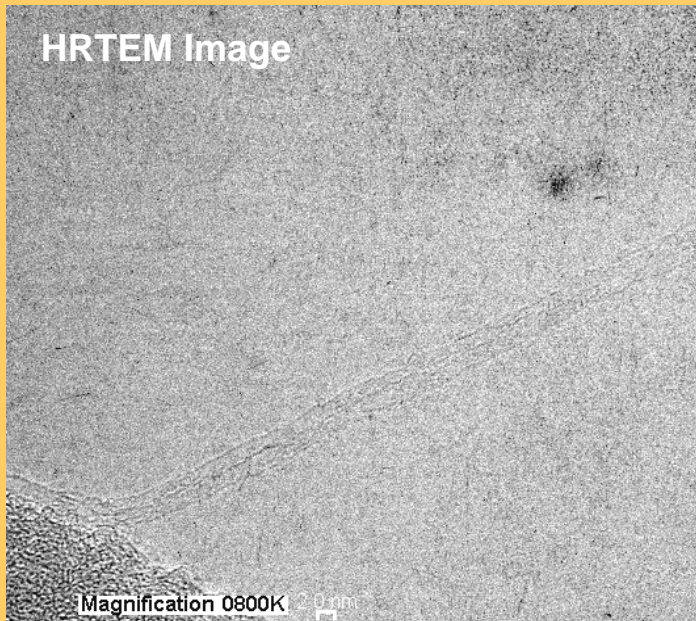
- the catalysts are hindered to aggregate to form large particles.
- provide more active nucleation sites.
- provide a porous underlayer, allowing for methane gas to flow to Fe surface.

## Function of Mo:

- Mo may help to promote the reduction of iron and retain catalytically active during the growth process.
- Mo is known to be a catalyst center for promoting the aromatization of methane, providing the intermediate aromatic species which can feed into the adjacent Fe sites with high efficiency.
- In the methane environment, Mo may exist in the form of  $\text{Mo}_2\text{C}$  and  $\text{MoO}_3$  which may probably inhibit the aggregation of iron particles. (but not observed in this study)

# Different Laser Wavelengths for Raman Analysis

Sample: Mo<sub>0.2</sub>/Fe<sub>1</sub>/Al<sub>10</sub>/Si



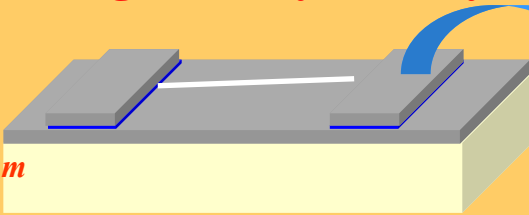
- There appeared RBM peaks in all different laser wavelengths in Raman analyses, and all have high *I*<sub>D</sub>/*I*<sub>G</sub> ratio.
- The only difference is the RBM position, and the resonance position is 199 cm<sup>-1</sup>, 196 cm<sup>-1</sup>, 187 cm<sup>-1</sup> in the wavelength 633 nm, 442 nm, 515 nm respectively.

*existing metallic and semiconducting tubes*

# Controlled *in-situ* Growth of Single-walled Carbon Nanotubes for Field-Effect-Transistor Application

- Lateral growth by a catalyst / SiO<sub>2</sub> double-layered structure

■ SiO<sub>2</sub>  
 ■ Ni 3 nm  
 ■ SiO<sub>2</sub> 100 nm

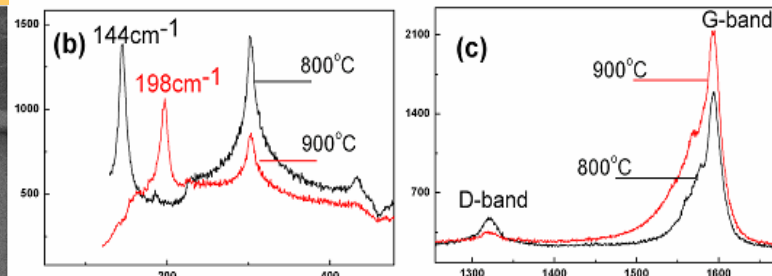
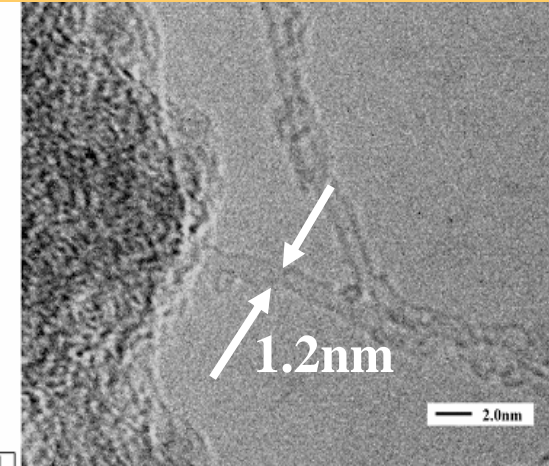
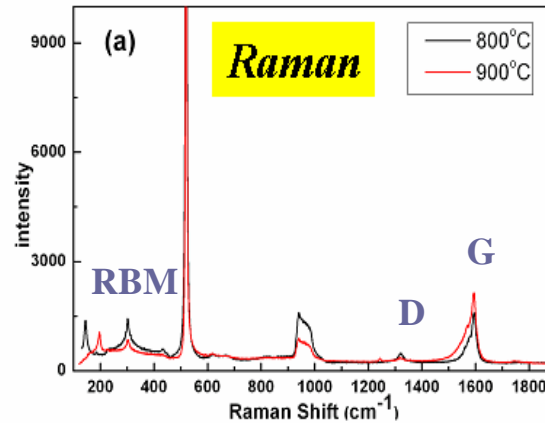
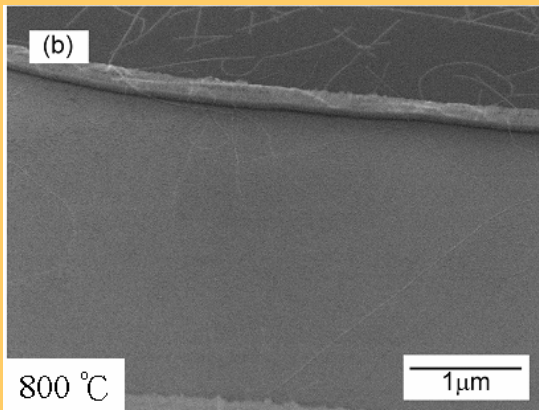
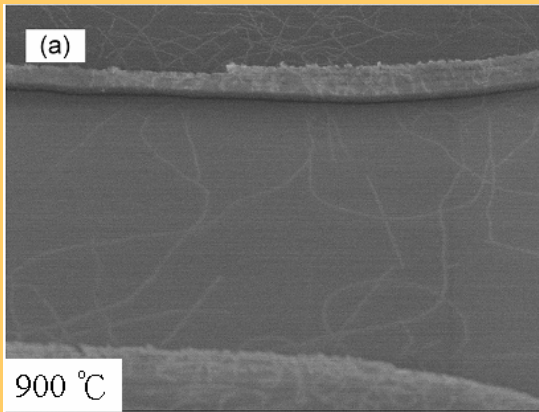


Double-layered catalytic pads

Ar:500 sccm ; CH<sub>4</sub>/H<sub>2</sub>:180/20 sccm

Temp: 800-900°C ; Pressure: 1 atm ;

Time: 30 min



HRTEM

The diameter of the SWNT's growing at 800-900°C range from 1.2 nm to 1.4 nm

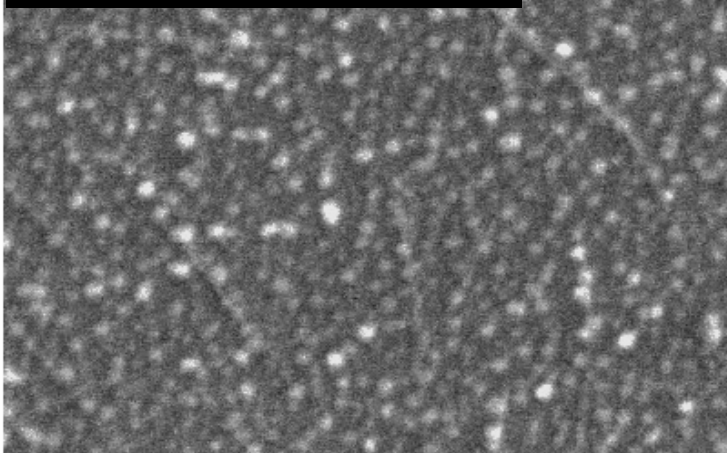
$$\lambda \text{ (cm}^{-1}\text{)}: d = 248 / \lambda$$

W.Y. Lee et al. *Diamond and Related Materials* 14 (2005) 1852.

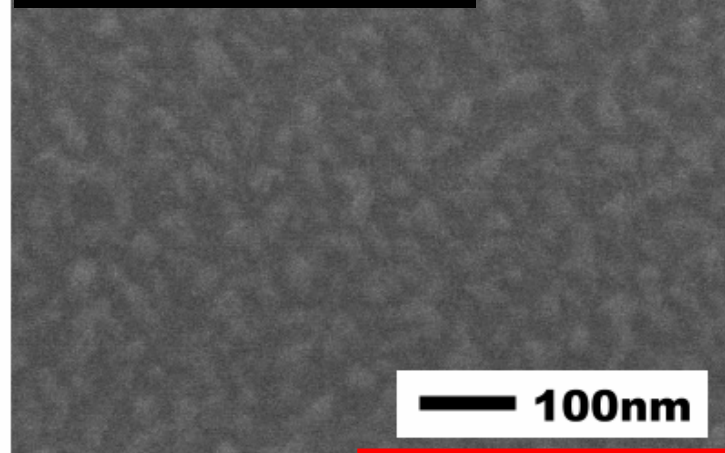


# Cross-section TEM of double layer

With upper SiO<sub>2</sub>

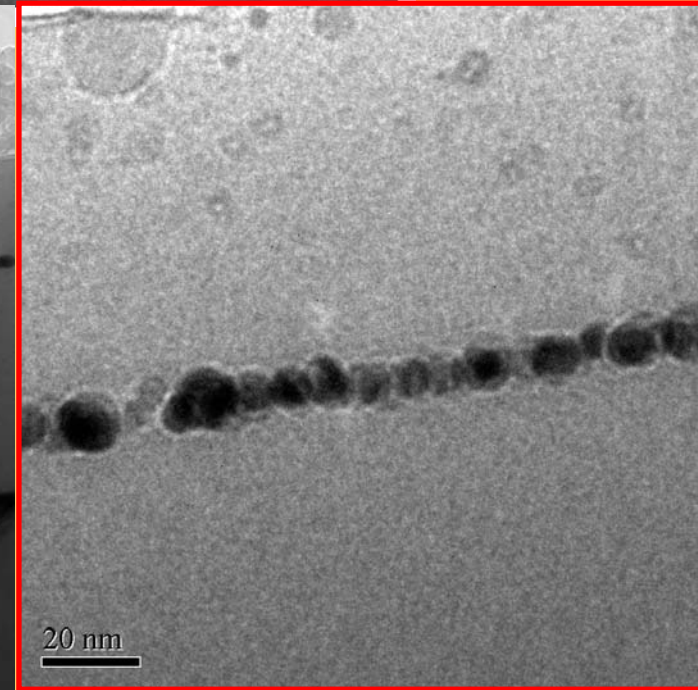
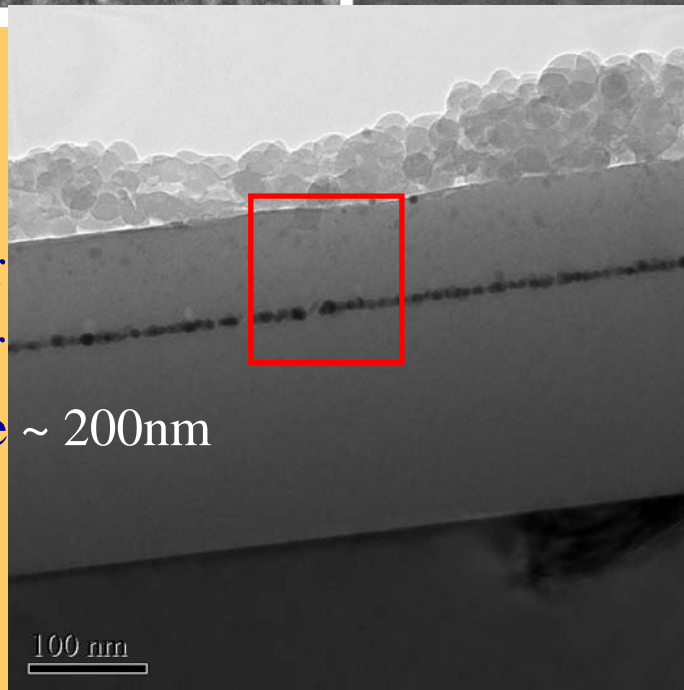


Without upper SiO<sub>2</sub>

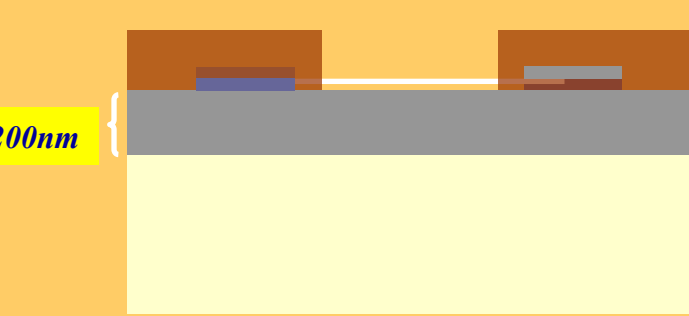






SiO<sub>2</sub> upper layer  
nickel layer

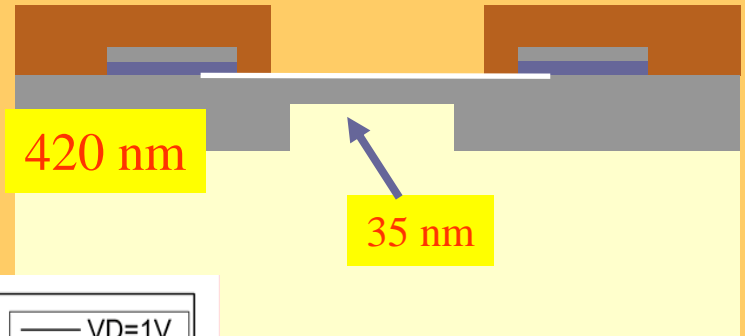
Thermal oxide ~ 200nm



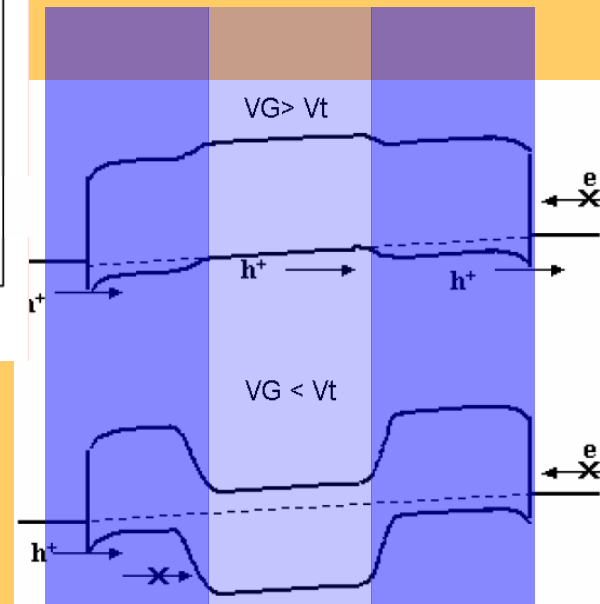
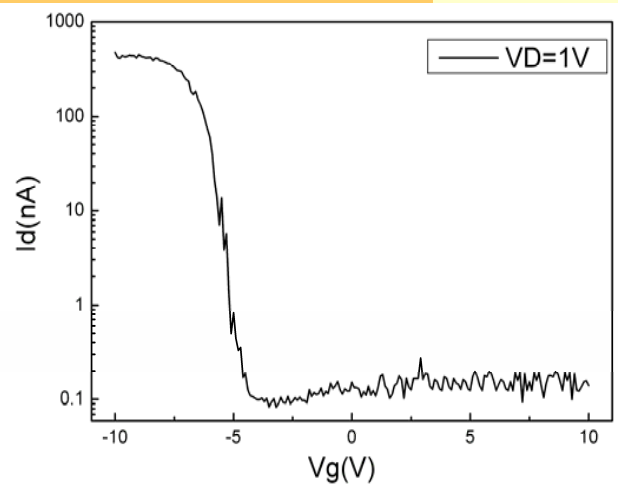
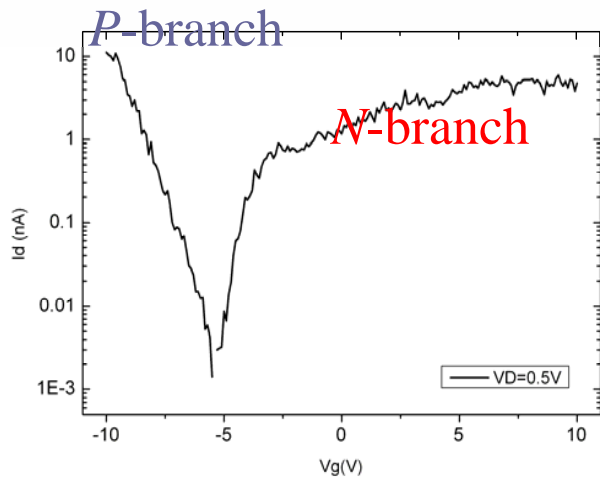
# Field Effect free-on source/drain electrodes



-   $SiO_2$
-  Si-wafer
-  Nickel (3 nm)
-  Ti (150 nm)



**Bottom gate CNT-FET**

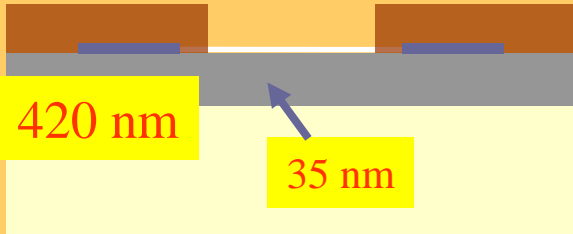


**Ambipolar to p-type unipolar CNTFET**

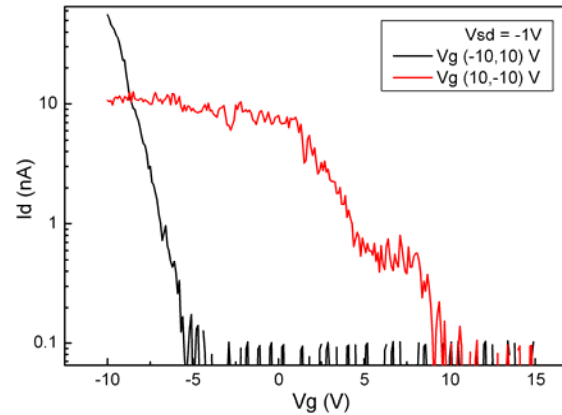
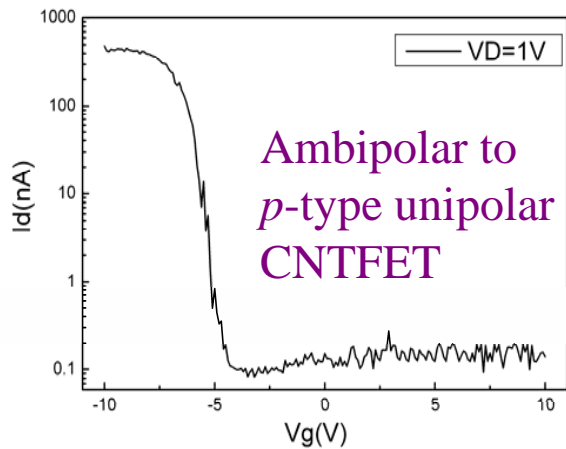
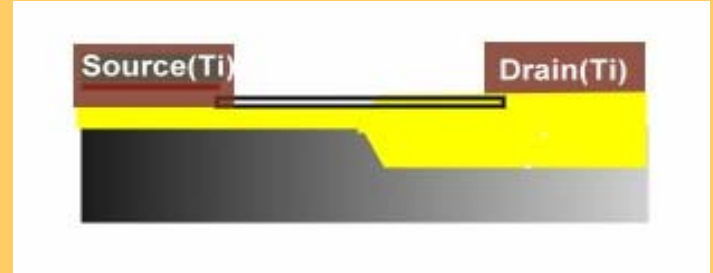
**Ambipolar transport**

# Asymmetric Structure CNTFET

Field Effect free-on source/drain electrodes → Asymmetric Structure CNTFET



$\text{SiO}_2$   
 Si-wafer  
 Nickel (3 nm)  
 Ti (150 nm)



*P*-type and hysteresis behavior in air

	Thin-oxide CNT-FET	CNT-FET with field-effect-free-on source/drain structure	Asymmetric CNT-FET
Threshold Voltage (V)	-7.1	-5.7	-9.8
Subthreshold Swing (mV/dec)	1170	543.1	429
$I_{\text{on}}$ (nA)	11.1	476.4	149
$I_{\text{off}}$ (nA)	0.0014	0.09458	0.02
On/Off Ratio	7929	5037	7450
Behavior	Ambipolar	Unipolar	Unipolar

# Charaterization by suspended structure

CH<sub>4</sub>/H<sub>2</sub>: 180/20 sccm, Temp: 850 °C, Pressure: 760 torr, Time: 20 min

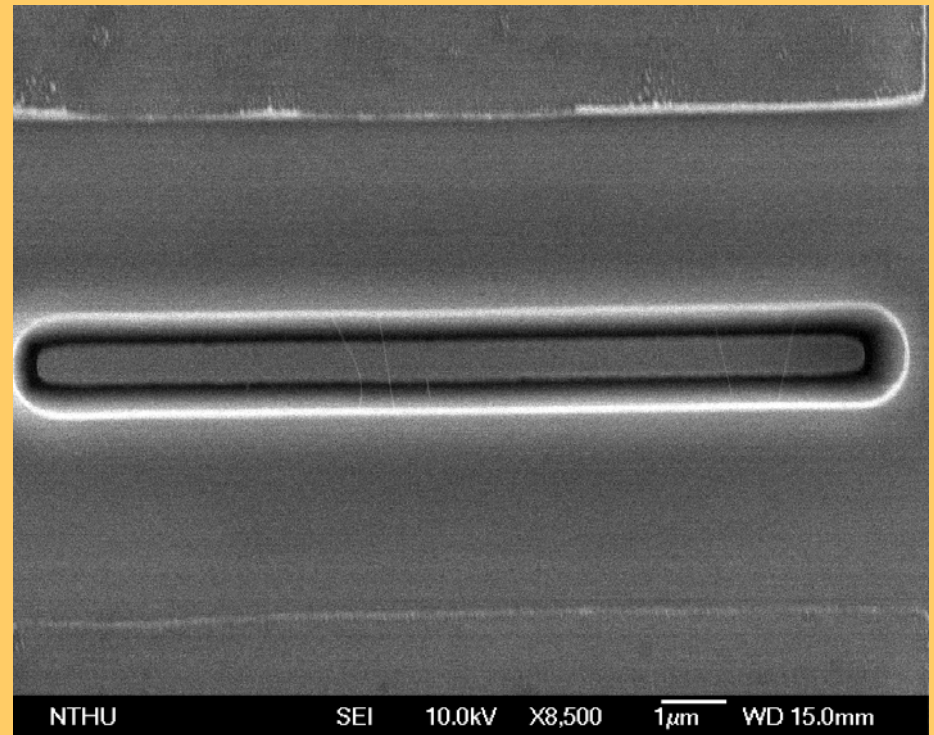
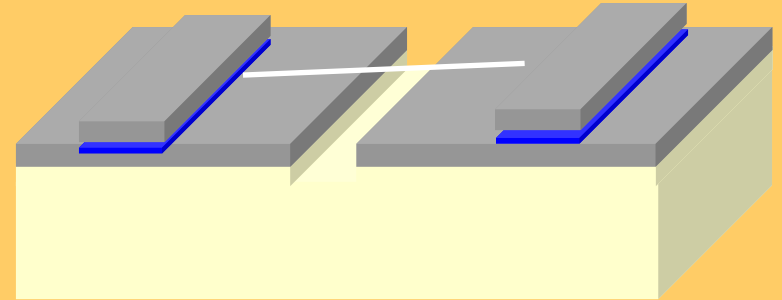
1. addressed by SEM  
Image

2.  $\mu$ Raman measurement

3. AFM  
measurement

10  $\mu$ m

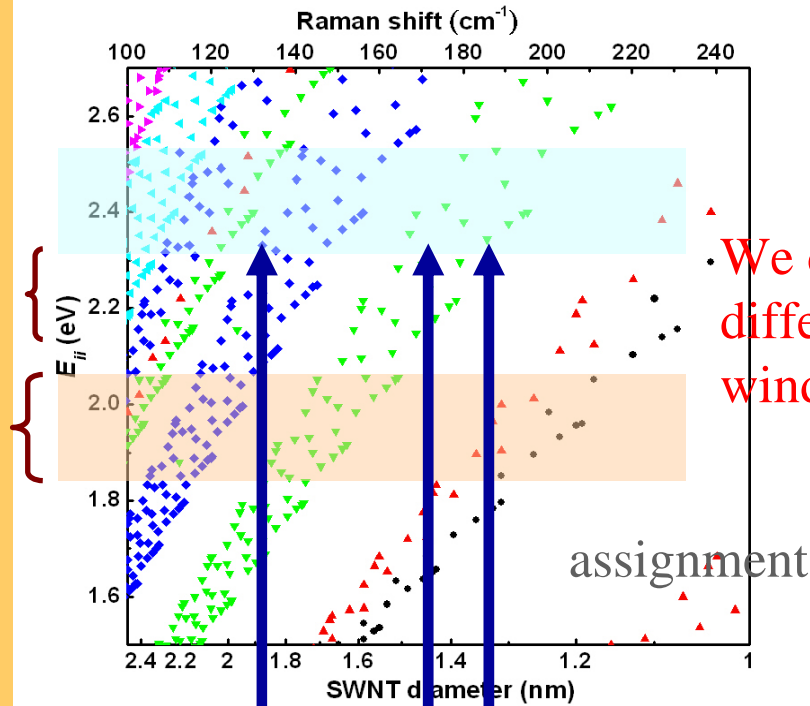
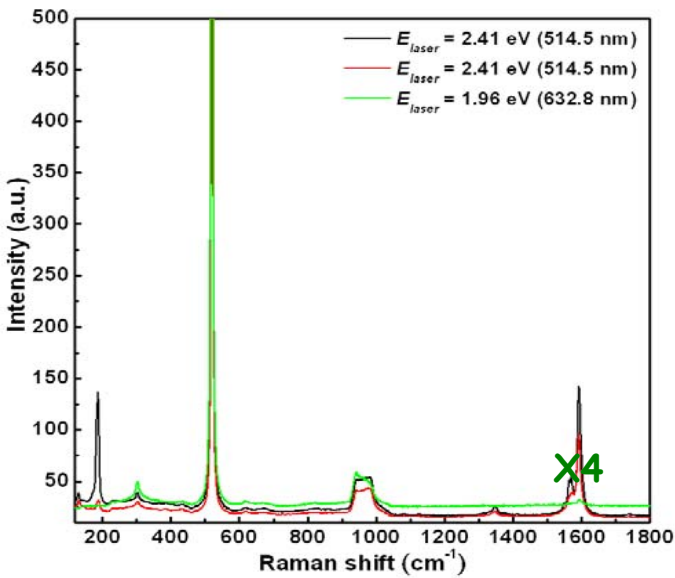
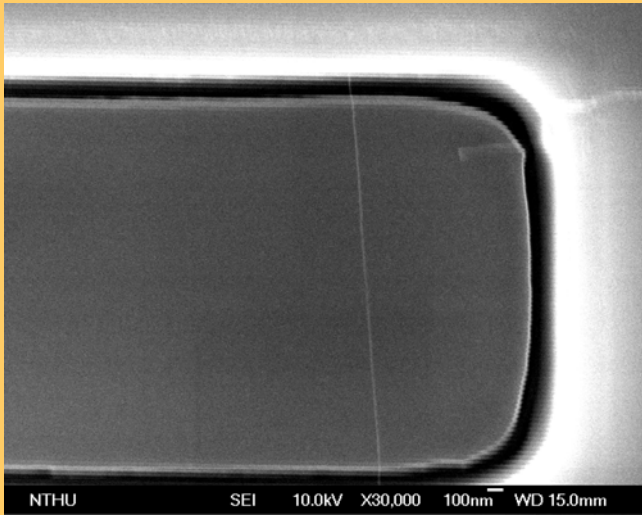
trench length : 20  $\mu$ m  
trench depth : 1  $\mu$ m  
trench width : 1, 2, 3, 4  $\mu$ m



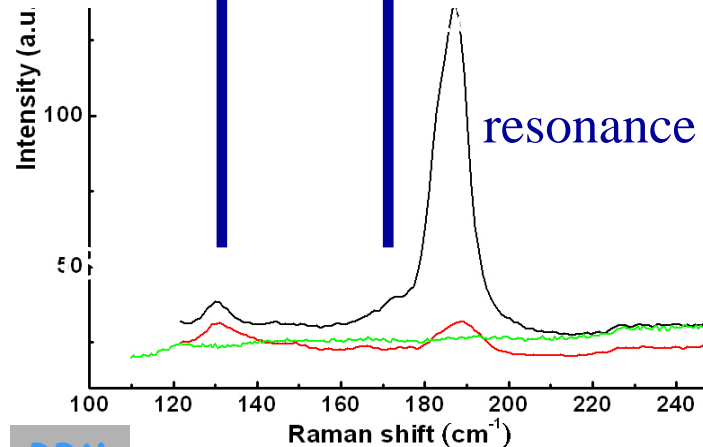
SiO<sub>2</sub>  
Si-wafer  
Nickel

the lateral growth SWNTs in thermal CVD (WY Lee)

# Raman spectrum of an assemble su-SWNTs



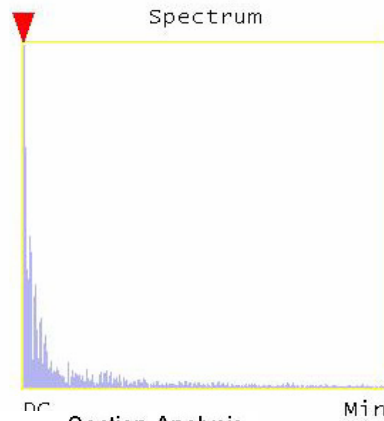
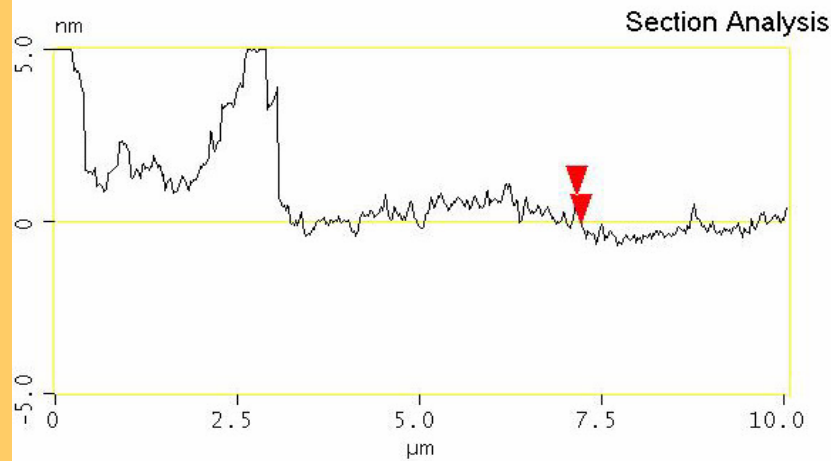
We can see the different resonant window !



no resonance

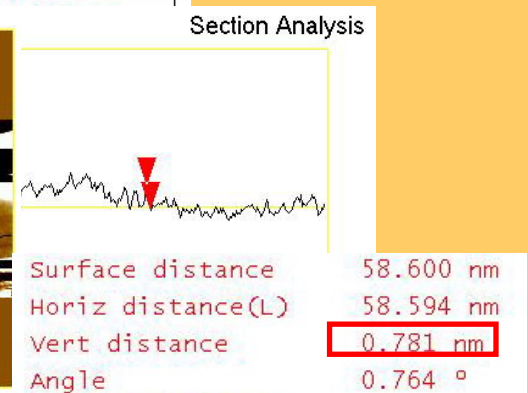
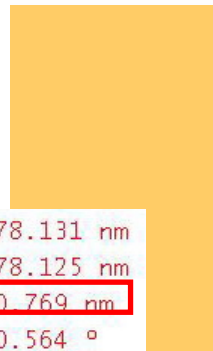
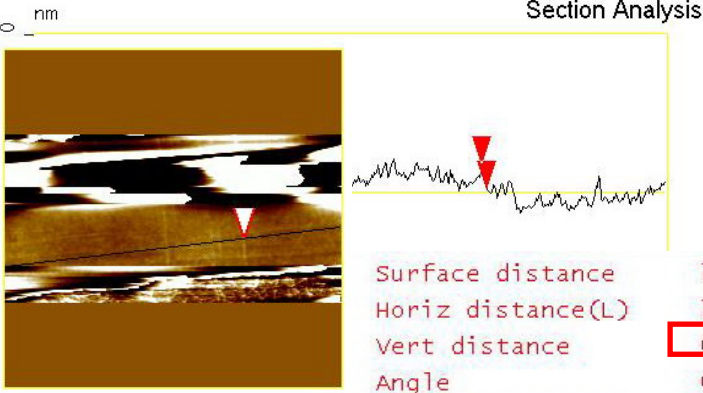
RBM

# Determine SWNT diameter by AFM analysis

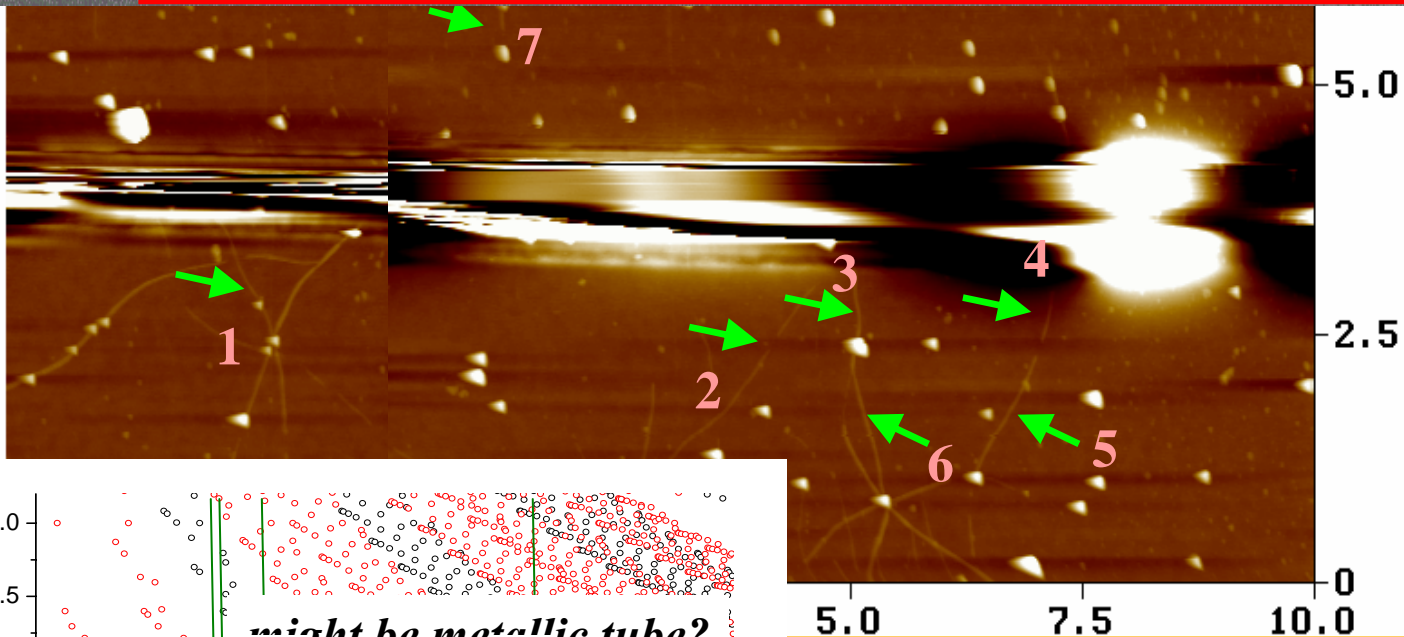
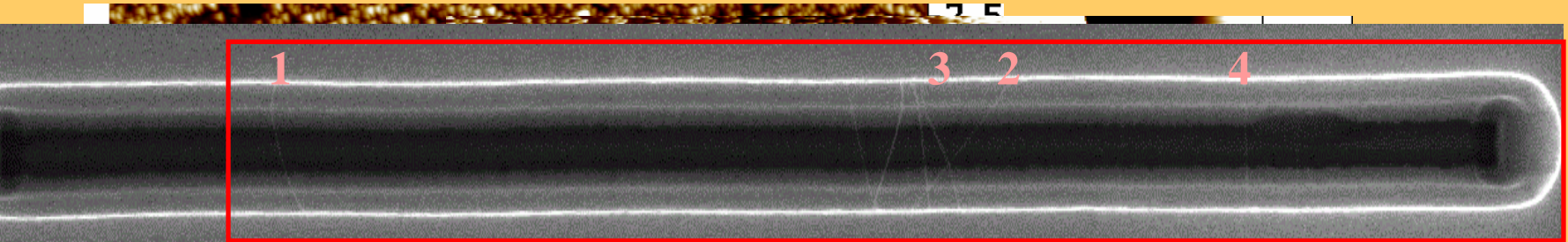


Surface distance	58.601 nm
Horiz distance(L)	58.594 nm
Vert distance	0.793 nm
Angle	0.776 °
Surface distance	
Horiz distance	
Vert distance	
Angle	
Surface distance	
Horiz distance	
Vert distance	
Angle	
Spectral period	DC
Spectral freq	0 Hz

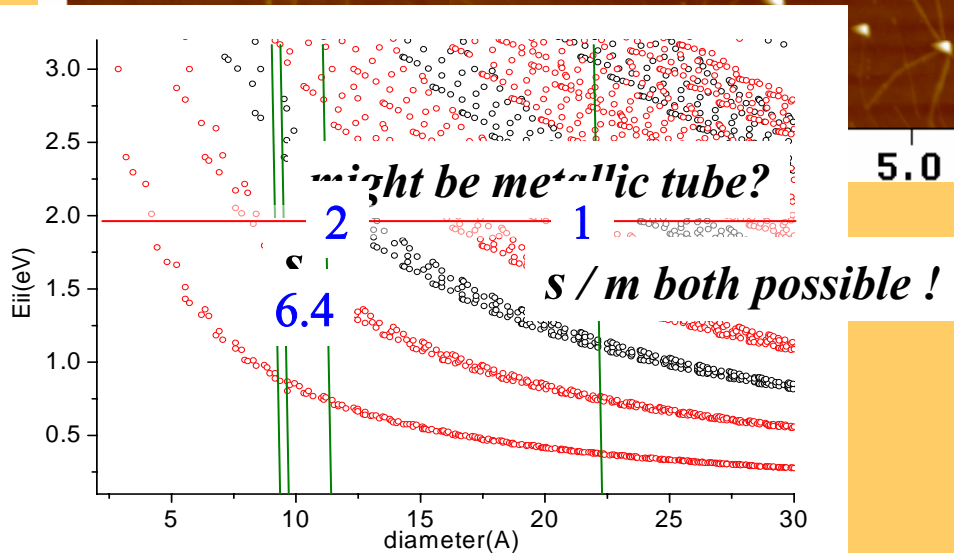
**Avg. diameter =  $0.78 \pm 0.01$  nm**



# Determine SWNT diameter by AFM analysis

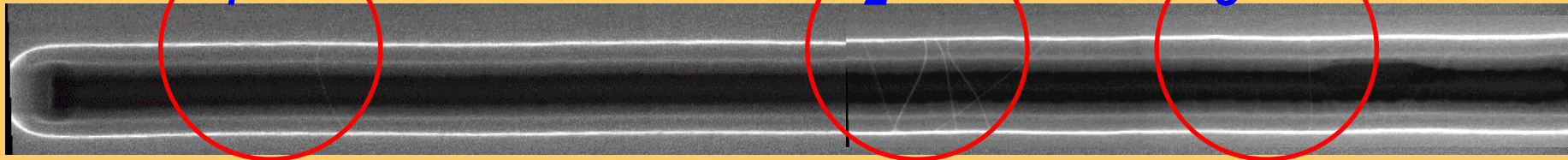


- 1. 2.21 nm (o)
- 2. 1.16 nm (o)
- 3. 1.98 nm (B)
- 4. 0.96 nm (o)
- 5. 1.15 nm
- 6. 0.85 nm (o)
- 7. 1.03 nm



# compared the AFM result with $\mu$ -Raman measurement

ESS 632.8nm



1. (1:dt=2.209nm)  $\omega_{G^-}$  : 1570.7  $\text{cm}^{-1}$   $\omega_{G^+}$  : 1589.4  $\text{cm}^{-1}$  :  
 $\ell = 91.25 \rightarrow$  might be metallic ! [o]
2. (6:dt=1.162nm)  $\omega_{G^-}$  : 1571.9  $\text{cm}^{-1}$   $\omega_{G^+}$  : 1591.3  $\text{cm}^{-1}$  :  
 $\ell = 26.19 \rightarrow$  might be semiconducting ! [o]
- (2:dt=0.854nm)  $\omega_{G^-}$  : 1571.9  $\text{cm}^{-1}$   $\omega_{G^+}$  : 1591.3  $\text{cm}^{-1}$  :  
 $\ell = 14.15 \rightarrow$  might be semiconducting ! [x]
3. (4:dt=0.957nm)  $\omega_{G^-}$  : 1576.3  $\text{cm}^{-1}$   $\omega_{G^+}$  : 1591.8  $\text{cm}^{-1}$  :  
 $\ell = 14.20 \rightarrow$  might be semiconducting ! [o]

$$\omega_{G^-} = \omega_{G^+} - \frac{\ell}{d_t^2}$$

in the same growth process and even in the same trench  
 $\rightarrow$  existing of mixing semiconducting & metallic tubes!

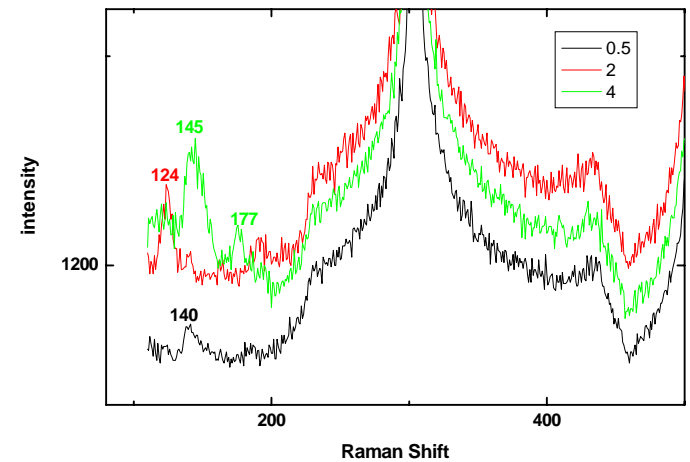
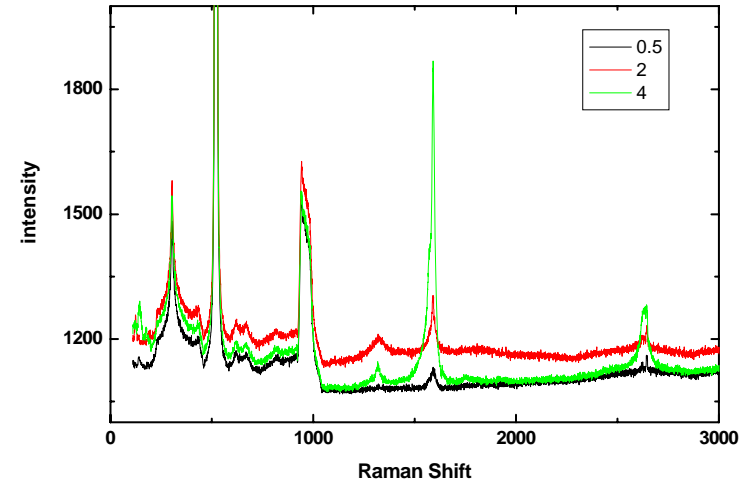
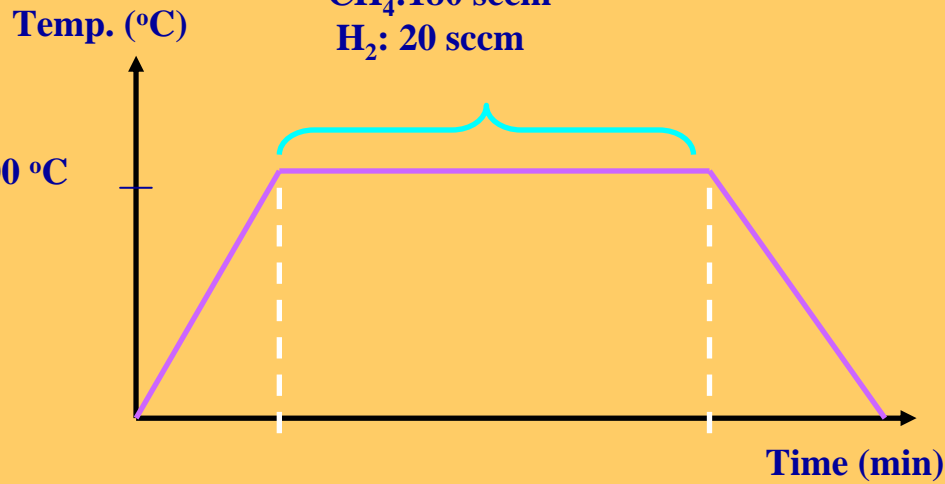


# Diameter Distribution Control

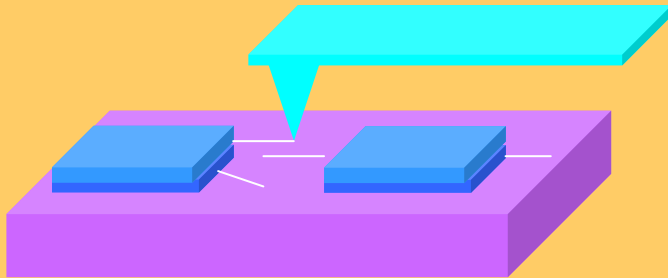
## Different deposition rates

Deposition rate of SiO <sub>2</sub> layer	0.5 Å/s	2 Å/s	4 Å/s
Thickness of nickel layer	3.3 nm	4 nm	3.5 nm

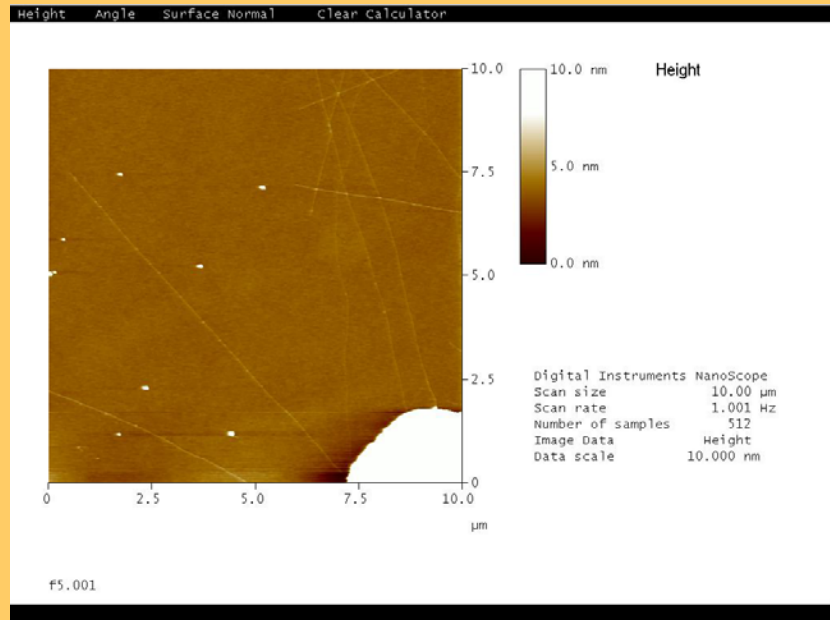
Growth condition  
CH<sub>4</sub>: 180 sccm  
H<sub>2</sub>: 20 sccm



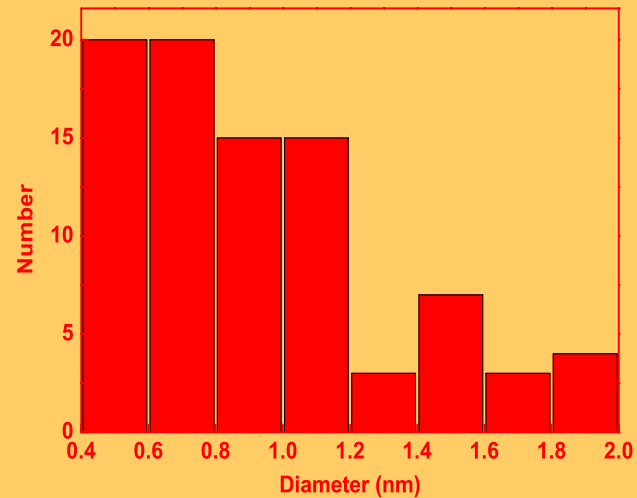
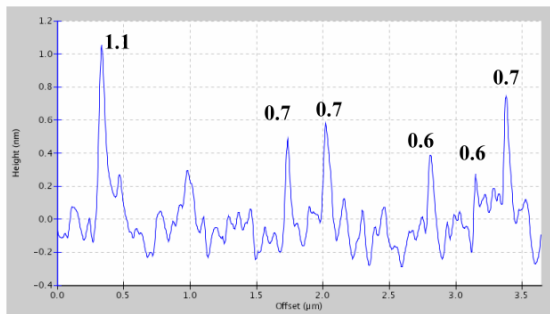
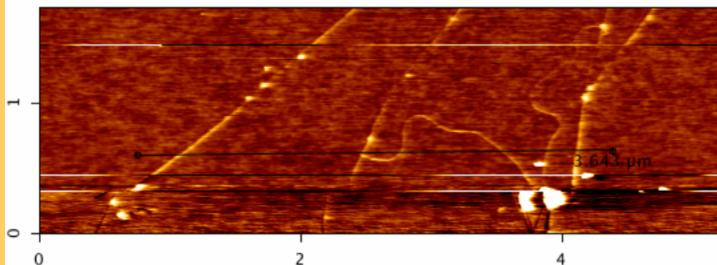
# SWNTs Characterizations



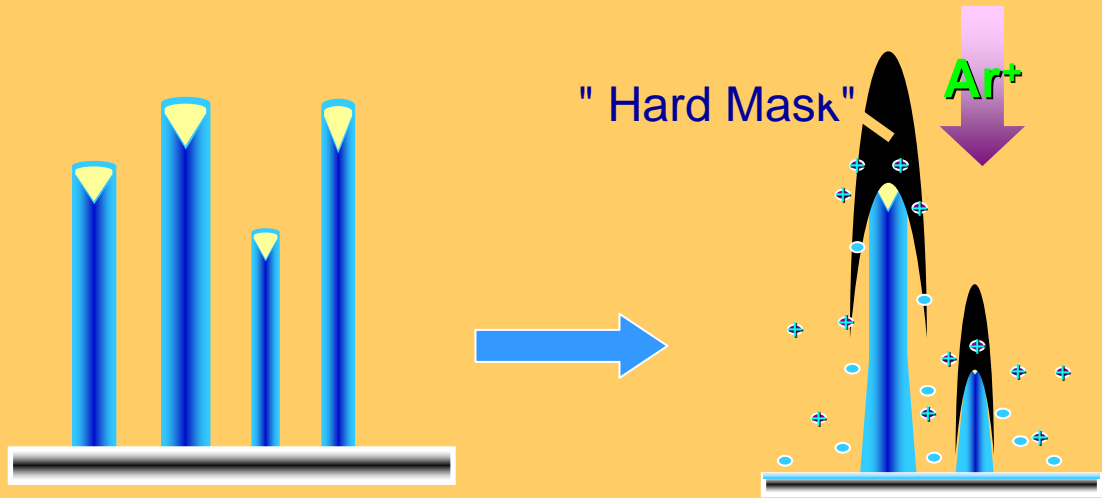
**SiO<sub>2</sub> substrate + Ni + SiO<sub>2</sub> (0.5 Å/s)**



**ESS NE101 (JPK AFM)**



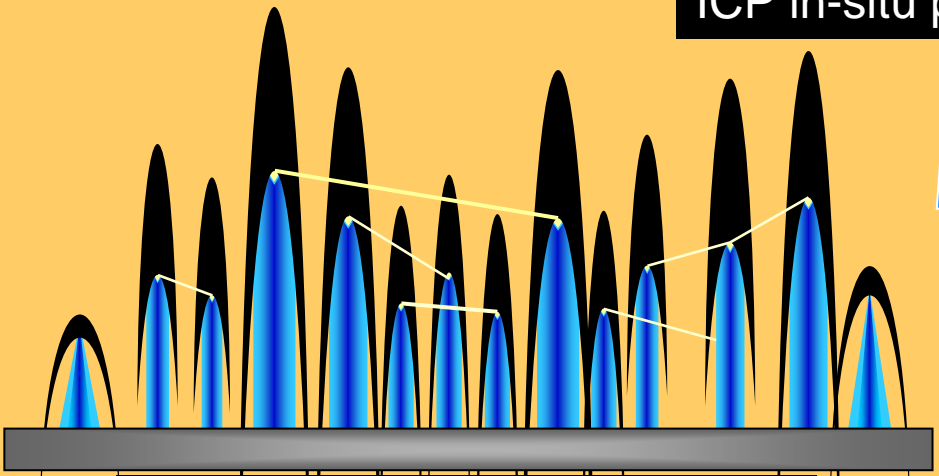
# Direct synthesis of SWNTs crossing plasma sharpened CNFs tips



ICP CNFs growth

ICP in-situ post-treatment

- CNFs growth
- Post-treatment
  - Ar plasma bombardment
  - Si layer co-sputtering



Re-growth SWNT

- Thermal CVD

Thermal CVD re-growth SWNT

# Controlled *in-situ* Growth of Single-walled Carbon Nanotubes for Field-Effect-Transistor Application

## Direct synthesis of suspended SWNTs using sharpened CNFs as templates

### • ICP-CVD growth

$C_2H_2/H_2/Ar$ : 8/24/0.5 sccm,

Pressure: 20 mTorr

ICP Power: 1000 W

RF Bias Power: 300 W

Surface Temp: 550 °C

Growth Time: 10 min

### • *in-situ* post-treatment

Feed gas: Ar 6 sccm,

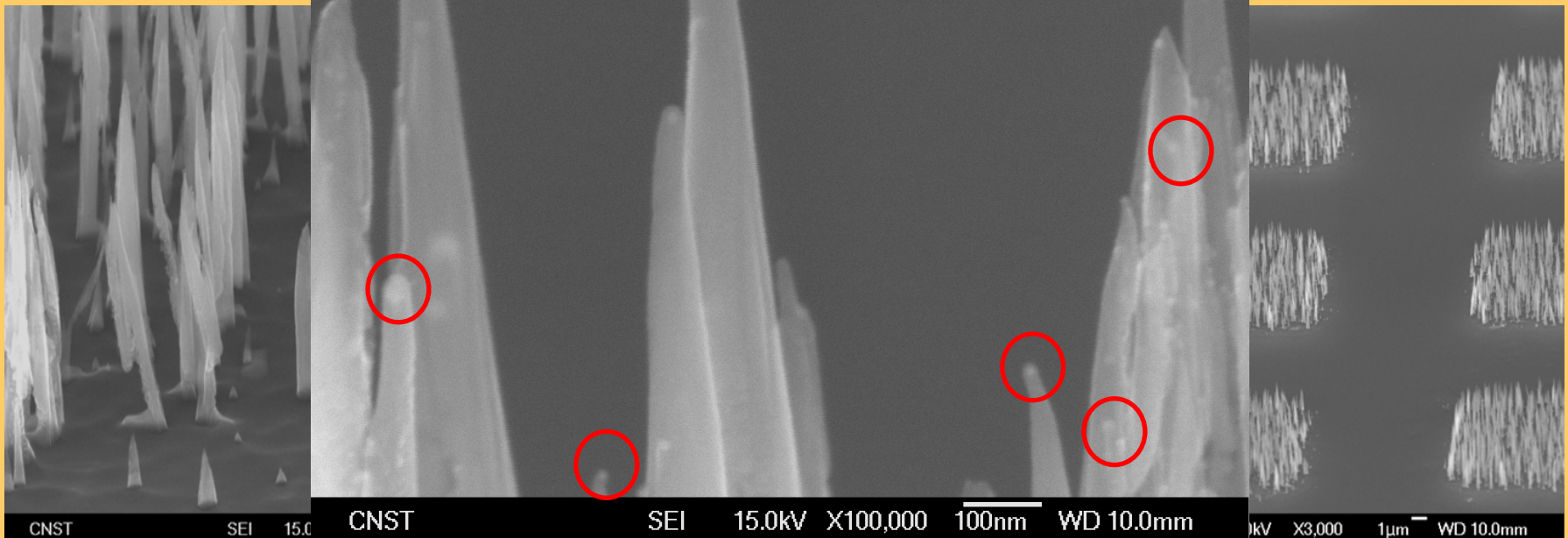
Pressure: 20 mTorr,

ICP Power: 1500 W,

RF Bias Power: 300 W, voltage: ~400 V,

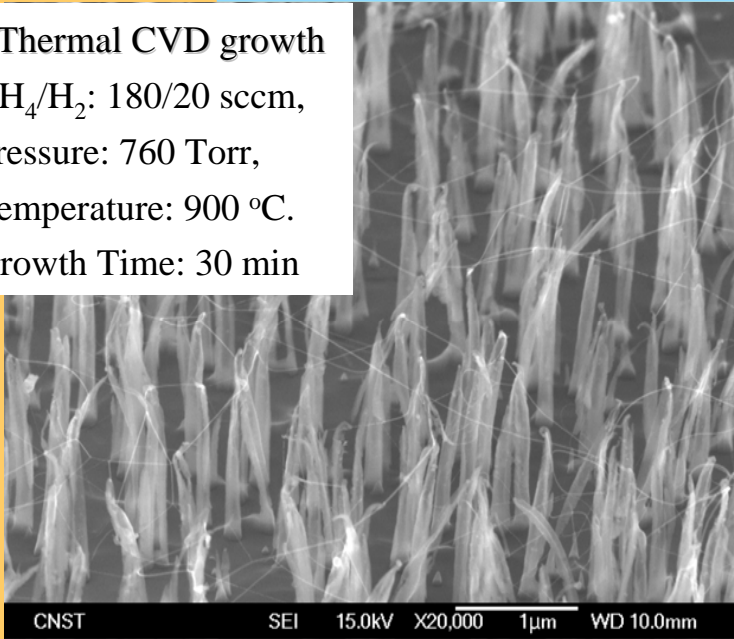
Surface Temp: ~550 °C,

Growth Time: 20 min

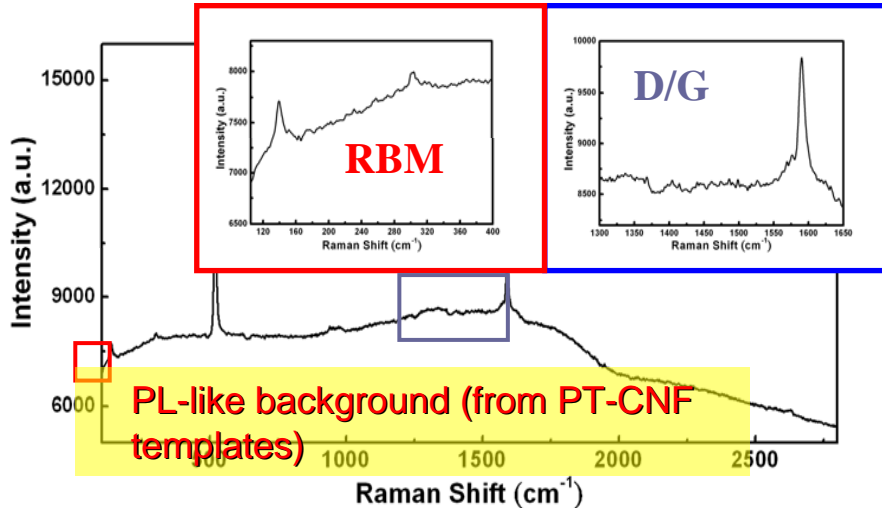
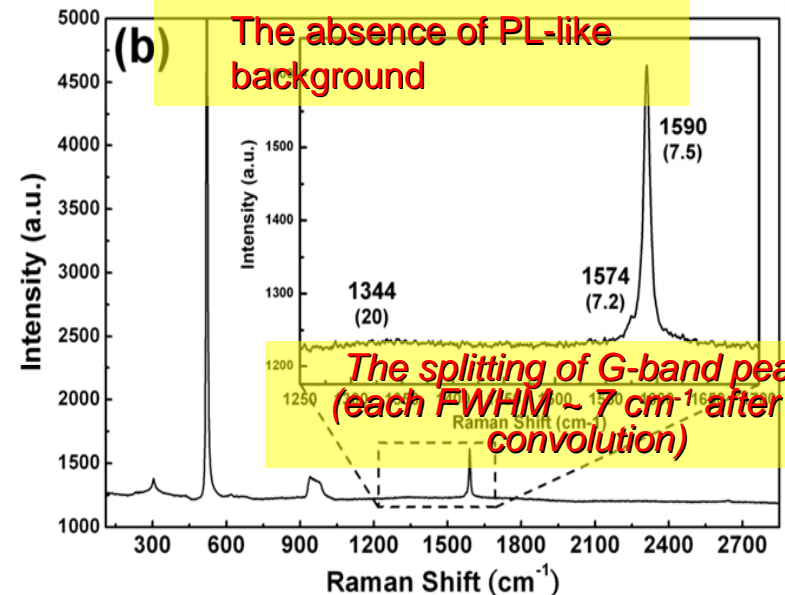
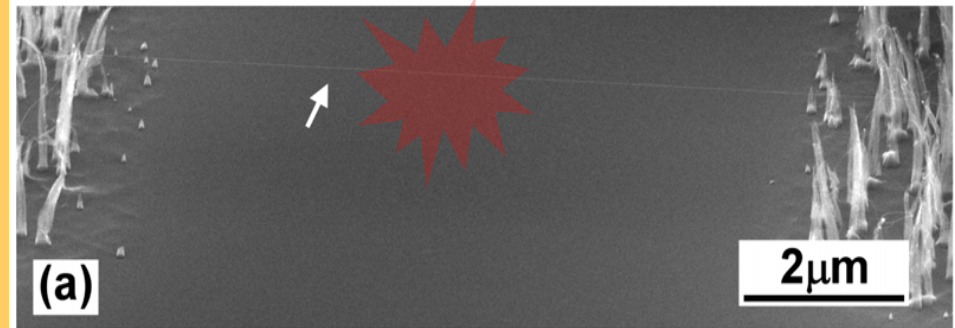


# Controlled *in-situ* Growth of Single-walled Carbon Nanotubes for Field-Effect-Transistor Application

- Thermal CVD growth  
 $\text{CH}_4/\text{H}_2$ : 180/20 sccm,  
 Pressure: 760 Torr,  
 Temperature: 900 °C.  
 Growth Time: 30 min



## Raman spectrum at *one SWNT level*



No RBM  
 (resonant with the scattered photons)

**“The principles of physics do not speak against the possibility of manufacturing things atom by atom.....”**

**“At the atomic level, we have new kinds of forces and new kinds of possibilities, new kinds of effects.**

**The problems of manufacturing and reproduction of materials will be quite different.”**



**Richard Feynman**

**“There’s Plenty of Room at the Bottom”  
1959, Caltech**



**Thanks for your attention**

## **Acknowledgement~**

### **Team Members:**

#### **• Field Emission Display :**

NTHU (清大): C.H. Tsai, K.C. Leou, C. Pan, N.H. Tai, T.L. Lin, Y. Hu,  
J.H. Huang, I.N. Lin

NTNU (師大): H.F. Cheng

CYCU (中原): T.S. Lai

#### **• Field Effect Transistors :**

NTHU (清大): C.H. Tsai, K.C. Leou, K.S. ChangLiao, T.L. Lin,  
N.H. Tai, H.Y. Huang, K.C. Hwang, W.K. Hsu

NCTU (交大): B.Y. Tsui, C.T. Kuo, H.C. Cheng

NCU (中央): C.H. Nien

### **Funded by:**

**National Science Council**

**Materials Research Laboratories, ITRI**

**Nano-Architect Research Corporation**

**Center for Nano Science & Technology, University System of Taiwan**

**Center for Measurement Standard, ITRI (for micro electron gun)**